AD-A132 462 FRACTO-EMISSION FROM POLYMERS(U) WASHINGTON STATE UNIV 1/2
PULLMAN DEPT OF PHYSICS J T DICKINSON JUN 83
N00014-80-C-0213

UNCLASSIFIED F/G 11/9 NL

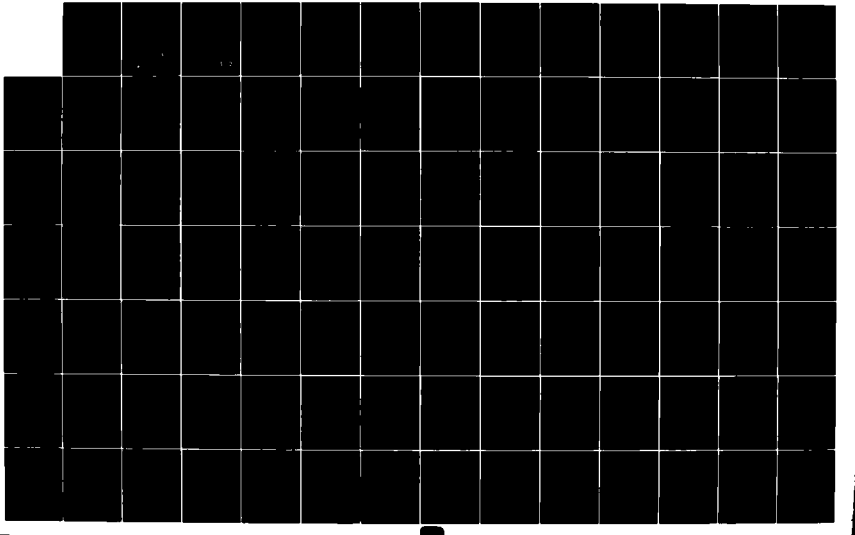

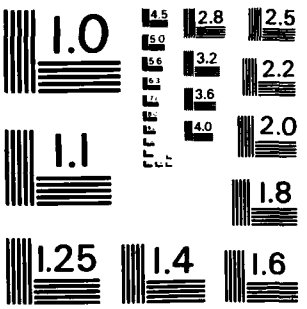

MICROCOPY RESOLUTION TEST CHART
NATIONAL BUREAU OF STANDARDS - 1963 - A

(12)

OFFICE OF NAVAL RESEARCH
Contract N00014-80-C-0213
Project NR 092-558

Annual Technical Report
June 1983

FRACTO-EMISSION FROM POLYMERS

J. Thomas Dickinson

DEPARTMENT OF PHYSICS
WASHINGTON STATE UNIVERSITY

OFFICE OF NAVAL RESEARCH
Contract N00014-80-C-0213
Project NR 092-558

Annual Technical Report
June 1983

FRACTO-EMISSION FROM POLYMERS

J. Thomas Dickinson

Department of Physics
Washington State University
Pullman, Washington 99164-2814

SECURITY CLASSIFICATION OF THIS PAGE (When Data Entered)

REPORT DOCUMENTATION PAGE

READ INSTRUCTIONS BEFORE COMPLETING FORM

1. REPORT NUMBER	2. GOVT ACCESSION NO. A132462
3. RECIPIENT'S CATALOG NUMBER	
4. TITLE (and Subtitle) Fracto-Emission From Polymers	5. TYPE OF REPORT & PERIOD COVERED Annual Technical Report June, 1982 - June 1983
	6. PERFORMING ORG. REPORT NUMBER
7. AUTHOR(s) J. Thomas Dickinson	8. CONTRACT OR GRANT NUMBER(s) N00014-80-C-0213
9. PERFORMING ORGANIZATION NAME AND ADDRESS Department of Physics Washington State University Pullman, WA 99164-2814	10. PROGRAM ELEMENT, PROJECT, TASK AREA & WORK UNIT NUMBERS
11. CONTROLLING OFFICE NAME AND ADDRESS Office of Naval Research Power Program Arlington, VA 22217	12. DATE ~~July 15,~~ 1983
	13. NUMBER OF PAGES
14. MONITORING AGENCY NAME & ADDRESS (if different from Controlling Office)	15. SECURITY CLASS. (of this report) Unclassified
	15a. DECLASSIFICATION/ DOWNGRADING SCHEDULE

16. DISTRIBUTION STATEMENT (of this Report)

Approved for public release; distribution unlimited

17. DISTRIBUTION STATEMENT (of the abstract entered in Block 20, if different from Report)

18. SUPPLEMENTARY NOTES

19. KEY WORDS (Continue on reverse side if necessary and identify by block number) fracture, delamination, crack propagation, fracture surfaces, surface chemistry, interfacial failure, exo-emission, electron emission, positive ion emission, photon emission, chemi-emission, tribo-luminescence, radio-wave emission, fracto-emission, surface charging, fracture-induced breakdown, gaseous discharges, fracture of: polymers, polybutadiene, elastomers, rubber, RDX, sucrose, quartz, SiO_2, epoxy

20. ABSTRACT (Continue on reverse side if necessary and identify by block number) Progress in the investigation of fracto-emission (FE) from polymers is reported. Measurements characterizing the FE, experiments concerning FE mechanisms, and studies of factors influencing FE are discussed. This work includes: experimental evidence for and presentation of a conceptual model for the charged particle emission mechanisms, studies of electron and positive ion emission from the organic crystal sucrose and from single crystals of RDX. Also included is a review paper on FE from filled and unfilled elastomers.

DD FORM 1 JAN 73 1473

SECURITY CLASSIFICATION OF THIS PAGE (When Data Entered)

TABLE OF CONTENTS

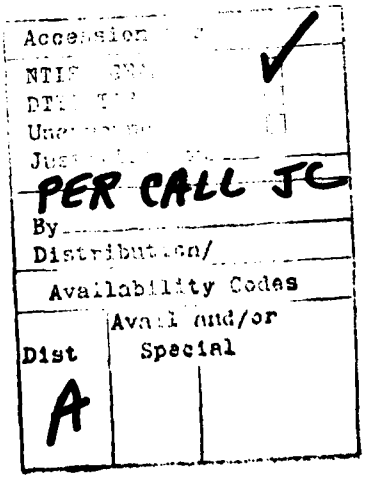

I. TECHNICAL SUMMARY

Crack propagation through an insulating material or at an interface produces regions of high electronic and chemical activity on the freshly-created surfaces. This activity causes the emission of particles, i.e. electrons, ions, and neutral species, as well as photons, from the surfaces both during and after crack propagation. This emission is called fracto-emission (FE), and in many ways serves as a probe of the electronic and chemical activity of the fracture surfaces. The work described in this report represents the results of our third year's research. Our primary goals have been to characterize FE from polymers, to further our understandings of the FE mechanisms, and to examine the dependence of FE on the nature of the fracture event and material properties. In Sections III - VII of this report we present recently written papers on the role of charge separation in producing charged particle emission both during and after fracture, the effect of cross-linking on FE, FE from the fracture of a molecular crystal (sucrose), FE from RDX, and a review paper on FE from filled and unfilled elastomers.

In addition, in Section VIII we present briefly the results of some of our work in progress, which includes:

1. Studies of the neutral emission and charged particle emission from a copolymer of 3,3-bis (azidomethyl) oxetane (BAMO) and tetrahydrofuran (THF),

2. Recent measurements of FE from inert inorganic single crystals, for the purpose of modeling hot spot mechanisms in explosive crystals (in

collaboration with K. C. Yoo, University of Maryland),

3. Recent measurements of FE from filled and unfilled polyurethane (in collaboration with Gene Martin, NWC),

4. Further investigation of FE from interfacial failure between polybutadiene and glass.

II. INTRODUCTION

Fracto-emission (FE) is the emission of particles (e.g. electrons (EE), positive ions (PIE), ground state neutrals (NE), excited state neutrals (NE*), and photons (phE)) during and following fracture. In Sections III - VII of this report we present recent studies of the characteristics of FE, FE mechanisms, and the dependence of FE on material and fracture parameters. These studies deal with fracture of filled and unfilled elastomers, crystalline materials - both organic and inorganic, and interfacial failure between polymers and both dielectrics and metals. Some of our recent results are summarized below:

Section III: FRACTO-EMISSION: THE ROLE OF CHARGE SEPARATION
(Submitted to J. Vac. Sci. Technol.)

Studies of EE and PIE mechanisms have been pursued, and in the systems where strong charge separation occurs we have found a mechanism that explains the intense, long-lasting emission. This model is consistent with a number of other characteristics of FE previously observed. The measurements supporting this model are presented, involving the <u>simultaneous</u> measurements of EE, RE (radiowave emission), and phE (photon emission) versus time for the fracture in vacuum of BR filled with glass beads. These results show that <u>during</u> fracture there are radio waves and accompanying visible photons due to an electrical discharge caused by the strong charge separation <u>and</u> the desorption of volatiles

and/or fracture fragments into the crack tip. This discharge only occurs during crack growth and ceases as soon as the surfaces separate. Thus the RE and the phE rise and fall during and immediately following fracture.

The EE rises with these emissions but then decays with a long tail. Because such emission is most evident where charge separation is strong and a discharge is more likely to occur, we hypothesize that during the discharge the fracture surfaces are bombarded by electrons and ions with relatively high energies. It is this bombardment which is the key stimulus for the EE and PIE which follows fracture.

Section IV: THE EFFECT OF CROSS-LINKING ON FRACTO-EMISSION FROM ELASTOMERS

(Submitted to J. Mater. Sci.)

We have measured the EE and PIE from the fracture of samples of unfilled polybutadiene (BR) (samples provided by Alan Gent, University of Akron) where the cross-link density was varied by changing the concentration of the cross-link agent (dicumyl peroxide). We have plotted the peak and total intensities of EE and PIE as a function of $1/M_c$, where M_c is the number average molecular weight between cross-links in BR. For increased cross-linking, we see an increase in emission. The increase in strength of the material is ultimately leading to more "damage" to the polymer surface.

Section V: ELECTRON AND POSITIVE ION EMISSION ACCOMPANYING FRACTURE OF WINT-O-GREEN LIFESAVERS AND SINGLE-CRYSTAL SUCROSE

(Submitted to J. Phys. Chem.)

We have examined the FE from sucrose and Wint-o-green Lifesavers to

compare fracture of a molecular crystal with the other types of materials studied. These particular materials are known to produce intense triboluminescence in air, and we were curious to see whether they emitted charged particles as well when fractured in a vacuum. The preparation and initial FE studies of single-crystal sucrose and Lifesavers was an undergraduate project carried out by L. B. Brix.

Section VI: FRACTO-EMISSION FROM RDX SINGLE CRYSTALS

(Rough draft. Final manuscript will be submitted to J. Appl. Phys.)

FE from the fracture of explosive crystals has been examined. We were able to observe charged particle emission from the fracture of RDX, a molecular crystal where little covalent bond breaking should occur. The important observation is that such organic molecular crystals do indeed emit charged particles. Furthermore, in RDX we are seeing a correlation between emission intensity and the particular crystal planes undergoing fracture. This could be due to different degrees of surface charging, as previously mentioned.

Section VII: FRACTO-EMISSION FROM FILLED AND UNFILLED ELASTOMERS: REVIEW PAPER

(To appear in Rubber Chemistry and Technology)

A review of FE from filled and unfilled elastomers, written for the ACS Symposium on Frontiers of Rubber Science (Toronto, 1983), is included.

Our work in progress, summarized in section VIII of this report, includes the following:

1. An examination of FE from unfilled BAMO/THF, concentrating on the EE and neutral molecule emission (NE). The unfilled BAMO/THF emits electrons but this emission has a strong strain-rate dependence (more emission at a higher strain rate). The changes in total pressure and mass 28 peaks accompanying fracture of notched samples of BAMO/THF have been examined at two different elongation rates. We observe a substantial increase in both the total pressure and the N_2 released during fracture. Our tentative conclusion is that the NE observed is in part a consequence of fracture-induced decomposition.

2. We have fractured a number of inorganic crystals such as LiF, MgO, and MgF_2 to first show that they emit. We have begun a study of the dependence of FE intensities on crystallographic orientation and have seen some interesting, reproducible differences.

3. We have fractured a few pieces of filled and unfilled polyurethane, and also looked at interfacial failure between this elastomer and inorganic surfaces. The latter leads to very intense EE and PIE.

4. Interfacial failure is believed to be the cause of the intense emission observed in the fracture of filled elastomers. A number of supporting experiments have shown that the likely cause of this increase is the interfacial failure between the polymer and the glass surface. We have recently performed peel tests with macroscopic surfaces of BR (samples provided by Alan Gent, University of Akron) and soda lime plate glass. The strong, long-lasting emission observed from such "fracture"

supports the hypothesis that interfacial failure is responsible for intense emission in the filled materials.

III. FRACTO-EMISSION: THE ROLE OF CHARGE SEPARATION

J. T. Dickinson, L. C. Jensen, and A. Jahan-Latibari
Department of Physics
Washington State University
Pullman, WA. 99164-2814

ABSTRACT

Fracto-emission is the emission of particles (e.g. electrons, ions, ground state and excited neutrals, and photons) during and following fracture. We have found that during fracture of adhesive bonds and crystalline materials involving large amounts of charge separation on the surface, the emission of charged particles, excited neutrals, light, and radio waves occurs with unique and revealing time dependencies. In this paper we report simultaneous fracto-emission measurements on several systems. We interpret the results in terms of a conceptual model involving the following steps: (1) charge separation due to fracture, (2) desorption of gases from the material into the crack tip, (3) a gas discharge in the crack, (4) energetic bombardment of the freshly-created crack walls, and (5) thermally stimulated electron emission, accompanied by electron stimulated desorption of ions and excited neutrals. In addition to evidence from fracture experiments, we present results from studies of electron bombardment of a polymer surface.

I. INTRODUCTION

Fracto-emission (FE) is the emission of particles (e.g. electrons, ions, ground state and excited neutrals, and photons) during and following fracture of materials. In past work we have observed intense, long-lasting emission of electrons (EE) and positive ions (PIE) from systems where high densities of surface charge develop on the fracture surface (see references contained in reference 1). Such systems include: 1) adhesive failure (e.g. peeling of pressure-sensitive adhesives from inorganic substrates, fracture of particulate-filled elastomers, fracture of fiber-reinforced epoxies), 2) fracture of piezoelectric materials such as crystalline SiO_2, sucrose, and polycrystalline PZT, and 3) a number of non-piezoelectric materials which still show intense charge separation, such as LiF, MgO, Al_2O_3, and mica.

In examining the various components of FE from these materials we found it useful to measure simultaneously two or more types of emission on various time scales, to provide further understanding of the emission mechanisms. Some of this work has been previously described for EE and PIE from polybutadiene filled with glass beads. The results previously obtained can be summarized as follows:

1. EE and PIE rise rapidly together during crack propagation, and decay immediately after separation of the fracture surfaces with identical kinetics (2-4).

2. On a submicrosecond time scale, a substantial fraction of the PIE

is in coincidence with the EE (3-5). This suggests that at least some of the electrons emitted are either created simultaneously with positive ions, or more likely, creation of the positive ions is accompanied by inelastically scattered electrons and/or Auger electrons from an ESD-like process (7).

3. There are neutral species emitted from materials undergoing fracture (6). These can be attributed to the release of absorbed species and/or fracture fragments (decomposition).

4. There are also excited neutrals emitted which are correlated in time with the EE (4). We have attributed these metastable molecules to ions neutralized in the process of leaving the surface.

In this paper we would like to report recent results involving simultaneous measurement of EE, photons (phE), and radio waves (RE) accompanying the fracture in vacuum of various materials where strong charge separation occurs. Also, measurements of EE and PIE induced by electron bombardment are presented for one material, polybutadiene. Finally a conceptual model is presented that ties together these new observations and those summarized above.

II. EXPERIMENTAL

The measurements described here were performed on materials fractured in a vacuum of 1×10^{-5} Pa. Samples were fractured either in tension or in three point flexure. The alumina-filled epoxy consisted of one part by weight EPON 828 (Z-hardener) epoxy to three parts of irregularly-shaped alumina particles with an average diameter of 10 μm. The 2mm X 17mm X 45mm samples

were notched with a sharp saw and fractured in tension in front of the detectors. The polybutadiene (BR) consisted of Diene 35NFA (Firestone Tire and Rubber Co.) crosslinked with 0.05% (by weight) dicumyl peroxide by heating for 2 hours at 150 ^{o}C. Some BR samples contained 30-95 μm glass beads (34% by volume). Samples were 2mm X 5mm X 20mm, and were notched slightly in the middle as before. The sucrose crystals were grown by allowing a saturated solution of sugar in water to evaporate for three weeks. These crystals were broken by applying a force perpendicular to the piezoelectric axis. Sucrose and quartz crystals were fractured in flexure. BR for electron bombardment studies consisted of Diene 35NFA dissolved in benzene and allowed to evaporate on a supporting Cu sheet. This resulted in a 0.8 mm thick BR film covering the Cu sheets. The SiO_2 crystals were x-cut disks, 6.5 mm in diameter by 1.2 mm thick, the disk face being the $(\bar{2},1,1,0)$ plane. The fracture surfaces tended to be perpendicular to the disk face.

The electrons were detected with a channeltron electron multiplier (background noise counts ranged from 1 to 10 counts per second). A Bendix BX754A Photon Counter Tube with an S-20 photosensitive surface and background count rate of 10-20 counts per second was used to detect visible photons. The two detectors were generally placed within 1 cm or less from the region where the crack would propagate. Both detectors yielded 10 ns pulses which could be treated with standard pulse counting techniques and stored in a multi-channel analyzer (MCA).

In addition to EE and phE, we detected the emission of radio frequency electromagnetic waves (RE) accompanying fracture in vacuum. RE has been detected previously by Derjaguin, et al. (8) during the separation of polymer films from dielectric surfaces at pressures considerably higher (10^3 -

10^5 Pa) than ours (10^{-5} Pa). The RE was detected using two different pickup coils: a 2.5 mH RF choke coil and a 20000 turn solenoid of No. 30 magnet wire. Either coil was connected to the input of a wide-band differential amplifier with high common mode rejection to minimize pick-up noise, and further amplified by a second amplifier. The response of each coil to a fracture event was a ringing signal with approximate frequencies and duration as follows:

2.5mH choke coil	600 khz	20 μs
20000 turn solenoid	8 khz	1 ms

The solenoid was 5 times more sensitive but because of the higher inductance and thus longer ringing it could only be used to determine the onset of detectable RE or the actual occurrence of RE emission, with approximate values of RE duration. The choke coil allowed more accurate time correlations but with reduced sensitivity.

Two methods of recording RE were used: the choke coil signals were fed into a discriminator, so that rings above a threshold produced pulses which were then counted with an MCA, thereby detecting the presence of bursts of RE as a function of time. The second method, used for the solenoid, consisted of digitizing the coil output with a wave-form digitizer. The rise of the RE ringing signal could then be correlated in time with other FE by the use of synchronized start pulses. Thus within one channel width on the MCA all three FE components could be compared. Previous experiments (2) correlating FE to video recording of crack growth indicated that EE intensity rises rapidly during crack propagation and falls upon separation of the fracture surfaces.

Although it has not been proven conclusively for rapid crack growth, we have assumed that the most intense EE is occurring during crack propagation.

III. RESULTS

The first set of data, shown in Fig. 1, is from the fracture of alumina-filled epoxy. The time scale chosen was in an intermediate range to assure aquisition of all three signals and still provide reasonably good time correlation information. In a separate experiment measuring crack motion in this material with a rotating framing camera, the duration of crack growth was found to be about 20 μs. The data in Fig. 1 was taken at 40 ms per channel and the count rate is plotted on a log scale vs. time. The EE burst occurring during fracture, seen in Fig. 1 as the point where the EE count rate is a maximum, is accompanied by a burst of RE as well as phE. The phE may show a weakly-defined tail; the RE drops off immediately after fracture. The results shown here were reproducible for 10 consecutive samples and show that in a vacuum there is an electrical breakdown occuring during fracture of this filled polymer.

Figs. 2-4 show similar results for polybutadiene (BR) filled with glass beads, single-crystal sucrose, and single-crystal quartz. All show the burst of RE and phE accompanying fracture. The BR and SiO_2 show clear evidence of tails following fracture, which may to a first approximation follow the electron decay in form. Note that for the filled BR we were able to follow phE and EE rising together, due to the much slower crack velocity. Also note that the drop in phE after the peak is for all of these material far more than a simple proportionality relative to the drop in EE; i.e., the phE during

fracture is much more intense than a phE mechanism that remains parallel to an EE mechanism would predict.

As a further test of the occurrence of a discharge during fracture, simultaneous PIE and RE measurements were taken for the fracture of the filled BR using the more sensitive solenoid coil (PIE was measured rather than EE because on faster time scales EE showed evidence of saturating the electron multiplier.). Of primary interest here was the onset of RE relative to the growth of PIE which we know rises with EE during fracture. The time of fracture has been reduced (by increasing the strain rate by approximately a factor of twenty) in order to increase the amplitude of the RE during fracture. The digitized waveform of the RE signal was squared, averaged, and the background subtracted to yield the average power in the ringing RE signal. This result is shown with the corresponding PIE count rate for the filled BR in Fig. 5, where great care has been taken to align the curves correctly in time. The RE is seen to break out of the background noise in the regions of most intense electron emission. The arrows indicate bursts of PIE and RE that are correlated in time. Also, the regions where the PIE is most intense correspond to regions where the RE is highest, where it has been shown (8) that the crack velocity is the highest. Thus, it appears that the RE intensity is velocity dependent also. The primary result here is that we can see RE during a considerable portion of the period in which we observe PIE.

In anticipation of a component of EE possibly produced by bombardment of the fracture surface by charged particles created in a discharge, we performed two experiments on a thick film of BR. At room temperature, the BR was bombarded with with 2 keV electrons at nanoampere currents for 5 minutes. As soon as the electron beam was turned off, a nearby channeltron biased to detect

electrons was turned on. Fig. 6a shows the resulting EE, with a long-lasting decay which is very similar to that of EE induced by fracture. This effect has been extensively studied on crystalline inorganic materials, such as oxides and alkali halides and is known as thermally stimulated electron emission (TSEE)(9). Here we see (to our knowledge for the first time) the same phenomenon, TSEE, at room temperature from a polymer.

Because of our extensive studies of fracture-induced PIE from this material (3,4), we also examined the emission of ions both during and after electron bombardment. For an energy of 2 keV and a current of 5 nanoamperes we see in Fig. 6b the PIE emitted during bombardment, which decays away as soon as the bombardment stops. The ions are not following a parallel mechanism to the EE but are following an ESD mechanism only. Thus we propose that the PIE observed during fracture is due to a portion of the EE which never completely escapes the sample but rather collides with the surface (probably at positive charge patches) and induces ESD of positive ions.

IV. CONCEPTUAL MODEL

At least in the cases illustrated here where significant charge separation occurs during fracture, we feel that the gaseous discharge that we detected using RE and phE is playing a very important role in the production of EE and PIE. In fact, variations in discharge intensity may explain the large variation in intensities observed for a wide range of materials, crack velocities, and other factors. The basic ideas we are proposing are:

1. The fracture event yields charge separation (usually patchy) producing an electric field, E, in the crack.

2. Desorption of volatiles and/or fracture products raises the pressure, P, in the crack tip.

3. A gas discharge (dictated by P, E, and a distance d which characterizes the crack width) occurs, producing the RE and phE. Electron and ion bombardment of the crack walls occurs during this discharge.

4. Bombardment of the fracture surfaces creates primary excitations, usually explained in inorganic crystals in terms of electron-hole production raising electrons into traps near the conduction band, which then undergo thermally stimulated migration until recombination with a hole occurs. This recombination can yield an emitted electron (thermally stimulated electron emission (TSEE)), say by an Auger process, or a photon (thermal luminescence, (TL) (12)).

5. A portion of the electron emission strikes adjacent patches of positive charge yielding PIE via an ESD mechanism. Some of these positive ions are neutralized as they leave the surface yielding the excited neutral component of FE that we have observed.

Consistent with this model are the observations that qualitatively, when charge separation is intense, so are EE and PIE. Secondly, the RE and phE peak intensities (i.e., during fracture) appear to be closely following the same trends. Third, in materials where charge separation is intense but the RE is weak, the EE and PIE tend to be small (e.g. an alkali halide). Fourth, the very close tie between EE and PIE count rates following fracture supports the ESD mechanism. Furthermore, the PIE kinetic energies we observe are often in the hundreds of eV (10,11) suggesting that the PIE originates from positive charge patches. Fifth, coincidence experiments showed that there was a finite probability of detecting an electron in close coincidence with an emitted

positive ion. This electron could be an inelastically scattered electron (creating the ESD excitation) or an accompanying Auger electron expected in the ESD process involving creation of a core hole. Sixth, in the case of sucrose and SiO_2 there is an observable phE decay that follows the EE decay after separation of the fracture surfaces, indicating a parallel de-excitation mechanism, similar to what is observed in TSEE and TL. Finally, the strong increase in EE with crack velocity observed in filled BR would be expected because: a) the surface charge densities may be higher due to the reduced reneutralization through conduction paths, and b) increased gas desorption into the crack tip occurs due to an expected increase in crack tip temperature with crack velocity.

V. CONCLUSIONS

These initial results and this conceptual model allow us to make a number of predictions concerning the dependence of fracture-induced EE on material properties, temperature, and crack velocity. Also, quantitative models relating various FE intensities to measurement of surface charge (measured in vacuum), surface conductivity, and separate TSEE, TSL, and ESD should be possible. We are currently pursuing these and a number of other features of fracture-induced particle emission.

VI. ACKNOWLEDGMENTS

The authors would like to express their gratitude to Alan Gent, University of Akron Institute of Polymer Science for contributing the BR samples and Lydia Brix, a Washington State University physics undergraduate, for growing the sucrose crystals. We also wish to thank B. H. Carroll for assistance in preparing this manuscript. This work was supported by the National Science Foundation, the Office of Naval Research, Sandia National Laboratory, NASA-Ames Resarch Center, and the M.J. Murdock Charitable Trust.

REFERENCES

1. H. Miles and J. T. Dickinson, Appl. Phys. Lett. 41, 924 (1982).

2. J. T. Dickinson and L. C. Jensen, J. Polymer Sci. Polymer Physics Ed. 20, 1925 (1982).

3. J. T. Dickinson, L. C. Jensen, and M. K. Park, J. Mat. Sci. 17, 3173 (1982).

4. J. T. Dickinson, L. C. Jensen, and M. K. Park, Appl. Phys. Lett. 41, 443 (1982).

5. J. T. Dickinson, L. C. Jensen, and M. K. Park, Appl. Phys. Lett. 41, 827 (1982).

6. L. A. Larson, J. T. Dickinson, P. F. Braunlich, and D. B. Snyder, J. Vac. Sci. Technol. 16, 590 (1979).

7. M. L. Knotek and P. J. Feibelman, Phys. Rev. Lett. 40, 964 (1978).

8. B. V. Derjaguin, L. A. Tyurikova, N. A. Krotova, and Y. P. Toporov, IEEE Transactions on Industry Applications IA-14, 541 (1978).

9. J. A. Ramsey, "Exoelectron Emission," in Progress in Surface and Membrane Science 11 (Academic Press, New York 1976) pp. 117-180.

10. J. T. Dickinson, E. E. Donaldson, and M. K. Park, J. Mat. Sci. 16, 2897 (1981).

11. J. T. Dickinson, M. K. Park, E. E. Donaldson, and L. C. Jensen, J. Vac. Sci. Technol. 20, 436 (1982).

12. R. Chen and Y. Kirsh, Analysis of Thermally Stimulated Processes, (Pergamon Press, New York, 1981), pp. 48-52.

FIGURE CAPTIONS

Fig. 1: Simultaneous emission of electrons, photons, and radio waves from the fracture of alumina-filled epoxy.

Fig. 2: Simultaneous emission of electrons, photons, and radio waves from the fracture of polybutadiene filled with small glass beads.

Fig. 3: EE, phE, and RE from the fracture of single-crystal sucrose.

Fig. 4: EE, phE, and RE from the fracture of SiO_2.

Fig. 5: PIE and RE during fracture of filled BR. Note the fast time scale.

Fig. 6: Consequences of electron bombardment on BR: a) EE following bombardment, and b) PIE during bombardment.

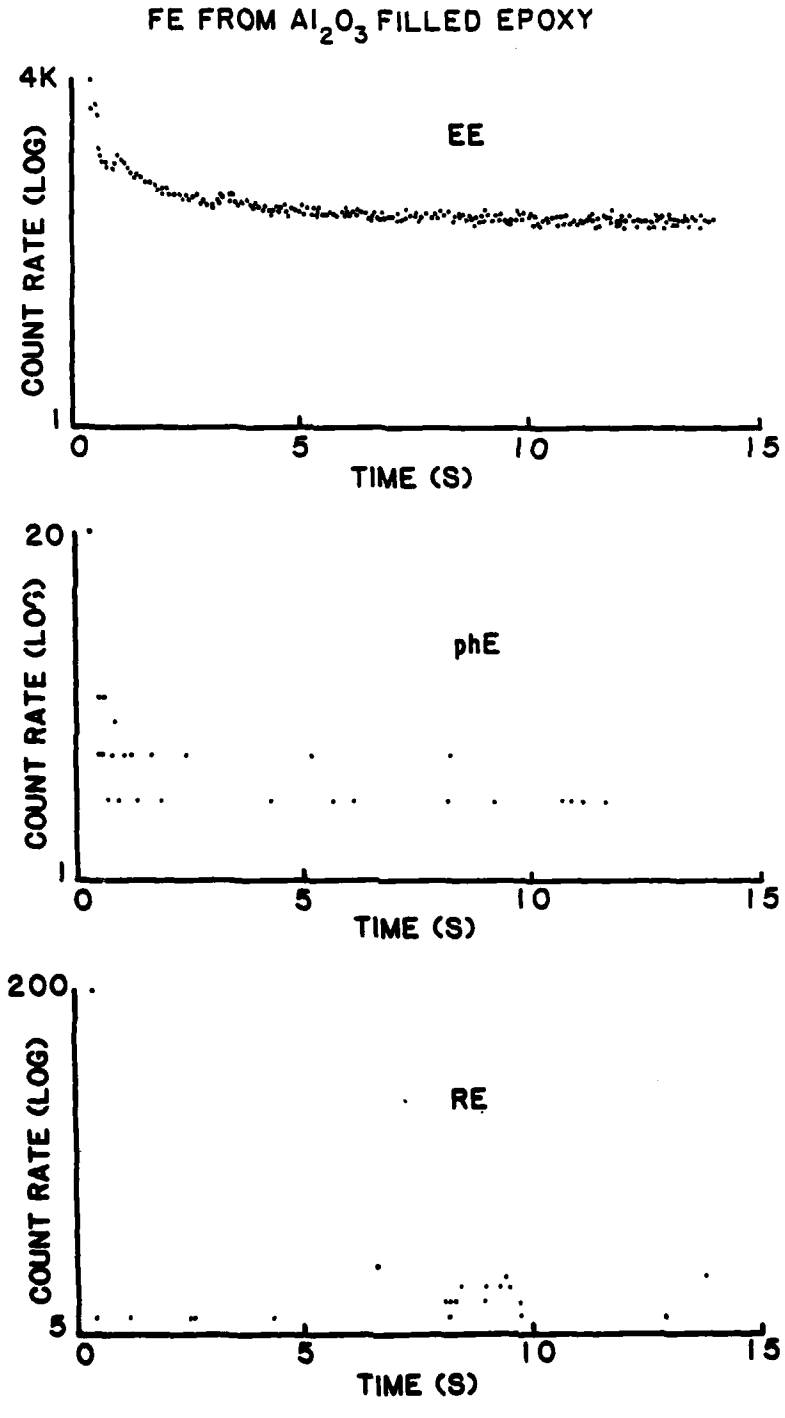
FE FROM Al_2O_3 FILLED EPOXY
4K
1
COUNT RATE (LOG)
EE
0
5
10
15
TIME (S)
20
1
COUNT RATE (LOG)
phE
0
5
10
15
TIME (S)
200
5
COUNT RATE (LOG)
RE
0
5
10
15
TIME (S)

Fig. 1

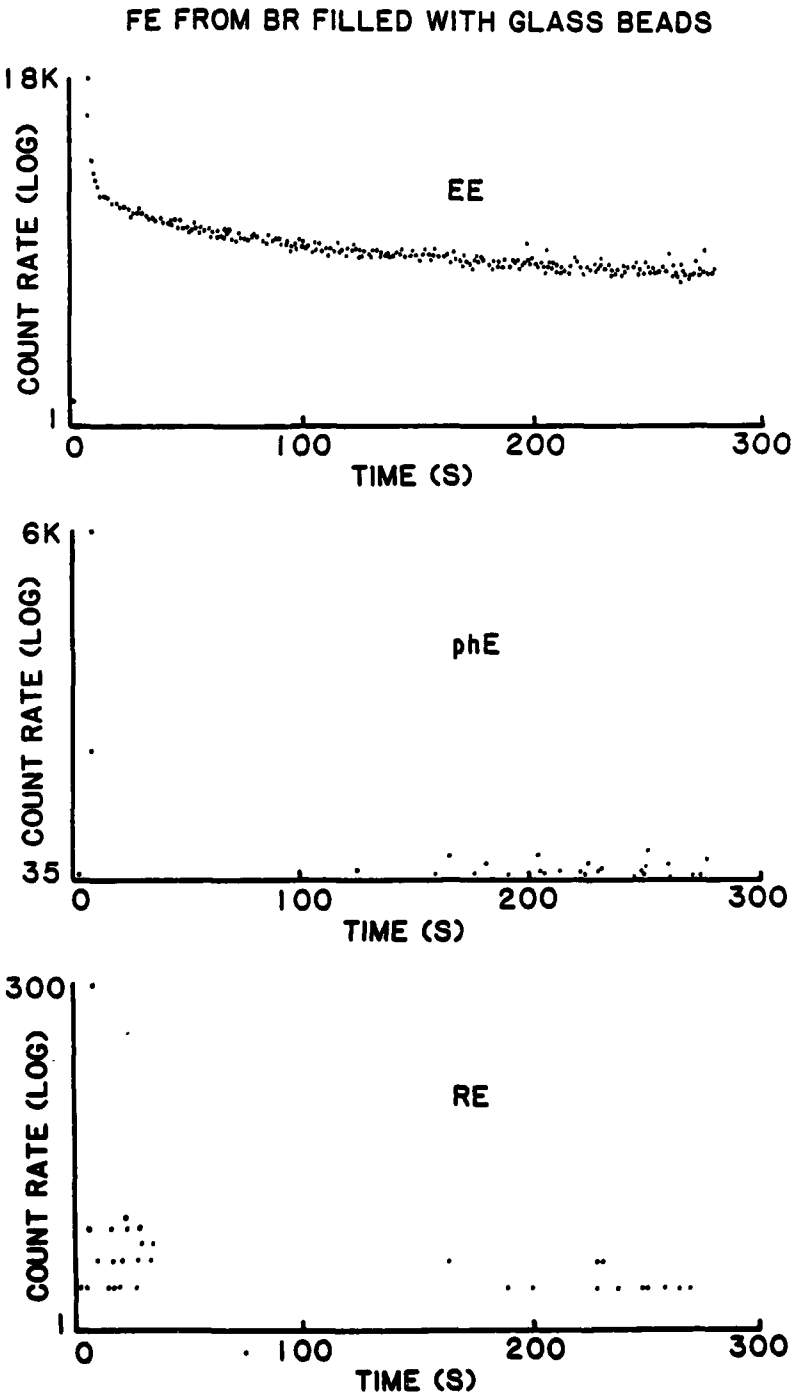
FE FROM BR FILLED WITH GLASS BEADS
18K
1
COUNT RATE (LOG)
EE
0
100
200
300
TIME (S)
6K
35
COUNT RATE (LOG)
phE
0
100
200
300
TIME (S)
300
1
COUNT RATE (LOG)
RE
0
100
200
300
TIME (S)

Fig. 2

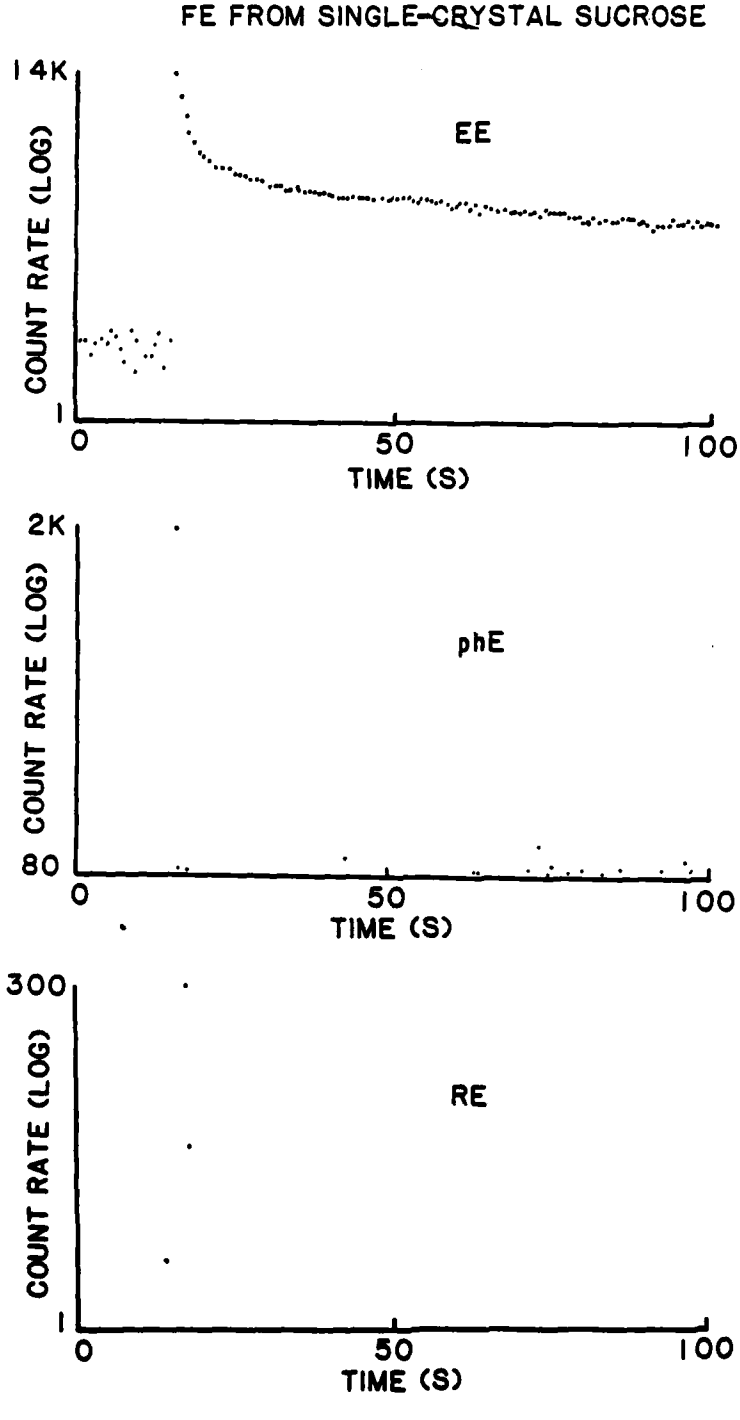
FE FROM SINGLE-CRYSTAL SUCROSE
14K
COUNT RATE (LOG)
EE
1
0
50
100
TIME (S)
2K
COUNT RATE (LOG)
phE
80
0
50
100
TIME (S)
300
COUNT RATE (LOG)
RE
1
0
50
100
TIME (S)

Fig 3

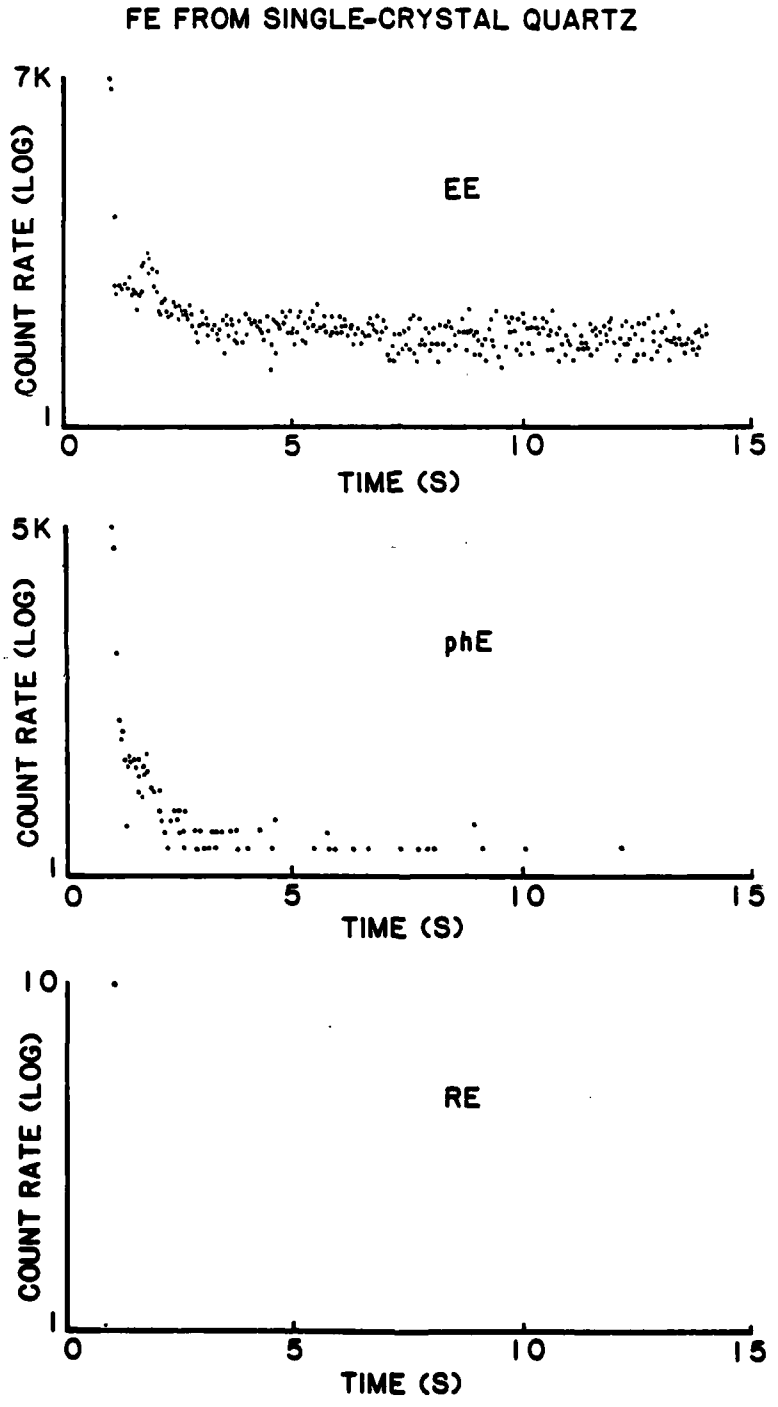
FE FROM SINGLE-CRYSTAL QUARTZ
7K
COUNT RATE (LOG)
EE
1
0
5
10
15
TIME (S)
5K
COUNT RATE (LOG)
phE
1
0
5
10
15
TIME (S)
10
COUNT RATE (LOG)
RE
1
0
5
10
15
TIME (S)

Fig 4

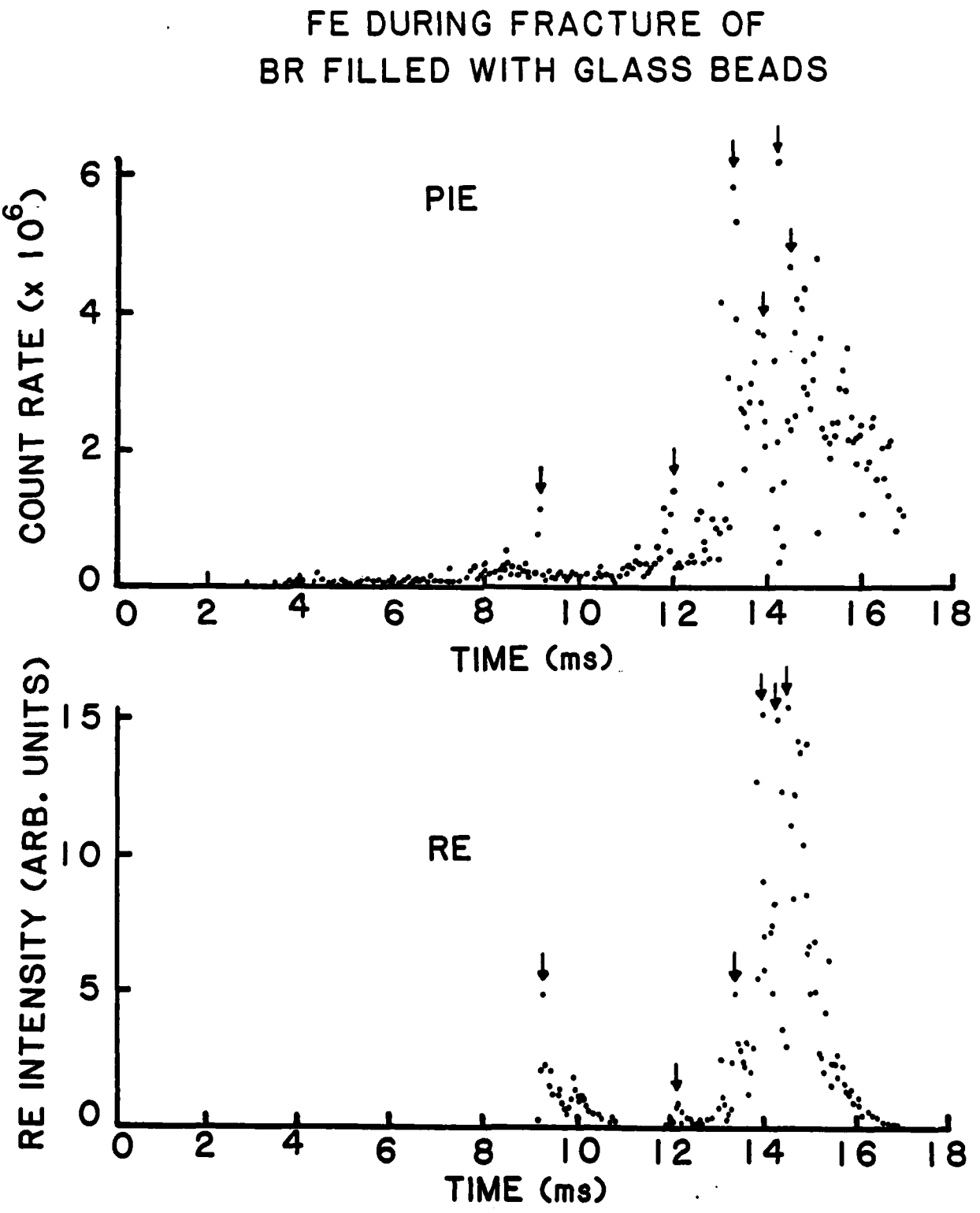
FE DURING FRACTURE OF
BR FILLED WITH GLASS BEADS
PIE
COUNT RATE (x 10^6)
0
2
4
6
0 2 4 6 8 10 12 14 16 18
TIME (ms)
RE
RE INTENSITY (ARB. UNITS)
0
5
10
15
0 2 4 6 8 10 12 14 16 18
TIME (ms)

Fig 5

EFFECT OF ELECTRON BOMBARDMENT OF POLYBUTADIENE

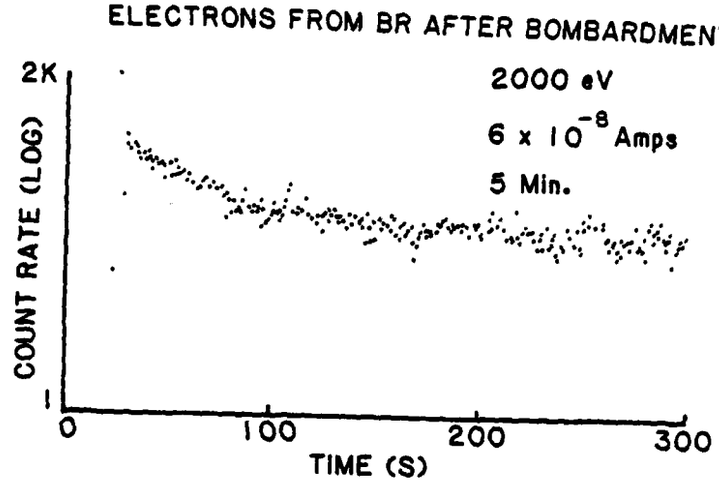

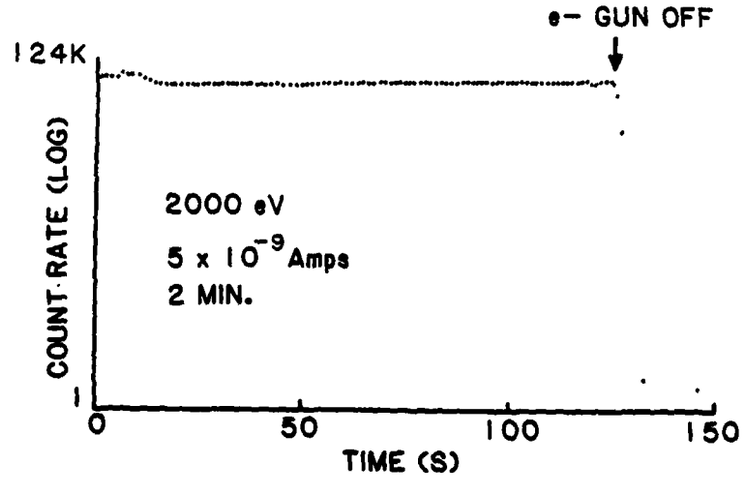

Fig. 6

IV. THE EFFECT OF CROSS-LINKING ON FRACTO-EMISSION FROM ELASTOMERS

J. T. Dickinson, L. C. Jensen, and A. Jahan-Latibari

Department of Physics
Washington State University
Pullman, WA 99164-2814

ABSTRACT

During the fracture of elastomers in vacuum, one frequently observes the emission of particles such as electrons, ions, neutral molecules, and photons, which we call Fracto-Emission. We report here measurements of electron emission and positive ion emission accompanying and following the fracture of polybutadiene (BR) and a styrene-butadiene co-polymer (SBR), where the degree of cross-linking has been altered either by varying the concentration of the cross-linking agent or by exposure of the material to UV or γ-ray radiation. Our results show that over the range of cross-link densities studied, both electron and positive ion emission increase with increasing cross-link density.

I. INTRODUCTION

Crack propagation through an insulating material or at an interface produces regions of high electronic and chemical activity on the freshly-created surfaces. This activity causes the emission of particles, i.e. electrons, ions, and neutral species, as well as photons, from the surfaces both during and after crack propagation; we call this emission fracto-emission (FE) (Photon emission during deformation and/or crack propagation is often called triboluminescence). The work presented in this paper will focus on electron emission (EE) and positive ion emission (PIE) induced by the fracture of elastomers in a vacuum.

Although a considerable portion of our work has concentrated on the fracture of filled elastomers (1-7), where interfacial failure yields extremely high emission rates, we have also investigated a number of unfilled materials. A summary of electron emission (EE) and positive ion emission (PIE) data, as presented in Table I, shows that these elastomers produce EE and PIE with a wide range of intensities and durations (decay times) of the emission following fracture. None of the unfilled materials show intensities that match the filled materials. The intense emission accompanying interfacial failure has been attributed (8) to the strong separation of charge that occurs due to contact charging between dissimilar materials.

In unfilled systems we suspect that the same mechanism could be responsible, but with weaker degrees of charge separation and reduced discharge, and thus less EE and PIE. However, the role of mechanical deformation and the scission of bonds in a unfilled polymer which would produce

this charge separation is not clearly understood.

The conceptual model we have presented (8) for the fracture-induced particle emission in cases where strong charge separation occurs can be summarized as follows:

1. The fracture event yields charge separation (usually patchy) producing an electric field, E, in the crack.

2. Desorption of volatiles and/or fracture products raises the pressure, P, in the crack tip.

3. A gas discharge (dictated by P, E, and a distance d which characterizes the crack width) occurs, producing radio wave emission (RE) and phE. Electron and ion bombardment of the crack walls occurs during this discharge.

4. Bombardment of the fracture surfaces creates exo-emission, usually understood in inorganic crystals in terms of electron-hole production raising electrons into traps near the conduction band, which then undergo thermally stimulated migration until recombination with a hole occurs. This recombination can yield an emitted electron (thermally stimulated electrom emission (TSEE) (9,10)), say by an Auger process (10), or a photon (thermoluminescence (TL) (9)).

5. A portion of the electron emission strikes adjacent patches of positive charge yielding PIE via an electron stimulated desorption (ESD) mechanism (12). Some of these positive ions are neutralized as they leave the surface, yielding the excited neutral component of FE that we have observed.

For crystalline materials that are known to be piezoelectric, e.g. SiO_2, PZT, and sucrose we were not surprised to detect the simultaneous emission of electrons (EE), photons (phE), and radiowaves (RE) during fracture - clear evidence for the occurrence of a gaseous discharge in the crack tip during fracture. We were also able to induce the EE by pre-bombardment with energetic electrons in unfilled, unfractured BR. This and other evidence supports the above model for materials exhibiting strong charge separation during fracture.

Unfilled elastomers could produce separated charges, most likely patchy, during fracture and yield the same effects at lower intensities due to weaker discharges occuring in the crack tip. For patches of both signs and of small dimensions, post-fracture probing of surface charge may yield nearly neutral results, making the charge separation difficult to detect. Nonetheless, we have recently detected both RE and phE during fracture of unfilled polybutadiene, supporting the idea that a discharge indeed occurs.

Presumably, the degree of charge separation should indeed be sensitive to the mechanical properties of the elastomers, namely that more rigid networks of cross-links would result in higher local stresses prior to fracture (inducing more charge separation) as well as the breaking of a larger number of principal bonds during fracture which may also contribute to charge separation. Thus in a more highly cross-linked material we might expect greater surface charging which in turn would cause a more intense discharge and result in more intense emission.

In this paper, we explore for the first time the possible influence of cross-link density on EE and PIE intensities during and following fracture of elastomers, where variations in cross-link densities were made by changing the

concentrations of the cross-linking agent and by exposure of the elastomers to UV and γ-radiation.

II. EXPERIMENTAL PROCEDURE

The materials used in this study were polybutadiene (BR) and a co-polymer of styrene-butadiene (SBR). Most of the samples used in this experiment were provided by The University of Akron, Institute of Polymer Science. The BR samples consisted of Diene 35 NFA, Firestone Tire and Rubber Co., mixed with dicumyl peroxide from 0 to 0.075% by weight.

The sample designations and the corresponding peroxide concentrations are as follows;

BR-0	0.000%
BR-1	0.025%
BR-2	0.050%
BR-3	0.075%
SBR-1	0.1%
SBR-2	0.2%

The SBR was made in the ratio of 25/75 styrene-butadiene (SBR 1502 Firestone Tire and Rubber Co.) with 0.1% dicumyl peroxide resulting in a very weak cross-linking and with 0.2% dicumyl peroxide showing increased cross-linking. Cross-linking was carried out by heating each mixture for 2 hours at 150 °C. For BR-0, the Diene 35 NFA was simply pressed and heated at 100 °C for 1 minute, which produced a very weakly cross-linked material.

As an additional means of varying the cross-link density, BR and SBR

samples were exposed to UV and γ-radiation. The UV source was a laboratory Hg lamp rich in 2500 Å light. Although UV intensities were not measured, all exposures were done at constant distance (20 cm) for 24 hours. The γ-radiation was from a calibrated 3000 Curie ^{60}Co source and exposures were again for 24 hours. The cross-link density was determined by swelling measurements in benzene using a technique described by Mullins and Mason (13).

The experiments were performed in vacuum at a pressure of 1×10^{-5} Pa. The vacuum system was equipped with a stress-strain device. The samples were supported in the pulling (tension) mechanism in clamps with an initial separation of 6 mm. The cross-section of these samples was 2 mm x 4.5 mm. The top edge of each sample was notched in the center so that the crack propagated in the vicinity of the detector. Samples were all elongated at a rate of 10% per second. The detectors used for charged particles were Channeltron Electron Multipliers (CEM) which produce a fast (10ns) pulse per incident particle with approximately 90% absolute detection efficiency for electrons and nearly 100% efficiency for positive ions with a gain of 10^6 to 10^8 electrons/incident particle. The detector was positioned about 2 cm away from the sample. The front of the CEM was biased with +300 or -2500 volts to attract electrons or positive ions, respectively. Background noise counts ranged from 1 to 10 counts per second. Standard nuclear physics data acquisition techniques, using a micro-computer based multichannel analyzer, were employed to acquire and store the emission data.

III. RESULTS

The results of EE and PIE measurements from the fracture of BR with

various concentrations of dicumyl peroxide are shown plotted on a log scale in Figs. 1 and 2. A comparison of both EE and PIE from different samples indicates the influence of the cross-linking agent and therefore cross-link density (CLD) on the emission. Both EE and PIE increase with the addition of more dicumyl peroxide. The data for EE measurements from the 0% dicumyl peroxide BR (BR-0) are also included in Fig. 1. We could not see any PIE from BR-0 samples, and the EE was relatively low. Variations in emission from sample to sample of BR-1 were quite high, about 50%. More consistency was observed for samples of BR-2 and BR-3, with variations of about 20%.

Fig. 3 shows the dependence of EE and PIE at fracture, i.e., the peak count rate, and the total emission (for equal time intervals of 400 seconds) on $1/M_c$ where M_c is the number average molecular weight between cross-links of BR. The CLD is proportional to $1/M_c$. It is clear from these curves that for this substance, increasing CLD yields noticeably more EE and PIE at fracture, which is particularly evident in the total emission curves. It should be noted that in these samples the CLD was not varied over a very large range.

The change in fracture behavior with increased CLD for notched samples strained at constant strain rate is evident in the observed rise in EE or PIE, which from previous measurements indicates the rate of crack growth and time required to fracture (2). The curves shown in Figs. 4a and 4b have been shifted and normalized so that the peak emission rates coincide for BR-1 and BR-3 for four diferent samples. One can easily see the effect of increased CLD on the fracture; BR-3 is fracturing considerably faster. Qualitatively, this can be understood from the fact that as stress is applied to a rubber sample, the shorter chains reach a breaking point before the longer chains. At higher

CLD, network chains become shorter and less extensible and hence prone to rupture before appreciable reorientation of the network as a whole occurs. On the other hand, at a low CLD it has been proposed that plastic flow of the chains is high. Therefore at low CLD the plastic deformation is high and thus it takes longer for the sample to break, while at high CLD the sample fractures in a more brittle manner.

The effect of irradiation of elastomers on EE alone is shown in figures 5-8 for BR-2 and SBR-1, which were strained at the slower rate of 5% per second (the changes in intensity and shape for BR-2 with and without UV irradiation were relatively small so they are not shown). Note that the irradiated materials have higher peak intensities and more emission after fracture, similar to the changes induced by variation in dicumyl peroxide content. Table II summarizes the measured emission totals amd $1/M_c$ values for these materials before and after irradiation. In these cases, the irradiated material shows the evidence of increased brittleness by yielding EE at earlier times, i.e. the crack started moving at a lower strain (see Figs. 5-7).

The most dramatic change in EE with irradiation is for the BR-0, which is shown in Fig. 8, yielding an increase in emission of up to 100 times. The cross-link densities of the irradiated BR-0 were not measured, but the exposed samples were considerably stronger, indicating an increased number of linkages over the weakly cross-linked BR-0.

IV. DISCUSSION

The results we have presented here clearly indicate that increasing CLD produces changes in the intensities and time dependence of the EE and PIE

accompanying fracture of these elastomers.

The time dependence effects observed are due to the influence of cross-linking on the time dependence of fracture at constant strain rates, namely the more brittle nature of crack motion with increasing CLD.

An explanation of the changes in intensity with CLD, which can be quite dramatic as shown for BR-0, demand a detailed understanding of the FE mechanisms in unfilled elastomers. We have implied in the introduction that localized charge separation occuring during fracture may be playing a crucial role even in "homogeneous" polymers. In fact we have recently detected RE and phE during fracture of BR-2, indicating that a discharge is occurring. We suggest that this in turn leads to or at least enhances EE and PIE because of the bombardment of the fracture surfaces by charged particles created in the discharge. Why BR should exhibit the charge separation necessary to yield breakdown is not clear. A piezoelectric effect is one likely candidate for the initial cause of charge separation. Wada (14) states that most polymers can exhibit piezoelectricity due to the presence of certain impurities or embedded charges in the bulk material. In addition, the fracture process itself, i.e. the breaking of bonds, may lead to charge separation due to some asymmetry in the electron clouds associated with the molecules undergoing scission, i.e. a non-adiabatic process. At this point, however, we cannot really distinguish between these possible causes nor provide details of the charge separation process.

V. CONCLUSIONS

The relationship between CLD and fracto-emission intensity has been

examined for unfilled BR and SBR. A clear increase in intensity with increasing CLD was observed. Previous results on systems exhibiting strong charge separation (including BR filled with glass beads) have indicated that particle bombardment during fracture is responsible for the resulting EE and PIE. The same mechanism may be involved in unfilled materials. This suggests that, on a local scale at least, charge separation is occurring in "homogeneous" elastomers. Although the cause of such charge separation in BR and SBR is not at this time fully understood, we have demonstrated that FE is sensitive to the microstructure and fracture-dependent properties of the material.

VI. ACKNOWLEDGEMENTS

We wish to thank Dr. A. N. Gent, University of Akron Institute of Polymer Science, for providing us with the samples of BR and SBR. We also thank E. E. Donaldson for helpful discussions. This work was supported by the Office of Naval Research, contract N0014-80-C-0213, and by a grant from the M. J. Murdock Charitable Trust.

REFERENCES

1. J. T. Dickinson, E. E. Donaldson, and M. K. Park, J. Mat. Sci. 16, 2897 (1981).

2. J. T. Dickinson and L. C. Jensen, J. Polymer Sci. Polymer Physics Ed. 20, 1925 (1982).

3. J. T. Dickinson, M. K. Park, E. E. Donaldson, and L. C. Jensen, J. Vac. Sci. Technol. 20, 436 (1982).

4. J. T. Dickinson, L. C. Jensen, and M. K. Park, Appl. Phys. Lett. 41, 443 (1982).

5. J. T. Dickinson, L. C. Jensen, and M. K. Park, Appl. Phys. Lett. 41, 827 (1982).

6. J. T. Dickinson, to appear in Adhesive Chemistry - Developments and Trends, L. H. Lee, Ed. (Plenum, New York).

7. J. T. Dickinson, L. C. Jensen, and A. Jahan-Latibari, to be published in J. of Rubber Chemistry and Technology.

8. J. T. Dickinson, L. C. Jensen, and A. Jahan-Latibari, submitted to J. Vac. Sci. and Technol.

9. R. Chen and Y. Kirsh, Analysis of Thermally Stimulated Processes, pp. 48-52 (Pergamon Press, New York, 1981).

10. J. A. Ramsey, "Exo-emission," in Progress in Surface and Membrane Science 11, pp. 117-180 (Academic Press, New York, 1976).

11. H. D. Hagstrum, in Inelastic Ion-Surface Collisions, edited by N. H. Tolk, J. C. Tully, W. Heil and C. W. White (Academic Press, New York, 1977).

12. M.L. Knotek, in Proceeding of the International Conference on X-Ray and Atomic Inner-Shell Physics "X-'82", AIP Conference Proceedings 94, 772 (1982).

13. L. Mullins and A. G. Mason, "The Chemistry and Physics of Rubber-Like Substances," L. Bateman, Ed., pp. 144-153 (John Wiley and Sons, 1963).

14. Y. Wada, "Electronic Properties of Polymers," edited by J. Mort and G. Pfister, pp. 109-160 (John Wiley and Sons, 1982).

LIST OF TABLES

TABLE I.

ELECTRONS

Material	Approx. Decay Times of Fracto-Emission	Ions Detected/ cm of Crack Wall
Neoprene	<1 s	10^2
Viton	<1 s	10^3
Buna N	<1 s	10^2
Natural Rubber	<1 s	10^3
Natural Rubber (abraded)	Minutes	10^7
Silicone Rubber	<1 s, minutes	10^5
Solithane	<.2 s	10^4
Vinyl Rubber (filled)	<1 s, minutes	10^4
Polybutadiene	0.04 s, minutes	10^3
Polybutadiene (filled)	<1 s, minutes	10^7
Nylon-66	<1 s	10^4
Isoprene	<1 s	10^6
Amber Rubber	<1 s	10^5
BAMO	<1 s	10^4

POSITIVE IONS

Material	Approx. Decay Times of Fracto-Emission	Ions Detected/ cm^2 of Crack Wall
Buna N	<1 s, minutes	10^3
Natural Rubber	<1 s	10^4
Natural Rubber (abraded)	Minutes	10^7
Silicone Rubber	<1 s, minutes	10^3
Solithane	<.1 s	10^6
Vinyl Rubber (filled)	<1 s, minutes	10^5
Polybutadiene	<.04 s, minutes	10^5
Polybutadiene (filled)	<.2 s, minutes	10^6
SBR - filled	<1 s	10^6

Table II

Material	Avg. Total EE	$1/M_c$
SBR-1	23000	0.00024
SBR-1 (UV-irradiated)	27000	0.00029
SBR-1 (-irradiated)	38000	0.00110
BR-2	35000	0.00100
BR-2 (UV-irradiated)	53000	0.00160
BR-2 (-irradiated)	84000	0.00500

FIGURE CAPTIONS

Fig. 1: Electron emission vs. time for Polybutadiene cross-linked with varying concentrations of dicumyl peroxide.

Fig. 2: Positive ion emission vs. time for Polybutadiene cross-linked with varying concentrations of dicumyl peroxide.

Fig. 3: EE and PIE vs. $1/M_c$, where M_c is the number average molecular weight between cross-links, and where $1/M_c$ is proportional to cross-link density.

Fig. 4: a) EE vs. time, and b) PIE vs. time for fracture of samples of BR with different cross-link densities, during fracture.

Fig. 5: EE for BR-2 with and without exposure to γ-radiation.

Fig. 6: EE for SBR-1 with and without exposure to γ-radiation.

Fig. 7: EE for SBR-1 with and without exposure to UV radiation.

Fig. 8: EE for BR-0 with and without exposure to UV and γ-radiation.

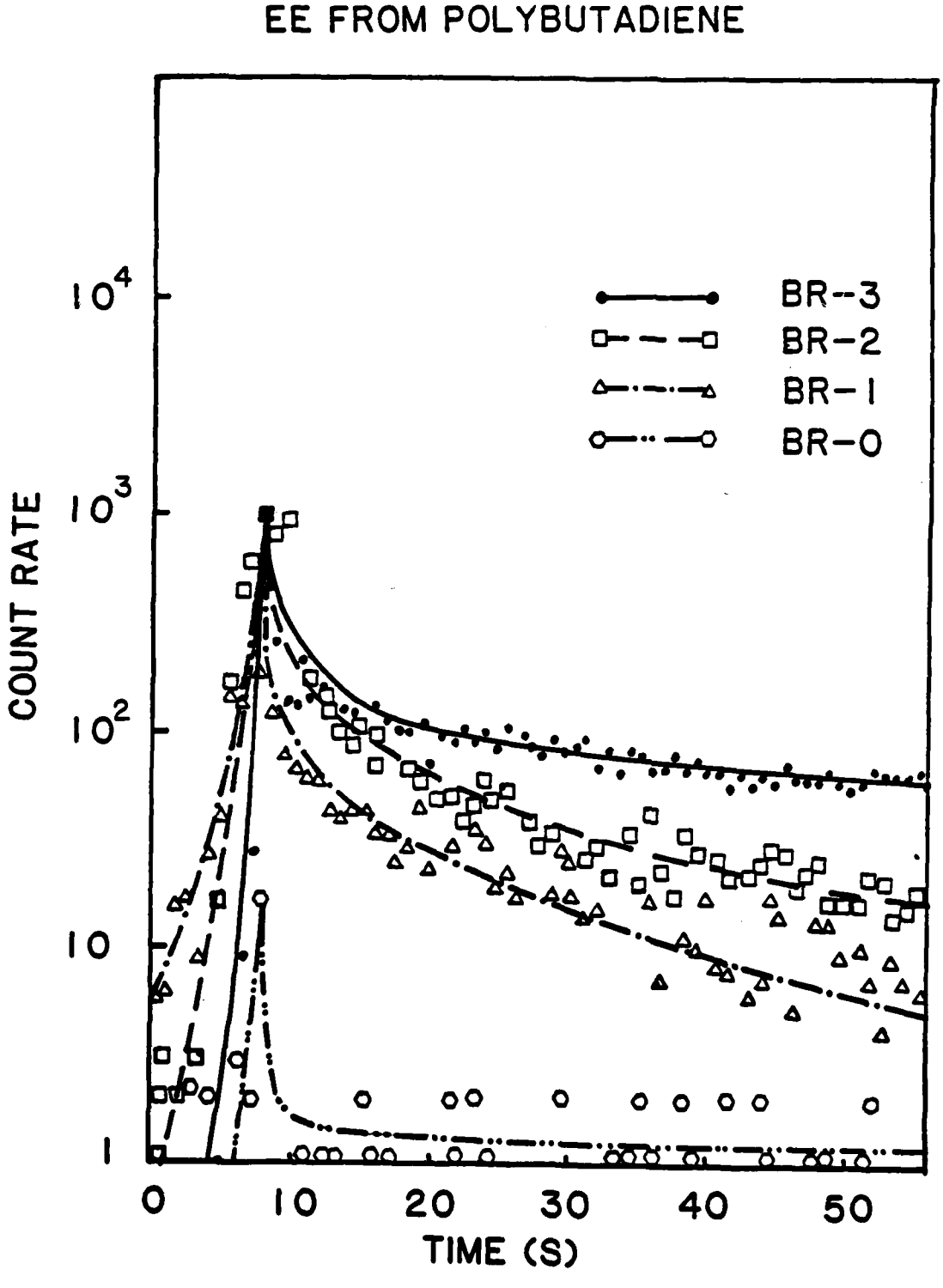
EE FROM POLYBUTADIENE
BR--3
BR-2
BR-1
BR-0
COUNT RATE
10^4
10^3
10^2
10
1
0
10
20
30
40
50
TIME (S)

Fig 1

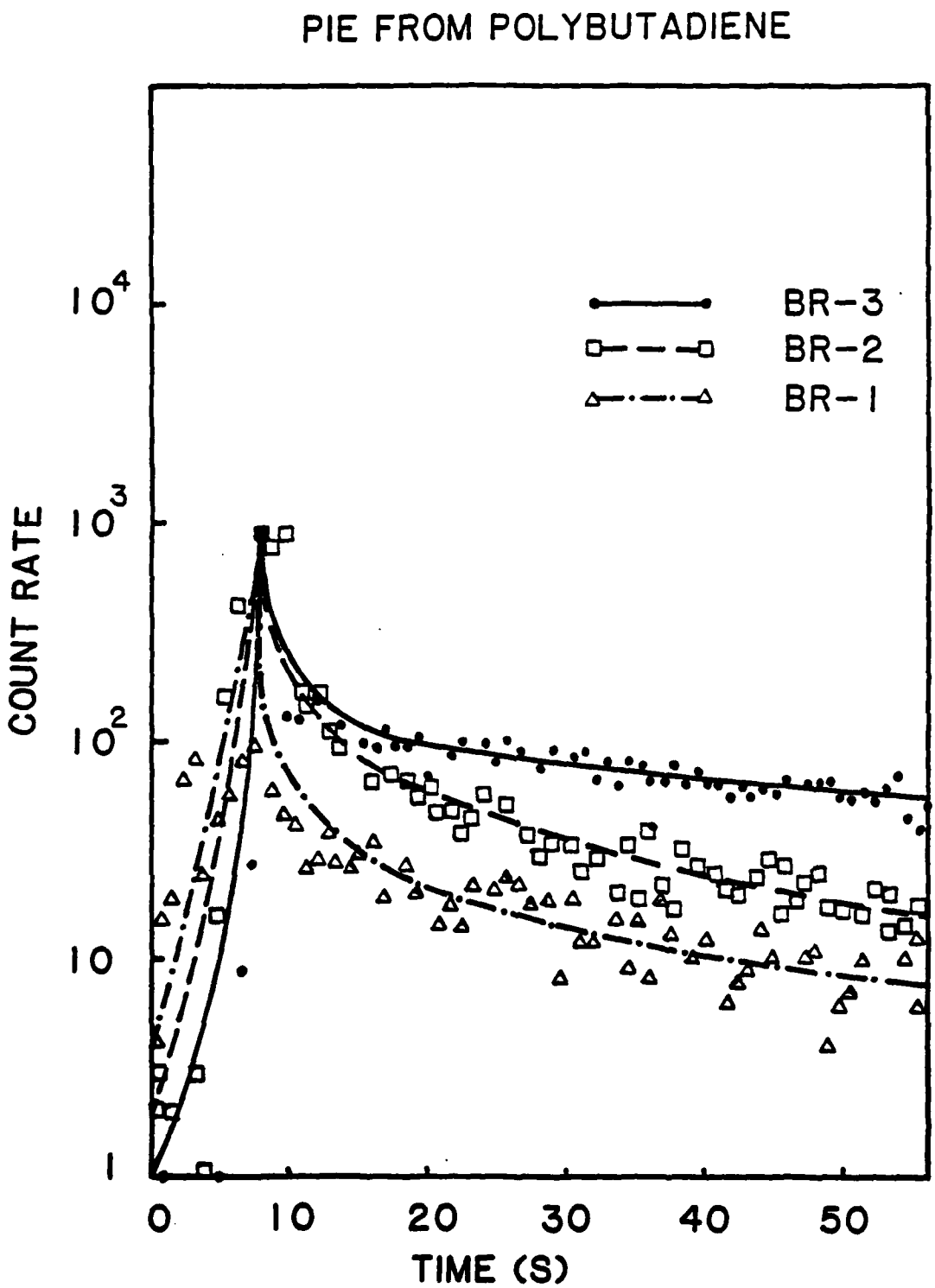
PIE FROM POLYBUTADIENE
BR-3
BR-2
BR-1
COUNT RATE
10^4
10^3
10^2
10
1
0
10
20
30
40
50
TIME (S)

Fig 2

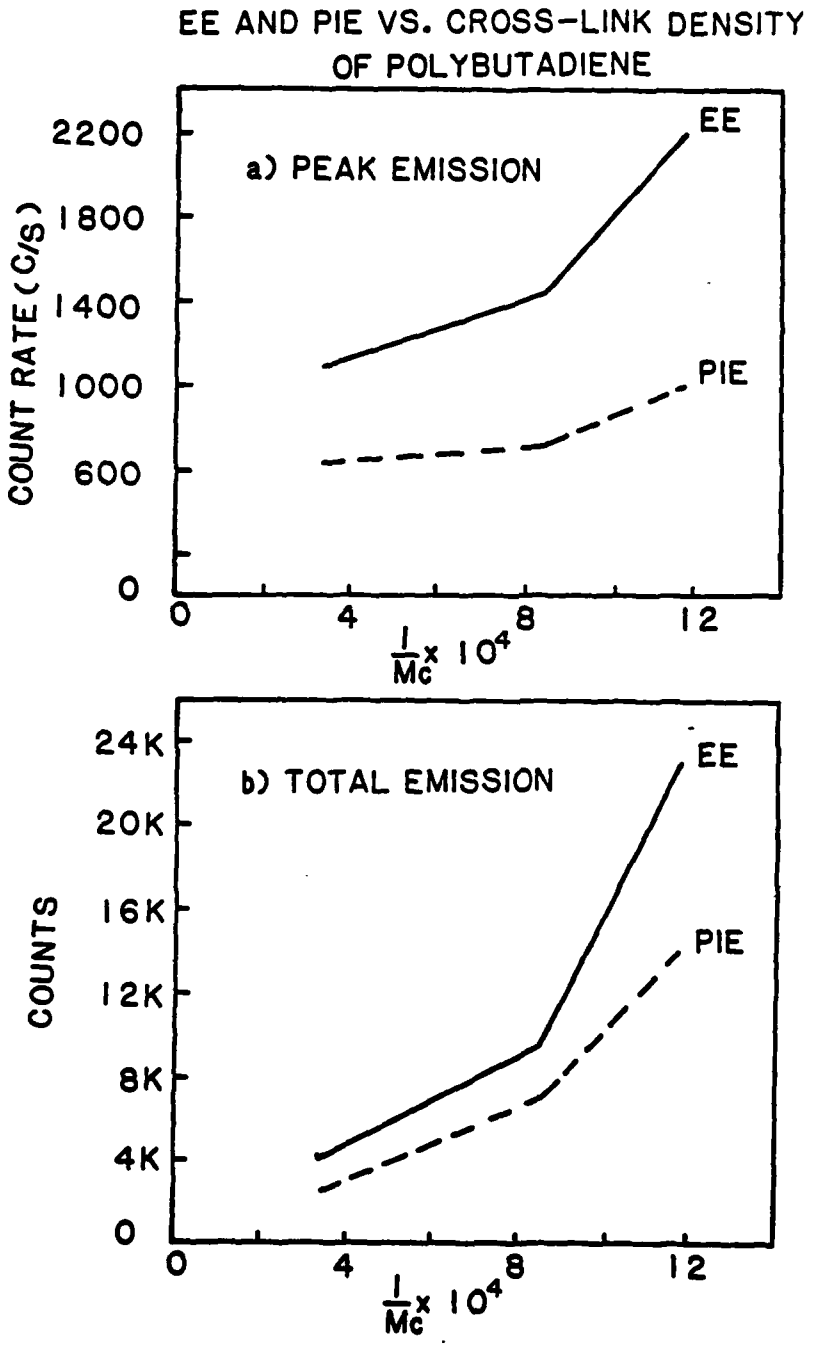
EE AND PIE VS. CROSS-LINK DENSITY
OF POLYBUTADIENE
a) PEAK EMISSION
EE
PIE
COUNT RATE (C/S)
2200
1800
1400
1000
600
0
0
4
8
12
1/Mc x 10^4
b) TOTAL EMISSION
EE
PIE
COUNTS
24K
20K
16K
12K
8K
4K
0
0
4
8
12
1/Mc x 10^4

Fig 3

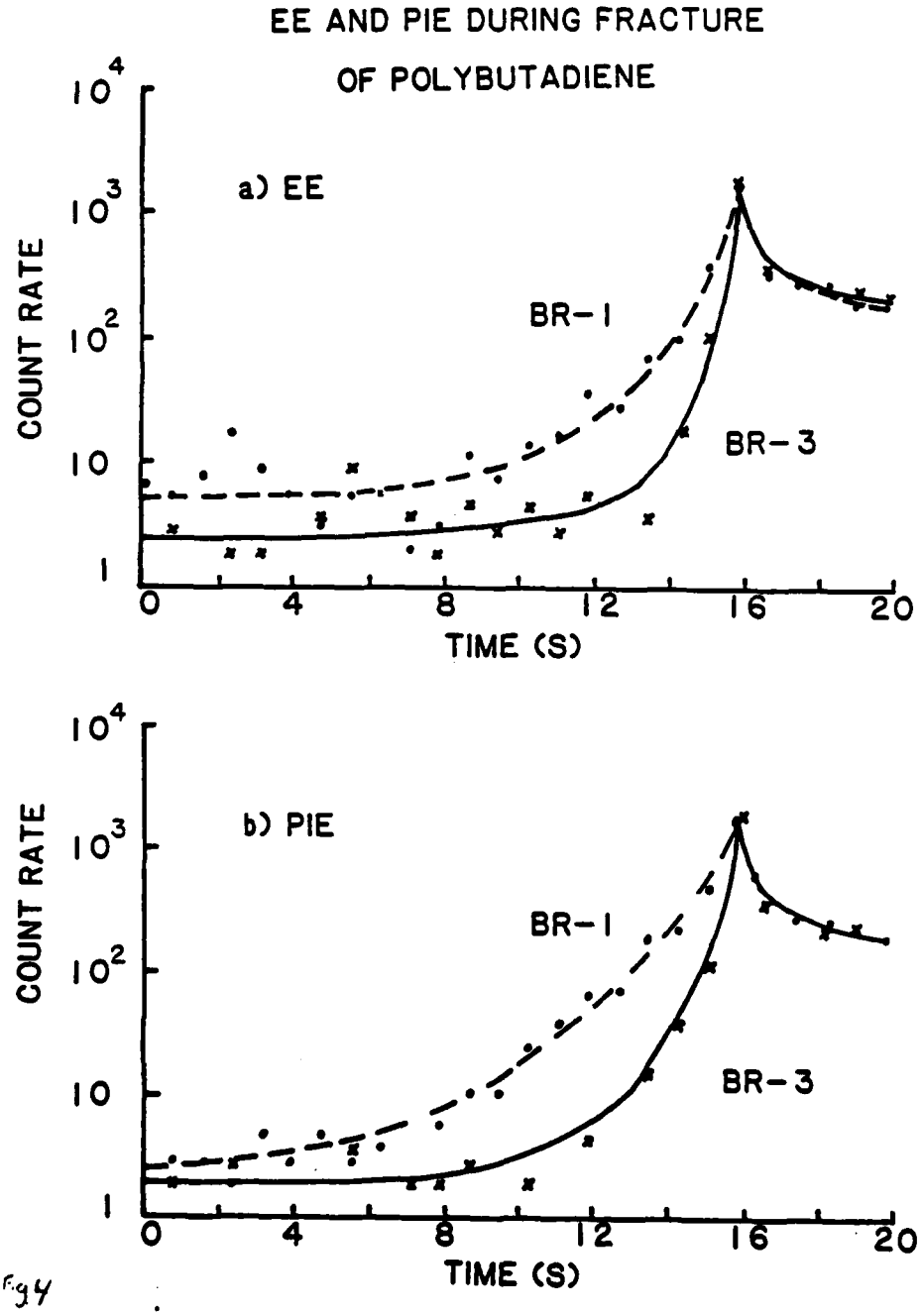
EE AND PIE DURING FRACTURE
OF POLYBUTADIENE
a) EE
b) PIE
BR-1
BR-3
COUNT RATE
TIME (S)
10^4
10^3
10^2
10
1
0
4
8
12
16
20

Fig 4

E E FROM POLYBUTADIENE

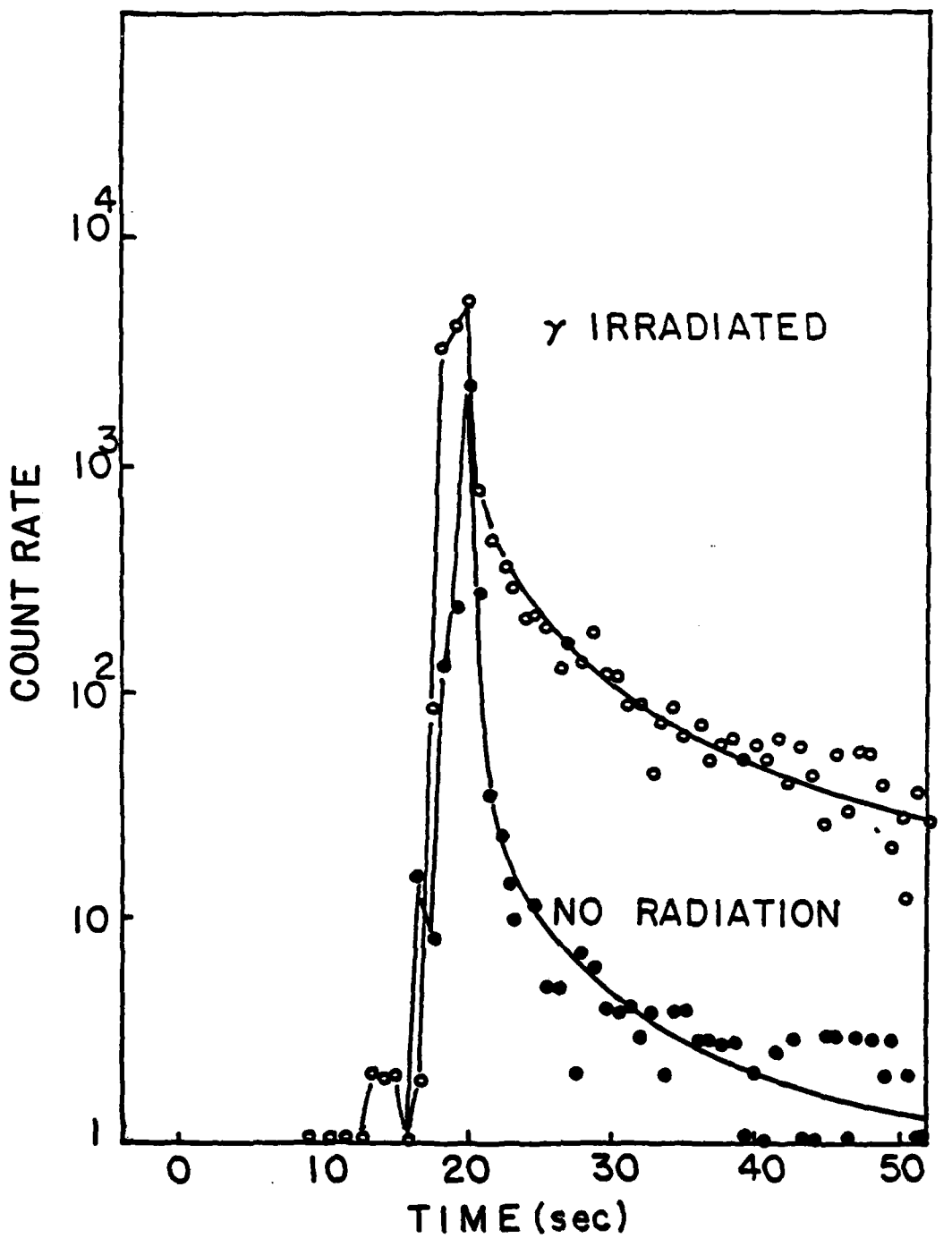

Fig. 5

EE FROM BUTADIENE-STYRENE CO-POLYMER

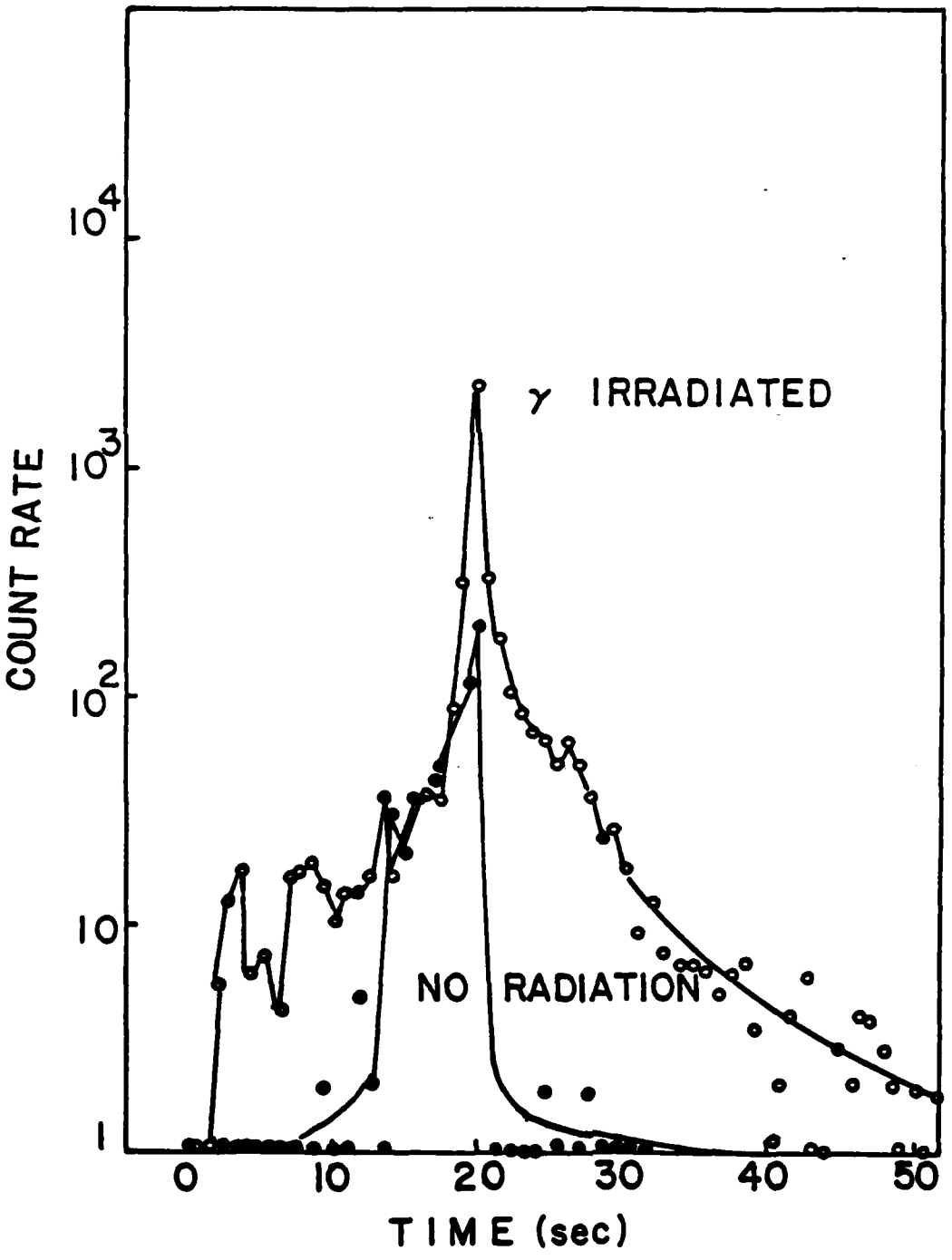

Fig. 6

EE FROM BUTADIENE-STYRENE CO-POLYMER

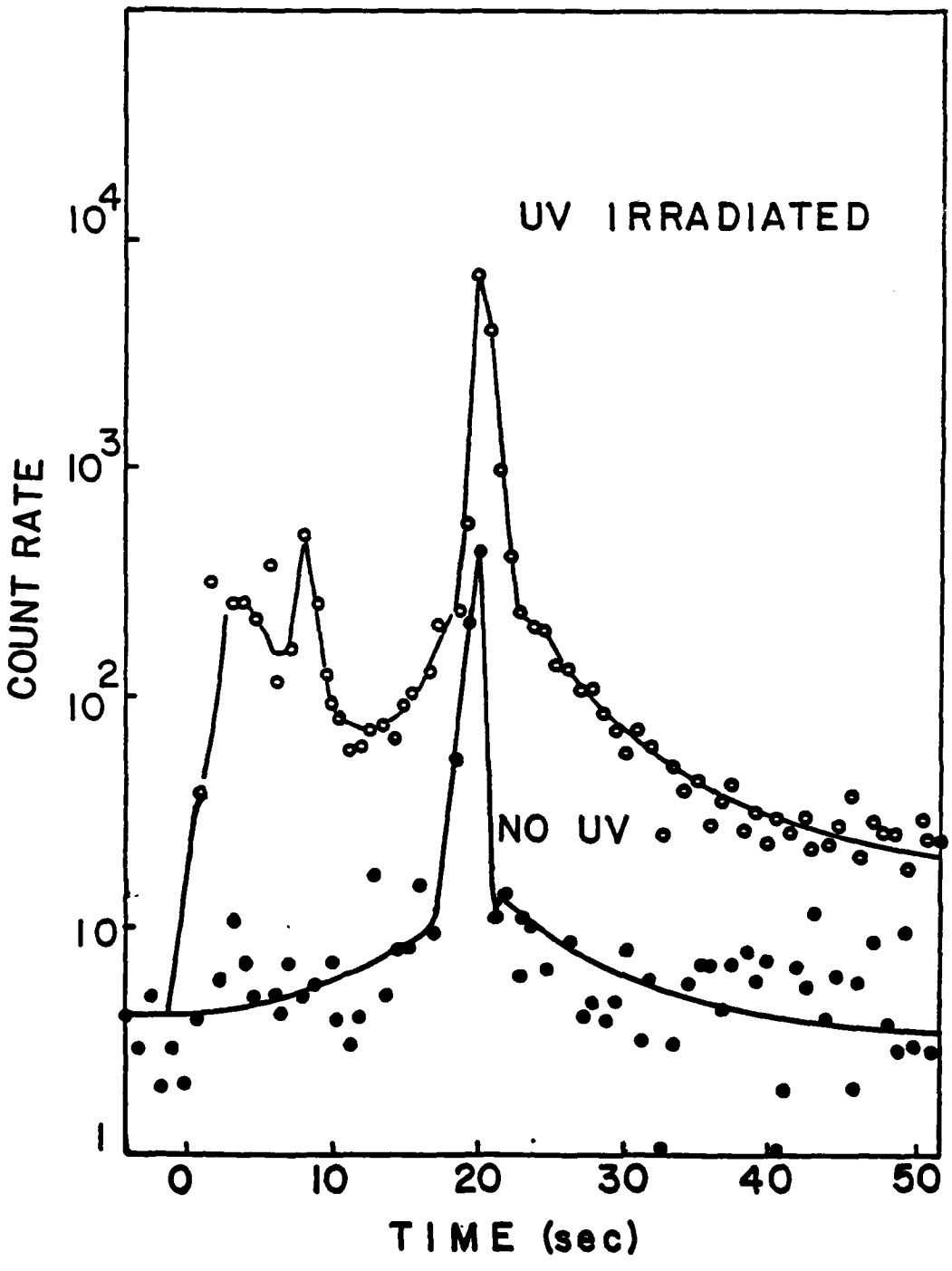

Fig. 7

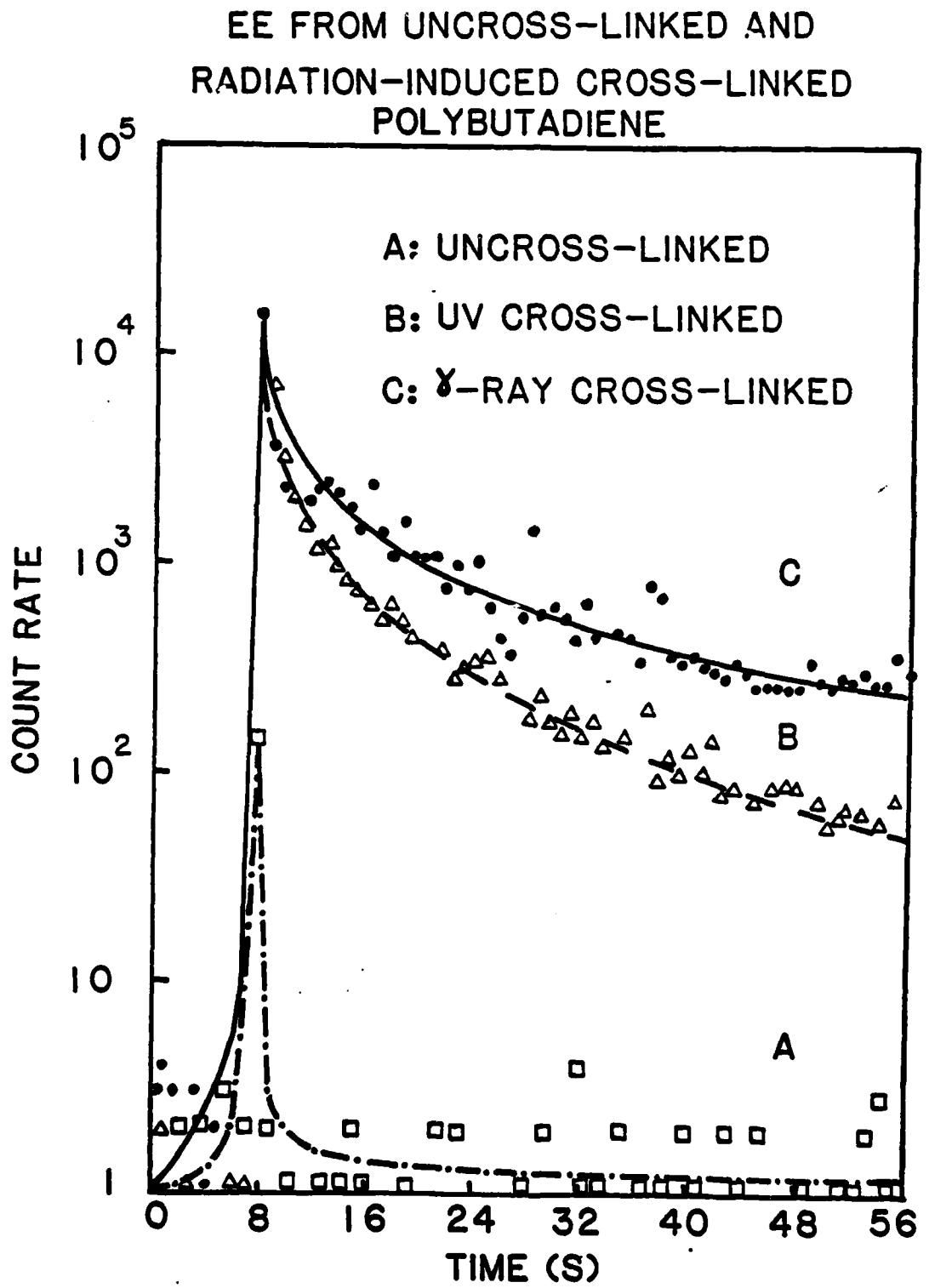
EE FROM UNCROSS-LINKED AND
RADIATION-INDUCED CROSS-LINKED
POLYBUTADIENE
A: UNCROSS-LINKED
B: UV CROSS-LINKED
C: γ-RAY CROSS-LINKED
COUNT RATE
TIME (S)
10^5
10^4
10^3
10^2
10
1
0
8
16
24
32
40
48
56
A
B
C

Fig 8

V. ELECTRON AND POSITIVE ION EMISSION ACCOMPANYING FRACTURE OF WINT-O-GREEN LIFESAVERS AND SINGLE-CRYSTAL SUCROSE

J. T. Dickinson, L. B. Brix, and L. C. Jensen
Department of Physics
Washington State University
Pullman, WA 99164-2814

ABSTRACT

It is a well-known fact that when Wint-o-green Lifesavers™* are broken in air one observes intense triboluminescence. We report here measurements of the emission of electrons and positive ions from the fracture of these Lifesavers in vacuum, as well as from single-crystal sucrose. The emission of photons and radiowaves during fracture in vacuum is also presented for sucrose, indicating the occurrence of a gaseous discharge in the crack tip during crack growth. Comparisons of the various emission curves are presented and discussed in terms of stress-induced charge separation.

* Lifesaver is a registered trademark of Lifesaver, Inc.

I. INTRODUCTION

Fracto-emission (FE) is the emission of particles, i.e. electrons, ions, neutral species, and photons, during and following the fracture of a material. In recent papers (see reference 1 and the references contained therein) we have shown that fracture in a vacuum of a large number of materials where charge separation occurs on the fracture surface leads to intense, long-lasting electron emission (EE) as well as positive ion emission (PIE). We have recently presented a qualitative model (2) for such systems which explains a wide range of observations. In this model, charge separation is accompanied by neutral emission (3) causing a gaseous discharge to occur in the crack tip region. This breakdown results in bombardment of the fracture surfaces by the charged particles produced in the discharge, which leads to eventual electron emission via electron-hole recombination (which can also yield visible photons, i.e. thermoluminescence (10)).

While carrying out studies verifying this model we became interested in systems where fracture produces triboluminesence, which has been attributed principally to charge separation (2), reasoning that there might also be observable EE and PIE from such samples. It is a well-known fact that when Wint-o-green Lifesavers are fractured in the dark one can easily observe the accompanying photon emission (phE) with the naked eye. Zink and co-workers (4-7) have attributed this triboluminescence in part to the electrical breakdown of air (N_2) at the crack tip due to the intense E-fields caused

by charge separation in the sucrose crystals contained in the Wint-o-green Lifesavers. Presumably these charged surfaces are produced by stress-induced polarization of sucrose crystals (a form of piezoelectricity) which, upon fracture, leads to charge separation.

In this work we first asked whether Wint-o-green Lifesavers fractured in a vacuum emit electrons and positive ions. Finding this to be the case, we then fractured single-crystal sucrose (the major ingredient in the Lifesavers) and found that it also emitted electrons and positive ions. We then sought evidence of a gaseous discharge occurring during fracture in vacuum, by detection of visible photons (phE) and radiowaves (RE), similar to the noise picked up on an AM radio during a lightning storm, but considerably less intense. The results presented here support the concepts suggested in our model (2) and also explain how the fracture of a molecular crystal, which should not yield substantial covalent bond breaking, can lead to energetic processes such as electron and ion emission.

II. EXPERIMENTAL

Single crystals of sucrose were grown by allowing a saturated solution of sugar in water to evaporate. Crystals began forming - usually growing down from the surface - within one week, and were large enough to use after two or three weeks. The crystals were then carefully removed from the container and left to dry in air for several days, after which the largest crystals were carefully separated from other crystals by cleavage.

The crystals were then prepared for use in a miniature three-point bending apparatus, which was used to fracture the samples inside a vacuum. A sample

could be cut to the proper size by cleaving a crystal along one of its axes with a sharp blade. Any irregularities or small crystals growing on the larger crystal were removed with an abrasive. Wint-o-green Lifesavers were prepared for breaking by simply cutting small rectangular sections with a jeweler's saw. Typical dimensions for both types of samples were 1mm x 3mm x 6mm.

The three-point bending apparatus held the ends of the sample fixed while applying pressure to the center until fracture occurred. The device was operated from outside the vacuum chamber by means of a bellows arrangement. The experiments were carried out at a pressure of 10^{-5} Pa.

Charged particles were detected with a channel electron multiplier (CEM), Galileo Electro-Optics Model 4039, positioned one cm from the sample surface. The front cone of the CEM was biased at +600 volts for efficient detection of electrons and at -2500 volts for detection of positive ions. The pulses out of the CEM were 10 ns in duration. Following amplification and discrimination, the pulses were counted and stored in a computer-based multi-channel analyzer set at 0.8 s/channel.

The photon detector was a Bendix BX754A Photon Counter Tube with an S-20 photosensitive cathode and a background count rate of 10-20 counts per second. The tube was placed in the vacuum a few millimeters from the sample looking into the region where fracture would occur. A CEM was placed as close as possible (approximately 5 cm from the sample) to simultaneously detect the charged particle emission.

III. RESULTS

The single crystals of sucrose tended to have rough fracture surfaces,

perhaps due to minor imperfections and impurities in the crystals. Both the sucrose crystals and Lifesaver samples sometimes broke into more than one piece or crumbled into many pieces. Qualitatively, in the case of EE from sucrose, the emission was roughly proportional to the cross-sectional area of the fracture surface.

Wint-o-green Lifesavers emitted both electrons and positive ions during and after fracture. Fig. 1 shows typical EE from a Wint-o-green Lifesaver. The PIE for a Wint-o-green Lifesaver is shown in Fig. 2 and is seen to follow closely the curve for the Lifesaver EE. We have observed similar behavior of EE and PIE in a number of other materials where charge separation is strong, including SiO_2, PZT, mica, and systems undergoing interfacial failure between polymers and both dielectric and metal substrates. Fig. 3 shows the EE from a sucrose crystal. The PIE from sucrose, shown in Fig. 4, again has the same general form as the EE.

The decay for sucrose is noticeably slower than that of the Wint-o-green Lifesavers. The peak counts for sucrose and Lifesavers are very nearly the same; the total counts for sucrose are approximately twice those obtained for the Lifesavers due to the longer tail. The total intensities per unit cross-sectional area for both these materials are above average for the wide range of materials we have examined (8).

Zink, et. al., have found that phE (triboluminescence) from Wint-o-green Lifesavers fractured in air appears to occur only during the propagation of the crack. The duration of phE from a single crack should be about the same as the time required for a crack to move through the sample, i.e. on the order of a few microseconds. EE and PIE from the Wint-o-green Lifesavers and sucrose, on the other hand, lasted many seconds, the emission intensity gradually decaying

over a period of time. Thus we see that phE produced in air and the EE and PIE produced in vacuum exhibit completely different behavior.

To compare the charged particle emission with possible phE occurring in vacuum, and to obtain further information on the mechanism, we examined the EE and phE, as well as the accompanying radiowave emission (RE), from the fracture of single-crystal sucrose in vacuum. The RE was detected with a small pick-up coil placed near the sample (2). As shown in Fig. 5, the RE and phE occur only during fracture, while the EE is, as before, most intense during fracture, followed by the usual tail.

For some sucrose samples, the phE was sufficiently intense that we were able to observe a component <u>after</u> fracture which showed evidence of decaying in step with the EE. Fig. 6 shows phE from two samples, taken on two different time scales: a) 40 ms/channel, and b) 0.8 s/channel. The second sucrose sample broke into several pieces, thus yielding multiple peaks. In both figures there are clear indications of a phE tail similar to the EE. In Fig. 6a, the peak phE (note log scale) is seen to be considerably higher than the remaining emission, suggesting two separate mechanisms for phE during and after fracture.

IV. DISCUSSION

Our data clearly indicate that fracture of Wint-o-green Lifesavers and single-crystal sucrose in vacuum is accompanied by EE and PIE which differ dramatically in form and time-dependence from the phE observed in air by Zink and from the vacuum phE data we have taken. The similarities between the Lifesaver and sucrose EE and PIE suggest that the basic cause of FE from the

Lifesavers is fracture of the sucrose crystals contained in the Lifesavers. The faster decays of the Lifesaver EE and PIE may be due to the influence of the flavoring agent (methyl salicylate) on the processes causing post-fracture emission.

RE has previously been observed by Derjaguin et al. (9) during the peeling of polymer films from dielectric substrates (at much higher pressures than in our experiments) and was attributed to electrical breakdown in the background gases. The RE we observe is not due to background gases, but to gases desorbing from the crack wall into the crack tip. Zink et al. (7) showed that vacuum-degassed sucrose would not produce triboluminescence when the crystals were broken in liquid benzene (free of N_2), which suggests that our undegassed samples may be evolving N_2 during fracture, leading to the discharge.

The detection of RE and the intense phE during fracture of sucrose in vacuum supports our hypothesis of a gaseous discharge, caused by strong charge separation, in the crack tip during fracture. The resulting charged particles in this micro-discharge should be strongly attracted to the oppositely charged surfaces, leading to bombardment of these surfaces. As we have shown in reference 2, this bombardment can lead to both EE and PIE. The mechanism for the EE is basically electron-hole recombination (10) where the necessary excitations were originally created by particle bombardment occurring during the discharge. Since trapped electrons must be mobilized in order to locate an appropriate hole, the rate of post-fracture EE will depend on electron and hole concentrations as well as the electron transport process. The phenomenon of radiation-induced electron emission, normally studied in inorganic materials, is called thermally stimulated electron emission (10). A process parallel to

this non-radiative electron emission is the emission of photons (thermoluminescence (10)), which accounts for the tail observed in the phE after fracture in vacuum. This tail may not be observable in the triboluminescence produced in air because of a quenching of the necessary excitations by reactions with air molecules.

The PIE is assumed to be due to self-bombardment, i.e. "self-flagellation," of the fracture surface with electrons which cannot escape due to electric fields from adjacent charge patches. This self-bombardment of the fracture surfaces induces PIE via an electron stimulated desorption (ESD) mechanism (11). The PIE rate should then follow the overall EE rate, explaining why we observe identical decay curves for EE and PIE.

In passing we should note that the shape of the EE and PIE curves, in particular the relatively rapid decay that occurs immediately after fracture, may be due in part to the temperature of the fracture surface being elevated by crack propagation, then cooling to room temperature in a few seconds via conduction and radiation. The EE and PIE intensities would follow this decrease in temperature. We are pursuing quantitative models of the kinetics of the EE processes and eventually hope to use the EE to obtain accurate measurements of the temperature rise of the surface produced by fracture.

V. CONCLUSIONS

The phE (triboluminescence) of Wint-o-green Lifesavers and sucrose for fracture in air has been strongly linked to charge separation on the fracture surfaces by Zink and co-workers (4-7). We have obtained similar results for phE in vacuum for the fracture of single crystals of sucrose. Furthermore, we

have shown that EE and PIE also occur in vacuum for both the Lifesavers and sucrose. The similarities of the time decays suggest that EE and PIE from the Lifesavers are due to fracture of the sucrose contained in the Lifesavers. The phE that we observed appears to have two components: 1) photons from a discharge in the crack during fracture, and 2) thermoluminescence after fracture. The latter is a relaxation process that occurs in parallel with the EE; both are due to electron-hole recombination. Strong evidence for the occurrence of the gaseous breakdown is the RE and the intense component of phE occurring during fracture.

One final result that was not reported above that should be noted is that after fracture in vacuum, the Wint-o-green Lifesavers tasted rather bland. Although we have not performed the control experiment, we are confident that fracture had nothing to do with the change in flavor. One must ask, however, what influence FE might have on the physiological experience of eating Lifesavers.

VI. ACKNOWLEDGMENTS

The authors would like to thank E. E. Donaldson and A. Jahan-Latibari for their contributions to this research and helpful discussions. This work was supported by the Office of Naval Research, the National Science Foundation, Sandia National Laboratories, NASA-Ames Resarch Center, and the M. J. Murdock Charitable Trust.

REFERENCES

1. J. T. Dickinson, L. C. Jensen, and M. K. Park, Appl. Phys. Lett. 41, 827 (1982).

2. J. T. Dickinson, L. C. Jensen, and A. Jahan-Latibari, submitted to J. Vac. Sci. Technol.

3. L. A. Larson, J. T. Dickinson, P. F. Braunlich, and D. B. Snyder, J. Vac. Sci. Technol. 16, 590 (1979).

4. J. I. Zink, Naturwissenschaften 68, 507 (1981).

5. B. P. Chandra and J. I. Zink, Physical Review B 21, 816 (1980).

6. R. Angelos, J. I. Zink, and G. E. Hardy, J. of Chem. Ed. 56, 413 (1979).

7. J. I. Zink, G. E. Hardy, and J. E. Sutton, J. Phys. Chem. 80, 248 (1976).

8. J. T. Dickinson, E. E. Donaldson, and M. K. Park, J. Mat. Sci. 16, 2897 (1981).

9. B. V. Derjaguin, L. A. Tyurikova, N. A. Krotova, and Y. P. Toporov, IEEE Transactions on Industry Applications, Vol. IA-14, 541 (1978).

10. R. Chen and Y. Kirsh, Analysis of Thermally Stimulated Processes (Pergamon Press, New York, 1981), pp. 48-52.

11. M. L. Knotek, in Proceedings of the International Conference on X-ray and Atomic Inner-Shell Physics, "X-'82," AIP Conference Proceedings 94, 772 (1982).

FIGURE CAPTIONS

Fig. 1: Electron emission (log scale) from the fracture of a Wint-o-green Lifesaver.

Fig. 2: Positive ion emission from the fracture of a Wint-o-green Lifesaver.

Fig. 3: EE from single-crystal sucrose.

Fig. 4: PIE from single-crystal sucrose.

Fig. 5: Simultaneous emission of electrons, visible photons, and radiowaves from single-crystal sucrose.

Fig. 6: Visible photon emission from fracture of single-crystal sucrose for two samples, taken on different time scales: a) 40 ms/channel, and b) 0.8 s/channel.

ELECTRON EMISSION FROM WINT-O-GREEN LIFESAVERS

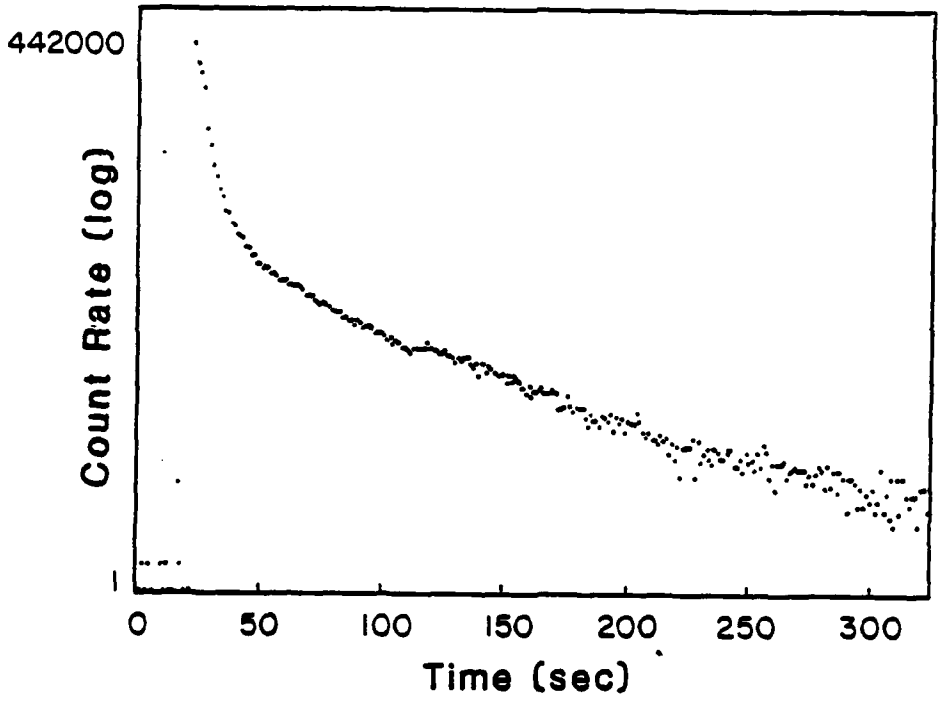

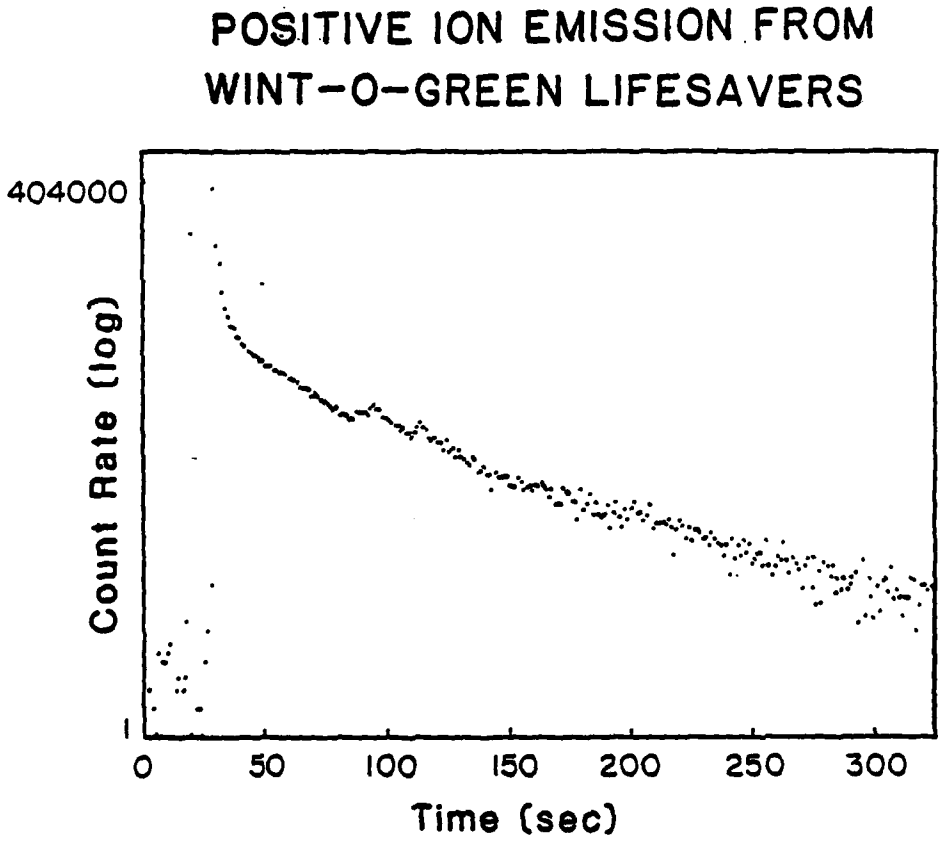
POSITIVE ION EMISSION FROM
WINT-O-GREEN LIFESAVERS
404000
1
Count Rate (log)
0
50
100
150
200
250
300
Time (sec)

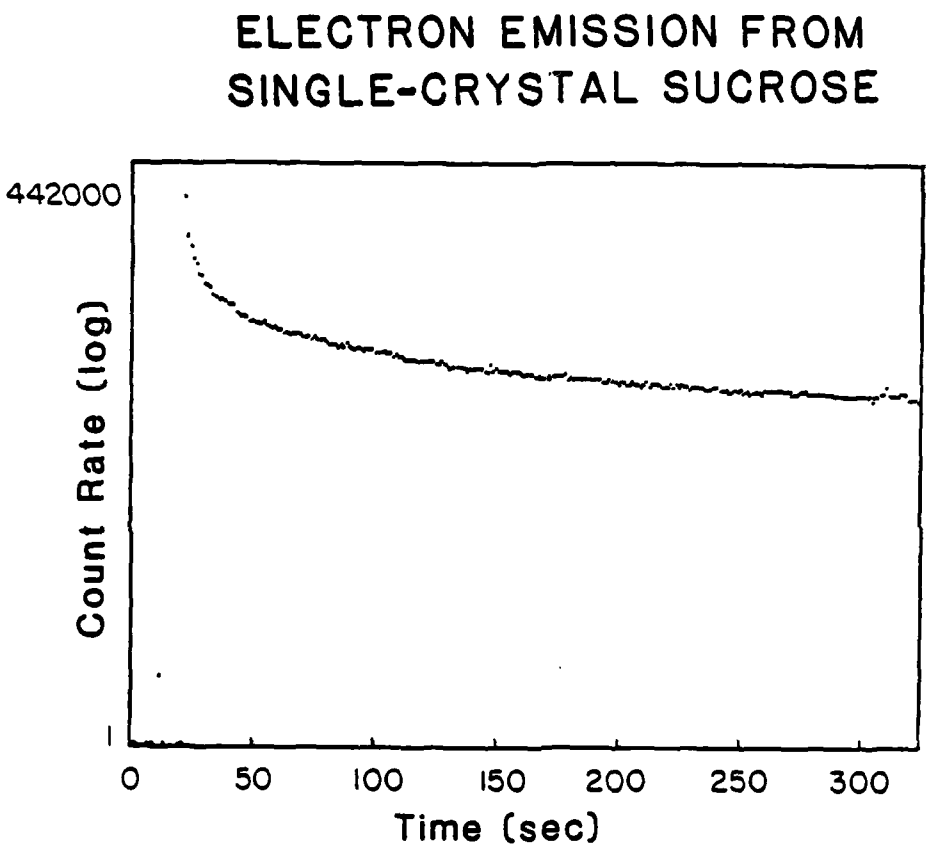
ELECTRON EMISSION FROM
SINGLE-CRYSTAL SUCROSE
442000
1
Count Rate (log)
0
50
100
150
200
250
300
Time (sec)

Fig. 3

POSITIVE ION EMISSION FROM SINGLE-CRYSTAL SUCROSE

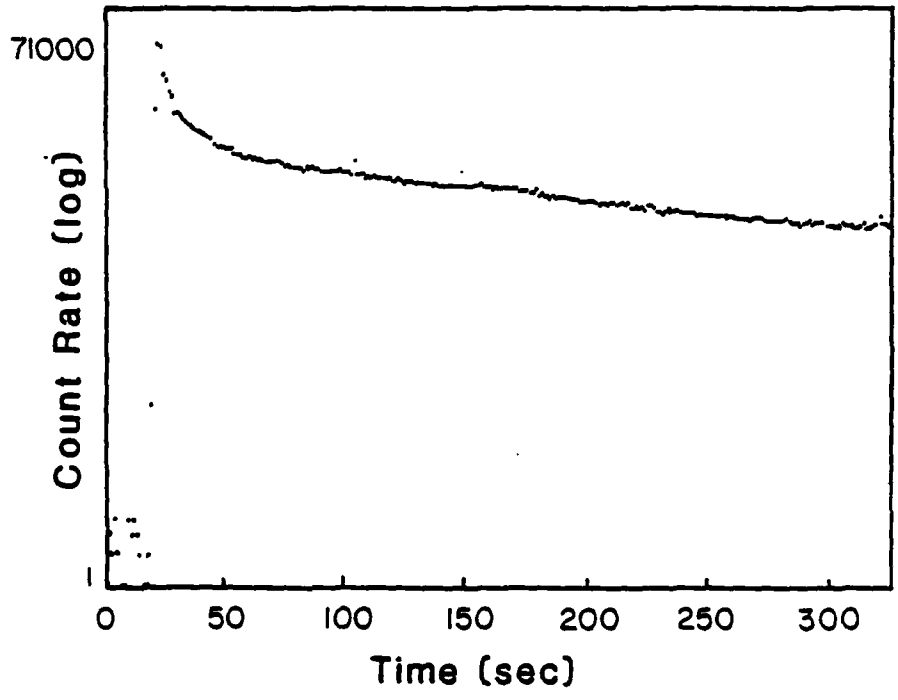

Fig. 4

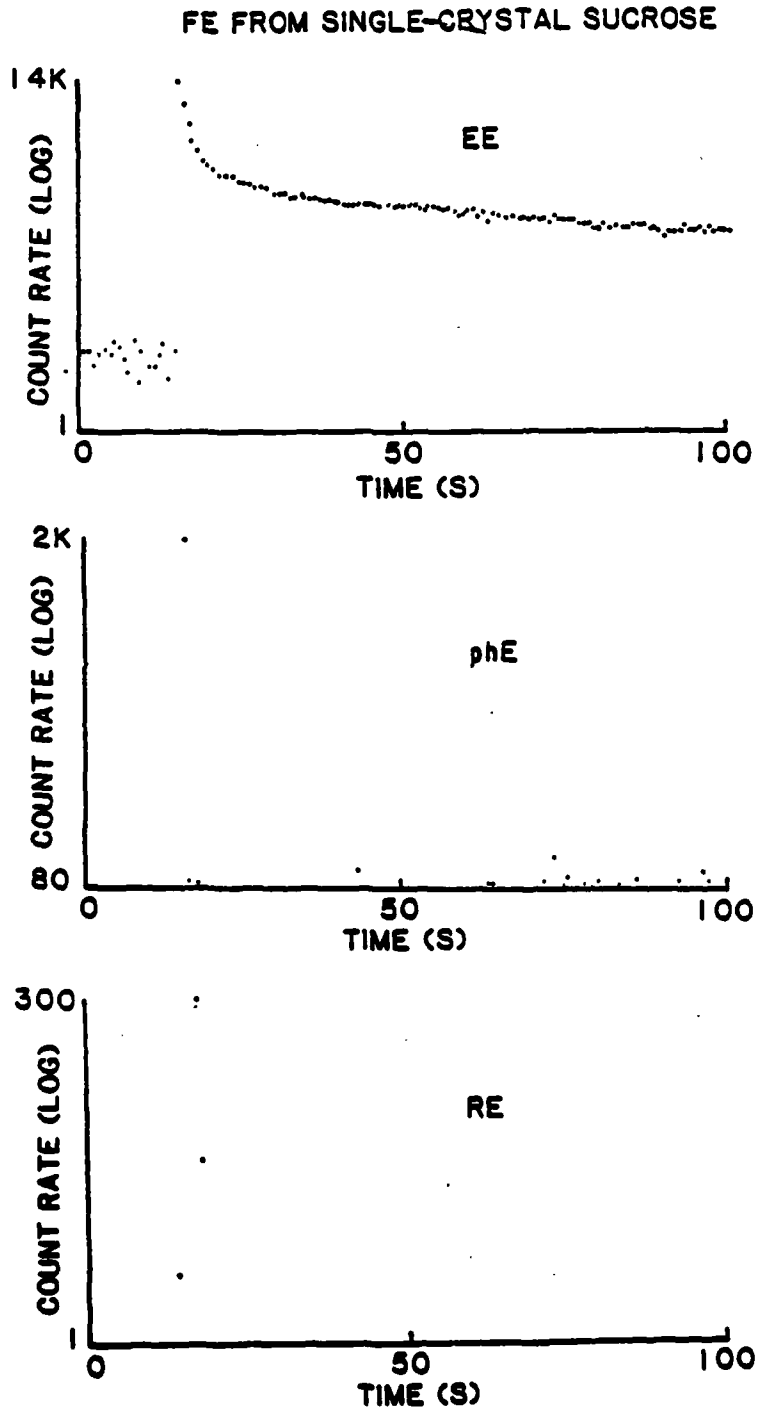
FE FROM SINGLE-CRYSTAL SUCROSE
14K
EE
COUNT RATE (LOG)
1
0
50
100
TIME (S)
2K
phE
COUNT RATE (LOG)
80
0
50
100
TIME (S)
300
RE
COUNT RATE (LOG)
1
0
50
100
TIME (S)

Fig. 5.

phE FROM SINGLE-CRYSTAL SUCROSE

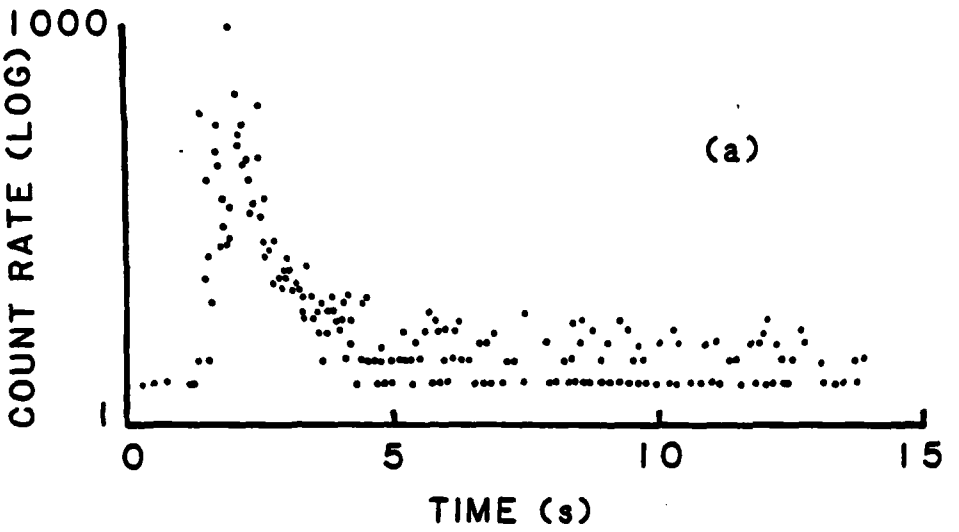

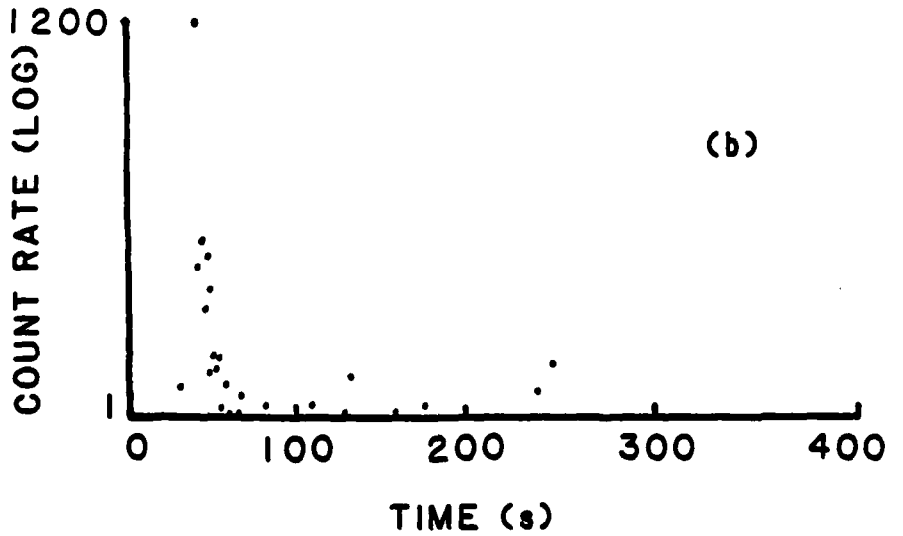

Fig. 6

VI. FRACTO-EMISSION FROM CYCLOTRIMETHYLENE TRINITRAMINE (RDX) SINGLE CRYSTALS

J. T. Dickinson and M. H. Miles
Department of Physics
Washington State University
Pullman, WA 99164-2814

W. L. Elban
Naval Surface Weapons Center
Silver Spring, MD 20910

R. G. Rosemeier
Department of Mechanical Engineering
University of Maryland
College Park, MD 20742

ABSTRACT

Single crystals of the explosive cyclotrimethylene trinitramine (RDX) were fractured in a vacuum while viewed by particle detectors biased to separate positive and negative charge. Fracture was achieved by compressive loading of small crystals and by three point bending. Cleavage type fracture exposing [001] crystal planes yielded a sharp emission peak followed by rapid decay. Multiple fracture involving surface frictional grinding yielded large emissions with emission continuing for several minutes after the mechanical damage. Results are discussed in terms of possible mechanisms.

I. INTRODUCTION

Fracto-Emission (FE) is the emission of particles--i.e. electrons, positive ions, neutral species, and photons--during and following the fracture of a material (see reference 1 and references contained therein). We have previously reported FE from single crystals of pentaerythritol tetranitrate (PETN) and cyclotetramethylene tetranitramin (HMX).[1] In this paper we present recent work on the electron emission (EE) and positive ion emission (PIE) from cyclotrimethylene trinitramine (RDX) single crystals fractured in vacuum. Fracture induced phenomena in these materials is of particular interest because of possible relevancy to their unusual decomposition modes wherein slow decomposition can revert to rapid modes of reaction releasing energy by atomic rearrangement. The role of the fracture process and the fracture surface in initiation is not clearly understood so that any new information would be of benefit. In this paper we show that like PETN and HMX, RDX also emits EE and PIE, and that the mode of fracture relative to the crystallographic orientation appears to effect the emission characteristics. We interpret these results in terms of a mechanistic model we have recently presented.[2]

II. EXPERIMENTAL

Single crystals of cyclotrimethylene trinitramine (RDX) were fractured in compression and three point bending. Two sizes of crystals were used: small class D crystals of about 1 mg and larger laboratory grown crystals of about 50 mg. The crystallographic orientation of the crystals with respect to the fracture mode were noted. Six of the small crystals and three of the large RDX crystals were fractured by compressive loading. Eight of the large RDX crystals were fractured in three point bending.

Charged particles were detected with Galileo Electro-Optics Model 4039 channel electron multipliers (CEM)[3] positioned about 1 cm from the sample. The front of the CEM was biased at +600 volts for efficient detection of electrons or at -2500 volts for detection of positive ions. Although these potentials do not guarantee exclusion of particles of the wrong sign nor the detection of excited neutrals, work on polymers indicate we will detect predominantly the EE or the PIE. The CEM detectors have typical gains of 10^6 - 10^3 electrons/incident particle producing fast (10 ns) pulses. For the work reported here the detection efficiency for both electrons and positive ions is near 100%, although we expect our collection efficiency to be as low as 10-20%. Background noise counts typically ranged from 1 to 10 counts/second. Standard nuclear physics data acquisition methods were used to convert and store pulses as a function of time.

For compressive loading two CEM detectors were used on opposite sides of the crystal under compression. Two detectors allowed observation of both negative and positive charges, although geometrially one detector was much closer to the fracture surface than the other and therefore was favored. For crystals fractured in three point bending a thin piece of metal with a rectangular window a few mm on a side was used to provide the end support of the crystals while a knife edge pushed from behind to fracture the crystal. For three point bending only one detector was used monitoring either electrons or positive ions.

Fracture was performed manually using a screw drive coupled to the translation of two parallel metal surfaces for compressive loading and to the motion of a knife edge for flex or three point bending. For some crystals we performed slow loading until an initial emission was observed. Other crystals received a faster loading which crushed the crystals, producing multiple

fracture. Various samples were recovered for subsequent microscopic examination of the fractured surfaces. The vacuum system used in this work produced a background pressure of 10^{-5} Pa.

III. RESULTS

We started our experimentation compressing the small class D RDX crystals. We tried two different orientations with respect to the loading direction. The crystals were tabular in shape with the major flat surfaces (001) type crystal planes. Four class D crystals were compressed normal to the tabular planes while two were compressed parallel to the (001) morphology. The results are summarized in Table I. A total collection time of 240 seconds is represented in Table I; background counts (typically 2 counts/sec) have been subtracted out. Even in these small samples definite emission is illustrated for electron emission in sample 368 shown in Fig. 1. The peak counts recorded recorded in Fig. 1 for one 0.8 second channel is 95. Figure 2 shows the ion emission for sample 369. Peak counts recorded here was 575. Low total counts generally corresponded to rapid emission decay. In contrast sample 366 yielded relatively large ion emission and was accompanied by slow decay.

Table I

Sample	Orientation	Electron Count	Positive Ion Count	Favoring
366	Normal	2,500	600	Electron
367	Normal	400	600	Electron
368	Normal	350	200	Electron
369	Normal	150	980	Ions
370	Parallel	100	200	Ions
371	Parallel	500	250	Electron

Five of the larger laboratory grown RDX crystals were fractured in compression. Table II Summarizes the results.

Table II

Sample	Orientation	Electron Count	Positive Ion Count
372 C-2	Normal	154,000 163,000	29,000 12,000
373 A-3	Parallel	3,000	3,500
374 A-2	Normal	8,000	20,000
384 A-4	Normal	17,000	32,000
385 C-5	Normal	52,000	143,000

Figure 3 shows the large slow decaying electron emission associated with sample 372 C-2. The positive ion emission decayed in a similar fashion. We have shown in a number of cases that the PIE and EE are kinetically equivalent.[1] Sample A-3 fractured and rotated in the compression fixture so that the fracture was not as extensive as for the other two samples.

Seven RDX crystals were fractured in three point bending. The knife-edge was perpendicular to the [001] crystal direction. Table III summarizes the results:

Table III

Sample	Electron Counts
375 A-1	1,000
376 B-4	31,000
377 C-4	1,000,000
380 C-1	9,000
381 B-3	6,000
382 B-1A	1,400
383 B-1B	54,000

Figure 4 shows the fast decay of electron emission from sample 375 A-1. In contrast to this fast decay low emission, some fractures produced emission thousands of times more intense with slow decay for long times following the fracture. Figure 5a shows an example of emission of this type for sample 377 C-4 which yielded extremely high emission. Figure 5b shows the initial emission on a faster time scale (50 ms/channel). One sees that the peak emission (during fracture) is considerably higher than the next few channels of after-emission. Note that the decay curve is very complicated, showing a minimum soon after fracture which then rises and falls fairly smoothly. With slow advances of the knife edge, it was possible to observe emission from the initial fracture event. Figure 6 shows electron emission for sample 380 C-1 at 0.8 s/channel; over half of the emission occurs during the first channel and then rapid decays back to zero. The same data displayed at 5 ms/channel shows in more detail the rapid portion of this decay. Sample 382 B-1A was also stressed slowly until emission occurred. Figure 8 shows two bursts of emission accompanying this initial fracture, each occurring in less

than a second. The crystal cracked but did not separate into two pieces. Presumably the two bursts correspond to two fracture events. Subsequent additional stress resulted in much larger and longer lasting emission indicated for the second stressing of sample B1, labeled 383 B-1B in Table III.

Correlations of the observed differences in FE with SEM analysis of the fracture surfaces is in progress at NSWC.

IV. DISCUSSION

We have demonstrated fracto-emission for single crystals of RDX. Both electron and positive ion emission occurs. Two extreme types of emission have been observed in RDX. Slow three point bending producing a fracture separating [001] planes yields a sharp emission peak followed by rapid decay. Total emission is of the order of a few thousand counts. More rapid loading that most likely involves surface frictional grinding produces intense emission that continues many seconds after the mechanical damage. Figures 3 and 5 are examples of this type. Figure 5 has a sharp initial emission with the subsequent emission slowly decaying. There may be some increases of emission occurring in the decaying region of the slow decay.

The correlation of FE with the fractography suggests that FE is indeed sensitive to the path of the crack. Details of this correlation will be available soon.

Recent FE studies on non-energetic materials at Washington State University have indicated that over a wide range of materials those that exhibit intense EE and PIE also exhibit easily measurable photon emission (phE) and radio wave emission (RE) during crack growth in samples fractured in vacuum. These latter two emissions are attributed to breakdown (a gaseous

discharge) occurring in the crack due to the separation of charge on the crack surfaces and the evolvement of gases into the crack. The charge density, gas pressure, and spacing are such that a gaseous discharge occurs, the intensity of which depends dramatically on crack velocity. The consequence of this discharge is the immediate bombardment of the crack walls with charged particles of reasonably high energies. This bombardment is then the basic cause of the post-fracture EE we have seen in so many materials. The bombardment creates electron-hole pairs. Their recombination releases electrons via non-radiative, Auger-like transitions. The accompanying PIE is explained in terms of self-bombardment of the surface by a portion of the EE attracted back to the surface by positive charge patches. The evidence in support of this mechanistic model has been recently presented in references 2 and 4.

One of the materials which produced strong EE, phE, and RE, and thus supporting our model, was the molecular crystal sucrose.[4] The phE of sucrose fractured in air (usually referred to as triboluminescence) is well known[5] and has been attributed to the breakdown of N_2 from air in the crack-tip. Sucrose is piezoelectric, thus the onset of charge separation due to the local stresses near the crack-tip are certainly expected. However, the details of the charge transfer process, or perhaps better stated, the barriers to charge transfer that ultimately yield charges on the fracture surfaces are not understood. In our studies[4] we showed that even when fractured in vacuum, single crystal sucrose yielded strong EE, phE, and RE during fracture and intense, long lasting EE after fracture.

In the molecular crystals PETN, HMX, and now RDX, the existence of FE and its similarities in form to other materials indicate that similar phenomena may be occurring. The major question that has troubled us in these

materials and sucrose (i.e. molecular crystals) as well as systems involving adhesive failure was how did electrons acquire the necessary energy to escape these materials. At first we considered fracture-induced bond scissons followed by "energy-releasing" recombination reactions. But the molecular crystals and systems failing adhesively really should not yield significant densities of primary bond scissions due to the weak inter-molecular forces normally expected. The particle bombardment mechanism, however, puts electrons in favorable, high lying energy levels which can undergo transitions producing EE, similar to exo-emission induced by radiation observed from inorganic insulators.[8] We therefore cautiously propose that in these explosive crystals, the observed emission following fracture is induced by a mechanism wherein a gaseous discharge produces particle bombardment of the fracture surfaces, thus creating electron-hole pairs whose recombination can lead to EE.

The sensitivity of EE and PIE in RDX to the type of loading and fracture path may be due to the differences in surface charge and/or release of gases into the crack during fracture. Certainly, the piezoelectric properties of crystalline materials tend to vary with crystallographic orientation, and thus could create different charge densities upon separation. Also, the crack velocity or rate of separation of the fracture surfaces, which would depend on which crystal planes are involved, would be expected to influence the intensity of the discharge.

The questions raised, suggested experiments, and implications of interpreting the observed emission in terms of these concepts are quite extensive. One major question is the details of creating a discharge in the crack tip and, of course, experimental verification of its occurrence (phE and RE) as well as the relation of EE and PIE to particle bombardment of these

crystals. In terms of implications, the presence and density of charge on the fracture surface should be particularly pertinent to the manner in which fracture is occurring in these materials. Furthermore, the consequences of particles bombarding the fracture surfaces in terms of potential chemistry on and near the surface should be of considerable interest.

V. ACKNOWLEDGMENTS

The authors would like to thank Les Jensen and K. C. Yoo for their assistance in this research. This work was supported by the Office of Naval Reseach and the Naval Surface Weapons Center.

REFERENCES

1. M. H. Miles and J. T. Dickinson, Appl. Phys. Lett. 41, 924 (1982).

2. J. T. Dickinson, L. C. Jensen, and A. Jahan-Latibari, submitted to J. Vac. Sci. and Technol.

3. E. A. Kurz, Am. Lab. 11 (3), 67 (1979).

4. J. T. Dickinson, L. B. Brix, and L. C. Jensen, submitted to J. Phys. Chem.

5. J. I. Zink, Naturwissenschaften 68, 511 (1981).

6. J. I. Zink, G. E. Hardy, and J. E. Sutton, J. Phys. Chem. 80, 248 (1976).

7. B. P. Chandra and J. I. Zink, Phys. Rev. B 21, 21 (1980).

8. R. Chen and Y. Kirsh, Analysis of Thermally Stimulated Processes (Pergamon Press, New York, 1981), pp. 48-52.

LIST OF TABLES

FIGURE CAPTIONS

Fig. 1. Electron emission accompanying the fracture of a single class D RDX crystal under compressive loading. Two peaks are observed probably due to two separate fracture events.

Fig. 2. Positive ion emission from the fracture of a single class D RDX crystal under compressive loading. A single peak lasting approximately 5s is observed.

Fig. 3. Electron emission from the compressive failure of a laboratory grown RDX crystal showing intense, long lasting emission.

Fig. 4. Electron emission from a laboratory grown RDX crystal loaded in a 3-point bending mode.

Fig. 5. Electron emission from sample 377 C-4 loaded in 3-point bending. a) data taken at 0.8 s/channel b) some data recorded at 50 ms/channel.

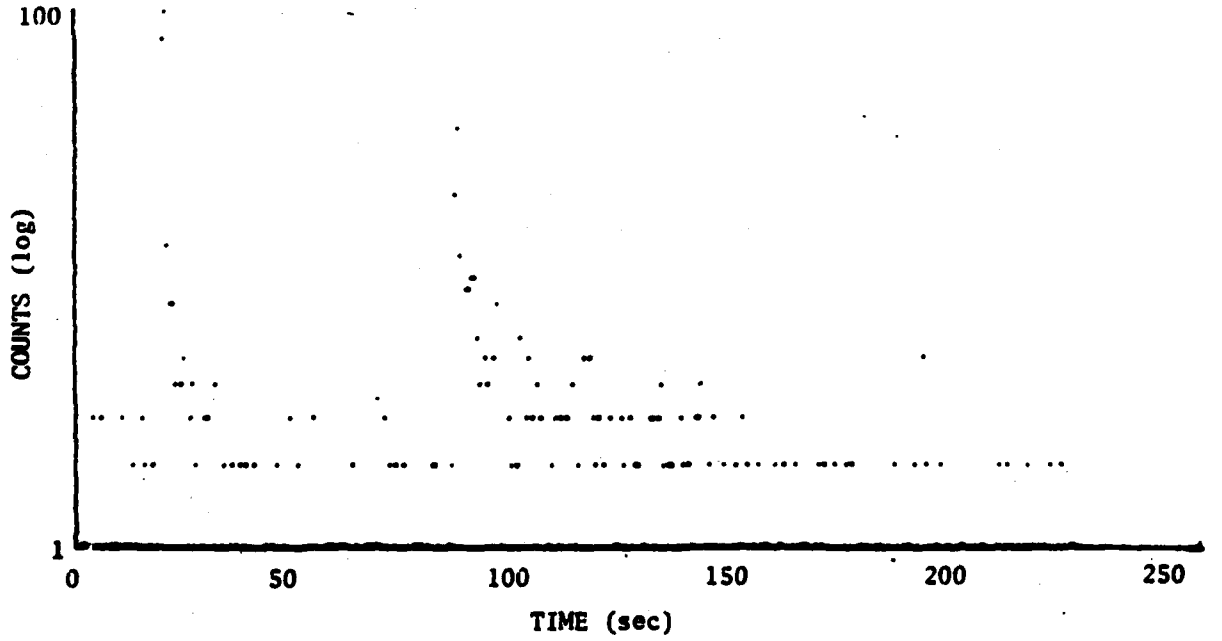

Fig. 1

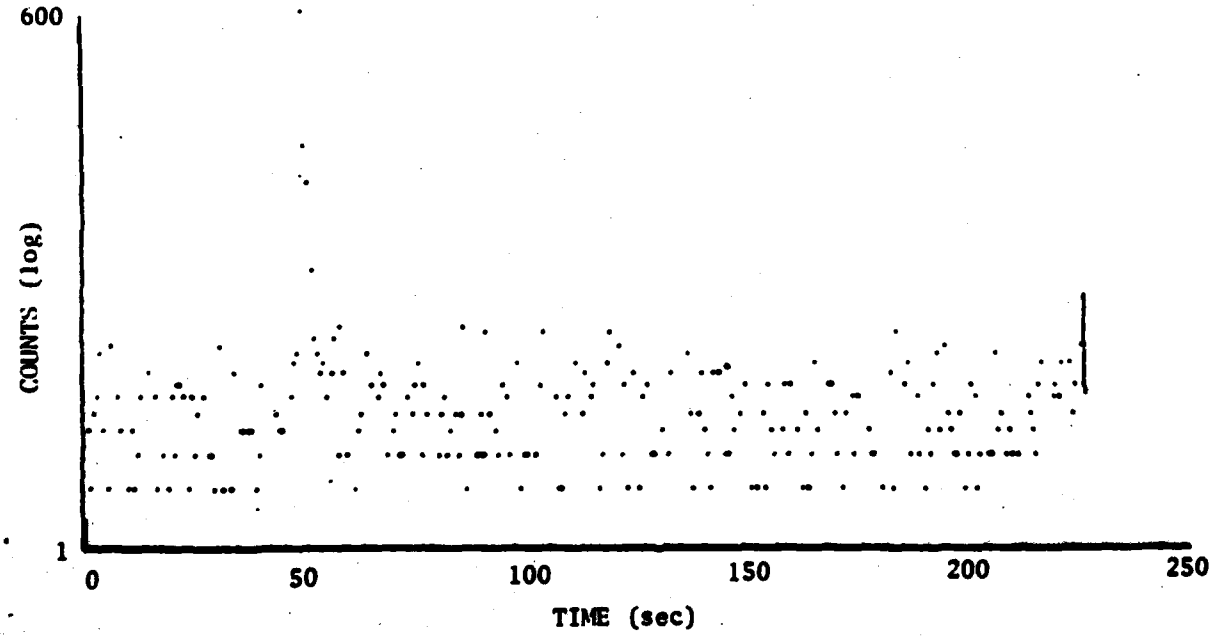

Fig.

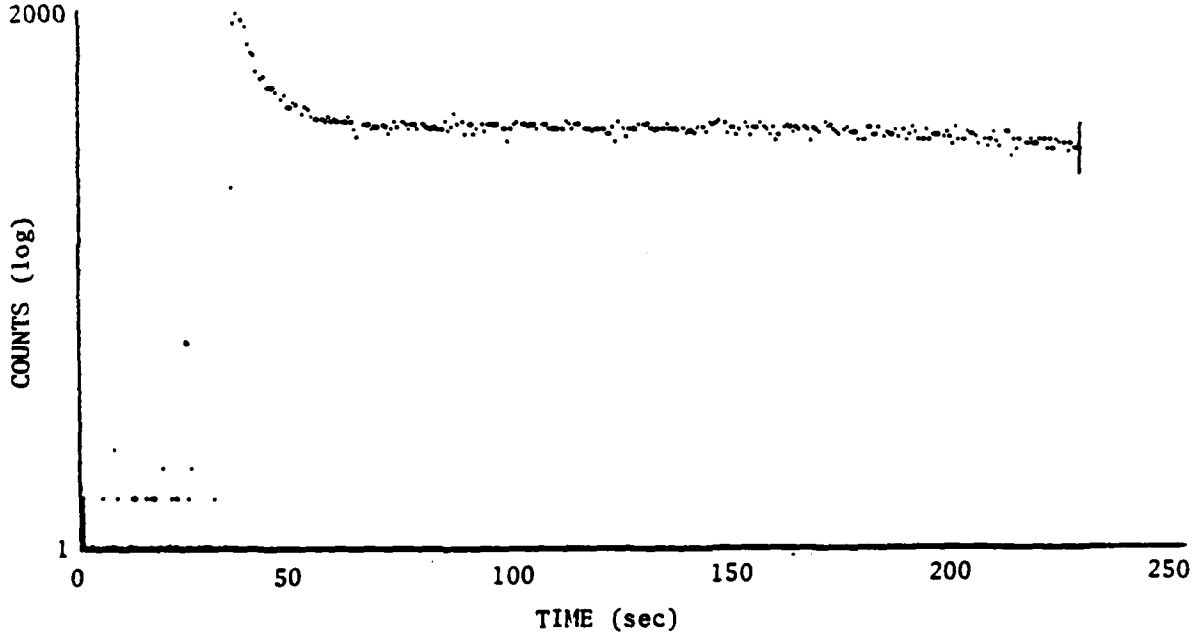

Fig. 7

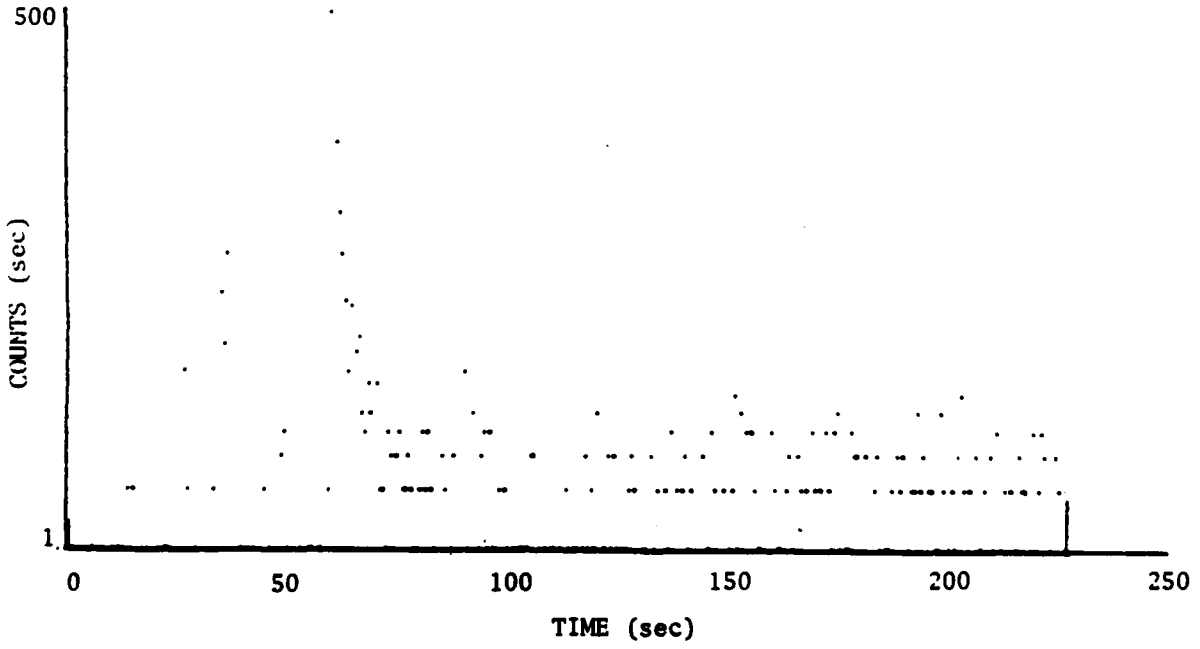

Fig. 4

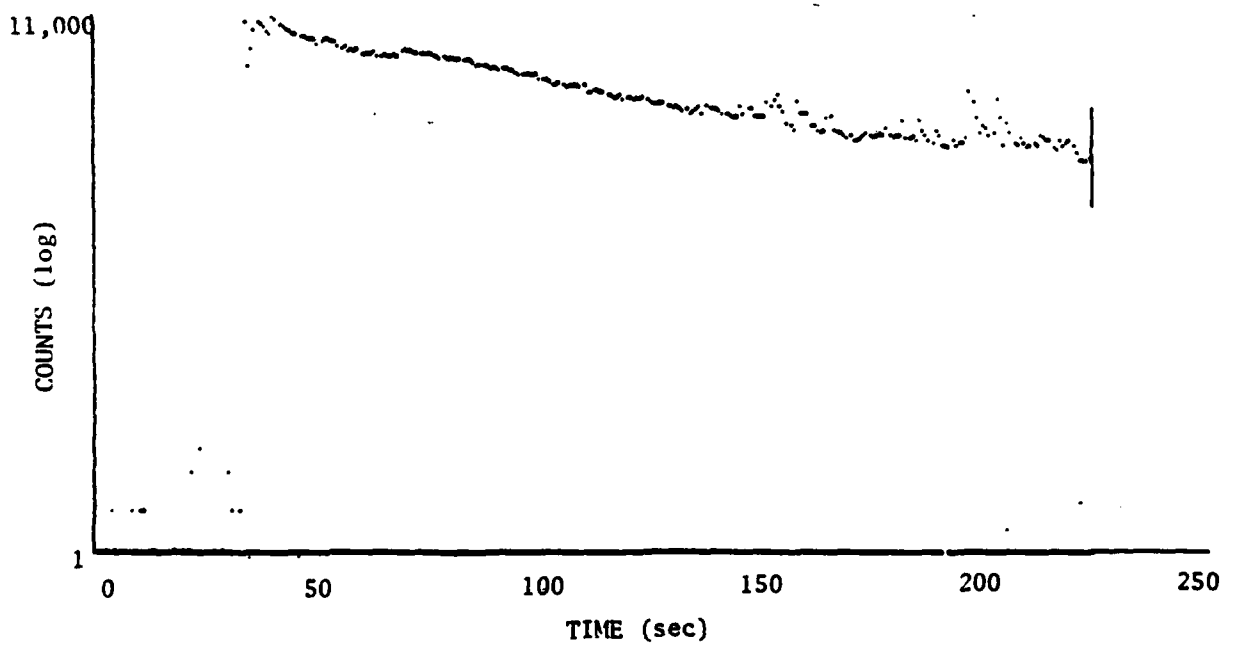

Sa

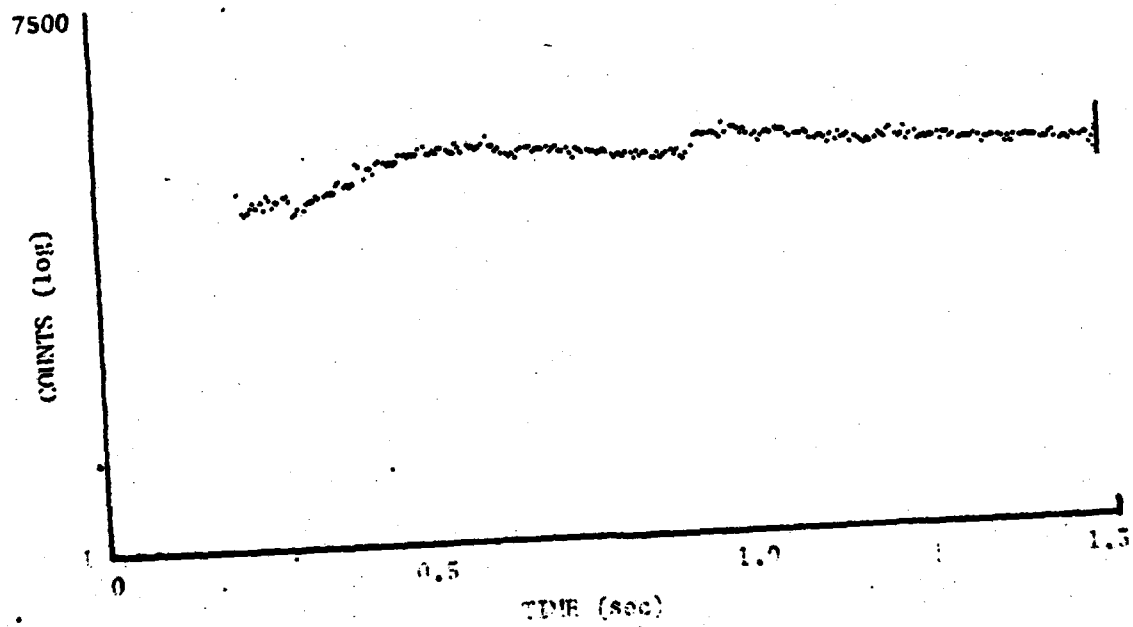
7500
COUNTS (log)
1
0
0.5
1.0
1.5
TIME (sec)

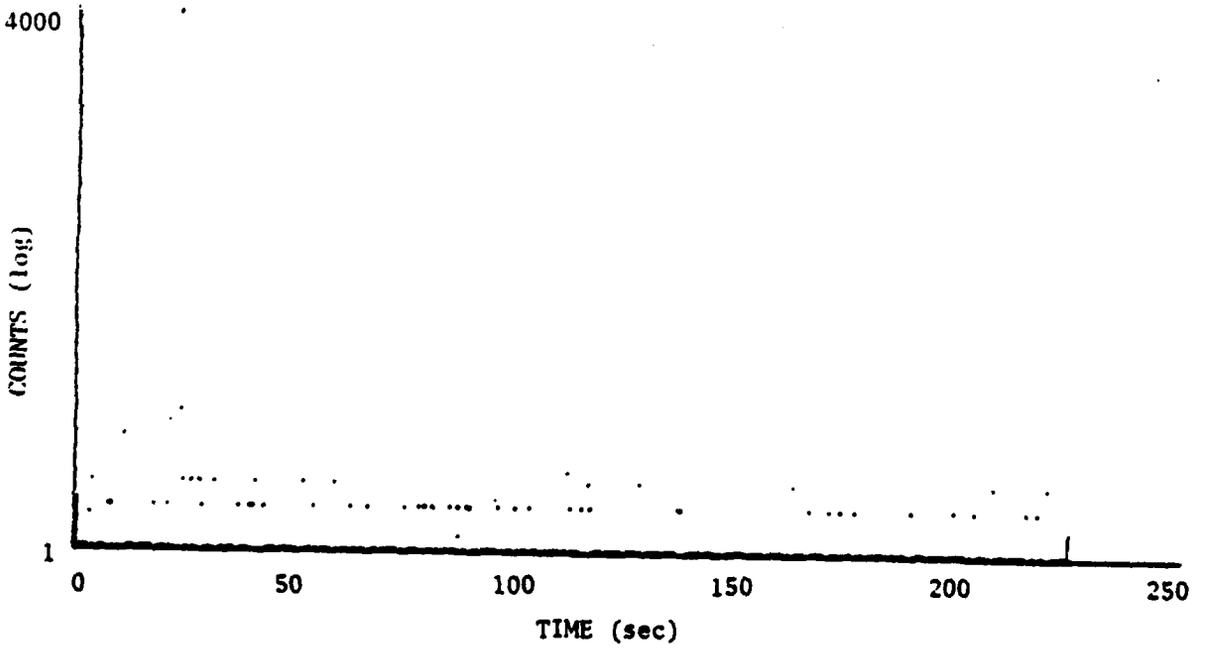

Fig 6

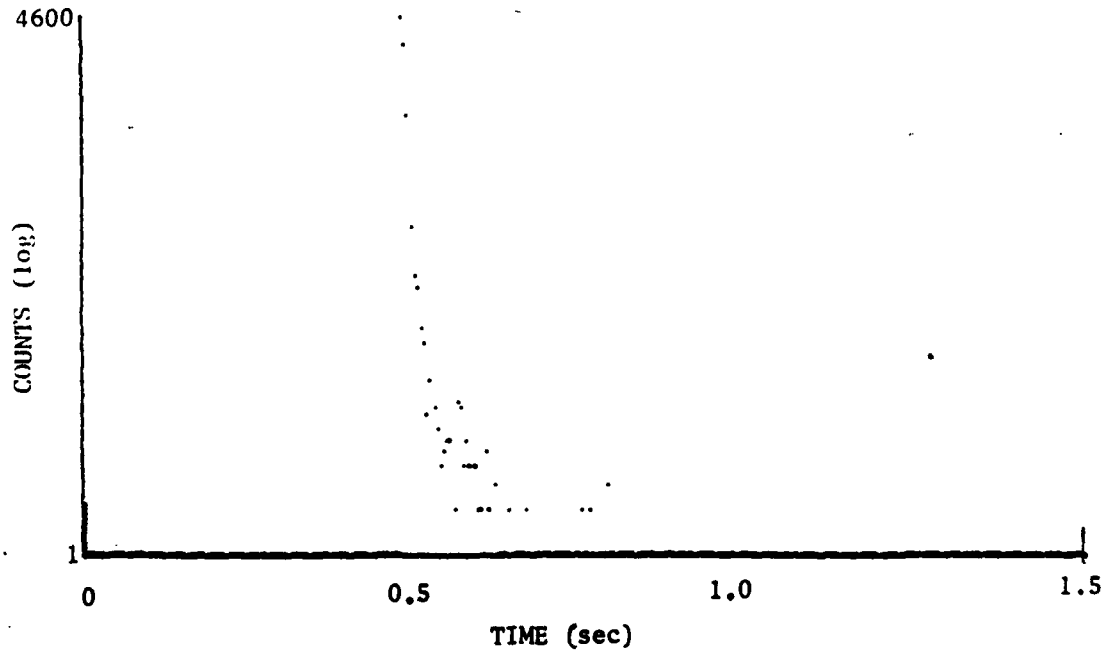

Fig

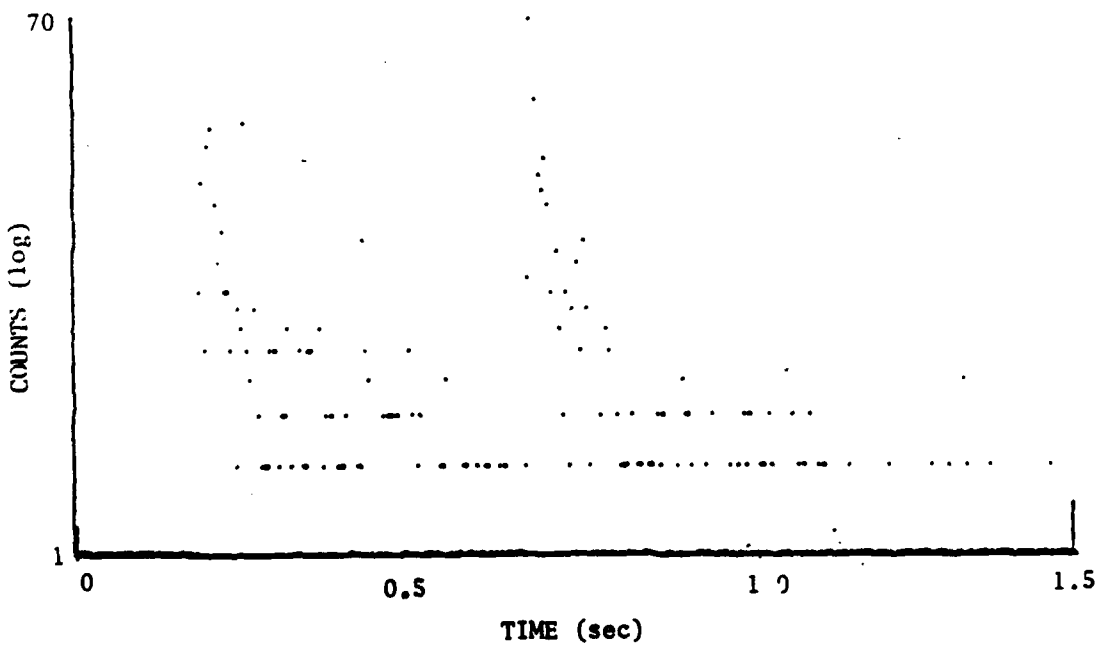

Fig 2

VII. FRACTO-EMISSION FROM FILLED AND UNFILLED ELASTOMERS

J. T. Dickinson, L. C. Jensen and A. Jahan-Latibari
Department of Physics
Washington State University
Pullman, Wa. 99164-2814

ABSTRACT

For a wide range of materials the emission of electrons (EE), positive ions (PIE), neutral species (NE), and photons (phE) has been observed accompanying fracture. We refer collectively to these emissions as fracto-emission (FE). In this paper we review our work on fracto-emission from filled and unfilled elastomers. When interfacial failure occurs it appears to lead to highly reactive surface species(perhaps free radicals), and charge separation. Subsequent chemical re ctions in the presence of surface charge produces intense, long lasting (several minutes) emission of charged particles and excited neutral species. The energies of the charged particle emission can be as much as several hundred electron volts. In this paper we describe measurements of the time dependence, energy distributions, crack velocity dependence, time correlations between EE and PIE, and PIE mass. We also discuss the effect of cross-link density on FE intensities.

I. INTRODUCTION

Crack propagation through an insulating material or at an interface produces regions of high electronic and chemical activity on the freshly-created surfaces. This activity causes the emission of particles, i.e. electrons, ions, and neutral species, as well as photons, from the surfaces both during and after crack propagation. This emission is called fracto-emission (FE). Electron emission from deformed materials for particular variations of mechanical stimulation has also been called tribo-stimulated exo-emission and mechano-emission. Photon emission during deformation and/or crack propagation is often referred to as tribo-luminescence.

In this paper we would like to review our work on FE at Washington State University concerning systems involving the fracture of filled and unfilled elastomers. The primary goals of our research have been to characterize fracto-emission from various materials, to further our understanding of the FE mechanisms, and to examine the dependence of FE on the fracture event and material properties. These studies (References 1-15) have included fracture of oxide coatings on Al (1-6), measurements of neutral molecule emission accompanying fracture (3), the examination of FE accompanying adhesive failure (7,9), measurements of the dependence of electron emission (EE) on crack velocity in filled elastomers (8), measurements of the mass of the positive ion emission (PIE) accompanying fracture (10-12), an examination of the time correlation between the EE and PIE being emitted from the same sample (11), and preliminary studies of imaging of EE and PIE coming from fracture surfaces.

FE studies are still quite new and considerable work is necessary to

AD-A132 462 FRACTO-EMISSION FROM POLYMERS(U) WASHINGTON STATE UNIV 1/2
PULLMAN DEPT OF PHYSICS J T DICKINSON JUN 83
N00014-80-C-0213

UNCLASSIFIED F/G 11/9 NL

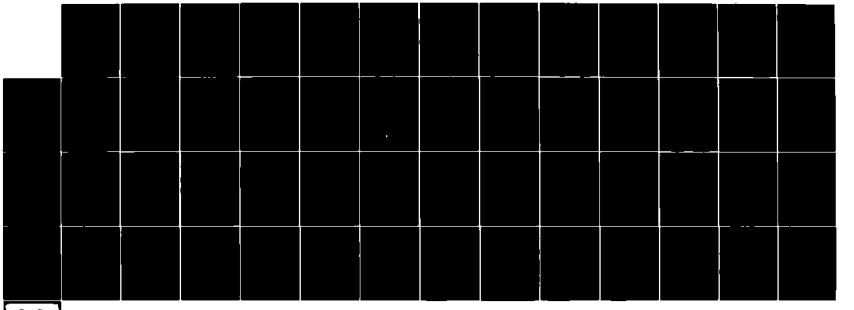

END
DATE FILMED
9 83
DTIC

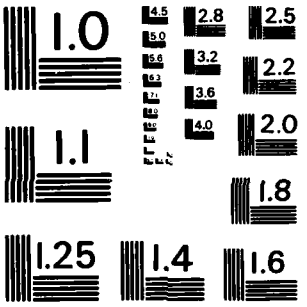

further characterize FE and to understand emission mechanisms. Nevertheless, we can speculate to some extent concerning potential applications to studies of fracture in general. The most obvious application is the sensitive detection of crack formation and growth where broken bonds are in communication with the surrounding vacuum (so that particles can be detected). The formation of surface cracks, crazing, micro-cracking, and finally a running catastrophic crack are examples of detectable events using FE. The motion of a crack as a function of time can be measured over a relatively wide range of time scales. In many cases, particle counting techniques used by nuclear physicists can be employed. We have examined, for example, the fracture of filled elastomers with 1 μs time resolution. Through the use of such techniques, FE may serve as a convenient way to measure the instantaneous crack velocity. Imaging of charged particles using image intensifier technology, as well as sensitive photon detection, may allow the use of FE to determine the location of damage, as well as providing temporal information during straining of a sample.

Examination of the emission kinetics immediately after the separation of the two fracture surfaces may serve as a way to measure the surface temperature at the crack tip. Models we have constructed for the post-fracture emission (or after-emission) all require a temperature rise with fracture that decays exponentially with a decay time of a few seconds.

Furthermore, FE has considerable potential as a probe of the locus of fracture in a multi-component system such as a filled elastomer. The intensity, time dependence, and species emitted appear to be sensitive to where fracture has occurred. For example, FE may be useful for determining when delamination or dewetting have occurred and to what degree.

Finally, FE may relate in important ways to fracture mechanics parameters and chemical bonding phenomena. If reliable connections can be made to such

parameters, FE could be used to measure them on an instantaneous and microscopic scale.

In references 14 and 15, we have reviewed the major characteristics that we have observed in the FE from a wide range of materials, including systems involving interfacial failure and composites. In brief, FE is a wide-ranging phenomenon; the characteristics appear to be sensitive to material properties, mode of fracture, crack velocity, and temperature. The emission mechanisms are not unique for each FE species but appear to involve fracture-induced mechano-chemistry and electrons trapped in shallow surface states produced and filled during fracture. These processes generally involve the consequences of broken bonds and we suggest, therefore, that FE is a probe of the degree of bond breaking that has occurred in producing the fracture surface.

In an elastomer, the degree of bond breaking is strongly dependent on the structure of the material (e.g. cross-link density), as well as the temperature, strain rate, and the presence of interfaces. In this paper we review our observations concerning the FE properties and some factors that influence the FE characteristics for filled and unfilled elastomers.

II. EXPERIMENTAL TECHNIQUES

Here we discuss brifly the general experimental techniques we use in our FE studies, in particular the charged particle work. Because we frequently deal with the detection of particles such as electrons, ions, and neutral molecules it is necessary to work in a vacuum. We have two vacuum systems that use liquid nitrogen trapped diffusion pumps to attain pressures of 1 - 10 x 10^{-5} Pa within a few minutes. We have one ultra-high vacuum system capable of reaching pressures below 10^{-7} Pa with a light bake-out. The latter

system is used in neutral emission studies to minimize interference from background gases in the mass spectra and to investigate the influence of the gaseous environment on the charged particle/photon emissions. The work presented in this paper has shown no evidence of a dependence on background gases in these pressure ranges.

For FE studies, our vacuum systems are equipped with devices to stress samples in various ways including tension, flex, and compression, while measuring stress and/or strain. Most of our experiments are performed in tension. Figure 1 shows a typical experimental arrangement.

The detectors used for charged particles are channeltron electron multipliers (CEM) which produce fast (10 ns) pulses with approximately 90% absolute detection efficiency for electrons and nearly 100% efficiency for positive ions. The gains of the CEM's used were typically 10^6 - 10^8 electrons/incident particle. The detectors were positioned 1 - 4 cm away from the sample with a bias voltage on the front cone of the CEM to attract the charged particles of interest. Background noise counts ranged from 1 to 10 counts/second. Standard nuclear physics data aquisition techniques were employed to count and store pulses, normally as functions of time. The time scales of interest are submicrosecond to several second intervals, which we can easily cover with commercial electronics.

In addition to the above capabilities, we also have a UHV system for the measurement of the neutral molecule emission accompanying fracture, devices for measuring charged particle kinetic energies, and photon detectors for measurements of photon emission accompanying fracture. In this review we will concentrate on our EE and PIE measurements.

The materials to be discussed in this paper include the following:

Samples of isoprene rubber (IR), provided by Alza Corporation, consisted of Goodyear Natsyn 2200 cross-linked with 0.025%dicumyl peroxide compression molded for 20 minutes at 165°C.

Samples of polybutadiene (BR) were provided by The University of Akron, Institute of Polymer Science. They consisted of Diene 35 NFA (Firestone Tire and Rubber Co.), mixed with dicumyl peroxide from 0.025 to 0.075% by weight. Cross-linking was carried out by heating each mixture for 2 hours at 150°C. Some BR samples contained small untreated glass beads 30-95 μm in diameter or 250 - 500 μm in diameter,mixed from 0 - 34% by volume. In addition we examined the peeling detachment of polybutadiene bonded to a macroscopic flat glass surface.

Commercial 50 Durometer Red Silicon Rubber (SI) samples filled 50% by volume with silica particles of irregular shape, typically 10 μm in diameter, and very fine Fe_2O_3 powder were used in the crack velocity studies.

The elastomers were fractured in tension at elongation rates in the range of 0.1 - 20 cm/s. Samples were usually notched so the fracture would occur in front of the detectors.

III. RESULTS AND DISCUSSION

Survey of EE and PIE: The first experiments we performed were to simply fracture various materials either in tension or, for brittle materials, in three point bending and detect the resulting EE and PIE. The integral under

the emission curves was divided by the cross-sectional area to give an intensity per unit area. The time for the emission to decay was also measured (or an upper bound determined when fast decays were not determined). Table I lists the results of this survey for a wide variety of materials including a number of elastomers. We have not examined as many materials for PIE; however it should be mentioned that for the materials examined, EE and PIE appear with approximately equal intensities.

Figure 2 shows the resulting EE (on a log scale) for isoprene rubber (IR) for a sample approximately 20 mm^2 in cross-section. The non-linear decay on a log scale indicates that the emission is not a simple first order process. Model fits of such decay curves indicate a second order, diffusion limited process is involved and a slight temperature rise at fracture is necessary, consistent with fracture-induced heating of the newly created surfaces, which then cool by conduction. Details of these model studies will be published at a later date.

Filled and Unfilled BR: Of considerable interest is the FE from filled materials in comparision to the unfilled material. The locus of fracture often involves the interface between the hard filler particles and the elastomer matrix. When a material such as polybutadiene (BR) filled with untreated glass beads is fractured, SEM studies show that the creation of fracture surfaces in these samples involves a high degree of interfacial failure. The EE and PIE for filled (34% by volume) and unfilled BR are shown in Figure 3. The peak intensity created during fracture and the after-emission are both considerably more intense when the glass beads are present. The detachment of the beads from the polymer tends to happen very quickly, and this interfacial failure is responsible for the enhanced emission. Figure 4 shows the dependence of the total emission (counts accumulated in 200 seconds) on the quantity of glass

beads in BR. Although we have drawn the graphs as straight lines, one sees a slight curvature in the data. Similar data taken with larger glass beads (250 - 500 μm in diameter), as seen in Figure 5, definitely show peaks in both EE and PIE intensities. The larger beads greatly reduce the strength of the material at a lower concentration than do the smaller beads. As a result, a crack begins moving through the material at lower strain and at considerably lower crack velocity. As we shall show in the following paragraphs, this rate of separation of the interfaces can greatly influence the emission intensity.

Crack Velocity: We examined the dependence of EE intensity on the instantaneous crack velocity, V_c, of two filled elastomers: BR and silicone rubber (SI) by measuring the crack-tip position as a function of time and EE intensity simultaneously. The former was done by using a video recorder with the camera imaging the region where the crack was propagating. Measurements of the crack position vs time from each frame (1/60 second) allowed calculation of V_c to values up to 20 cm/s. At a constant strain rate, the crack would accelerate until separation. Figures 6-7 show the resulting EE counts per channel (1 ms) vs. crack velocity for both BR and SI. Figure 6 represents the initial data for low velocities ($\leq$7 cm/s) where non-linear rise is observed. Figure 7 shows both low and high velocities. Comparing the two curves we see the remarkably strong dependence of EE intensity on crack velocity, namely nearly an exponential dependence at higher velocities.

Qualitatively, we have observed in a number of systems involving adhesive failure a strong dependence of FE intensity on the rate the surfaces separate, i.e. crack velocity. This suggests the interface is left in a higher state of non-equilibrium, perhaps because of a higher degree of bond breaking and a higher concentration of free radicals and/or trapped electrons near the

conduction band. This higher concentration may be a consequence of the fact that more rapid loading does not allow local molecular stresses in the region of the interface to be relieved via viscoelastic relaxation mechanisms, leading to a higher degree of bond scissions. These results suggest FE may be a sensitive probe of the microscopic events occuring during fracture.

As a verification that the enhanced, long lasting EE and PIE in the BR filled with glass beads was indeed due to interfacial failure, we obtained samples of the same polymer, cross-linked with 0.075% dicumyl peroxide, in contact with untreated soda-lime glass plates (intended to simulate the surface of the soda-lime glass beads). The elastomer layer, which was only weakly adhering to the glass surface, could be peeled from the glass surface while the FE was monitored with a particle detector. Typical PIE results are shown in Fig. 8, where the time $\mathcal{T}_2$ is the interval over which the peeling occured and during which approximately 2 cm^2 of area was exposed. The emission is once again intense and long-lasting. Qualitatively, the shape of the decay curve holds up longer and the total counts obtained in a 400 sec time interval increased with increasing peel velocity. Results for EE are essentially identical. We thus conclude that the interfacial failure in the BR filled with glass beads is indeed responsible for the intense, long-lasting emission observed and that the rate of surface separation is an important parameter effecting FE.

EE and PIE Time Correlations: Similar to a number of materials examined, in the BR filled glass beads we found identical intensity vs time curves for EE and PIE when the two were normalized at a single point. This result led us to ask if the two types of particles, electrons and positive ions, were possibly coincident in time on a faster time scale. Use of two detectors, as shown in Fig. 9, and associated pulse circuitry (e.g. coincidence circuits) showed that

on time scales of sub-microseconds there was a high degree of real coincidence between EE and PIE. A time correlation could also be found by use of time-interval circuits to measure the time between the detection of an electron and the next positive ion. The resulting Time-Delay Spectrum is shown in Fig. 10 for two different voltages applied to the front cone of the PIE detector. The first peak (0-0.5 μs) is due to positive ions that are in near coincidence with an electron. The width and shift of this peak is due to the finite time-of-flight (TOF) of the ion relative to the negligible TOF of the electron. The peak at 1.5 μs which does not shift with PIE accelerating potential has been assigned to a neutral molecule in an excited state (e.g. a metastable state), perhaps a re-neutralized ion. Thus it appears that a good fraction of the EE and PIE are sharing a common mechanistic step.

PIE Masses: The coincidence between the EE and PIE can be exploited to measure the mass-to-charge ratio of the PIE using a TOF method. Fig. 9 is a schematic diagram of the TOF arrangement with a drift tube of 25 cm in length. By using the electron pulse as a start, the flight time of the positive ion can be measured easily. A TOF spectrum of the PIE from BR filled with glass beads for a drift tube potential of -2 kV is seen in Fig. 11. Four major peaks are observed where positions in time can be shifted with changes in the voltage, V, applied to the drift tube. Analysis of the positions for these four peaks led to the M/q values given in Table II. Also shown are structures of likely fragments from BR which could give such M (assuming q=e). It appears that PIE may include fragments produced from the polymer during fracture.

Cross-link Density: Increasing cross-link density in an elastomer might be expected to cause an increase in particle emission because of the higher density of broken bonds. We have compared the EE and PIE for three different cross-link densities in unfilled polybutadiene, produced by varying the

concentration of diucumyl peroxide (0.025,0.05, and 0.075% by weight). The peak emission (highest count rate reached during fracture) and the total emission acquired (in a 400 second time interval) for both EE and PIE are shown in Fig.12 on a log scale plotted against $1/M_c$, where M_c is the number average molecular weight between cross-links of the BR. The increases in emission are readily seen over this fairly small change in cross-link density. This suggests that the expected increase in bond scissions causes an increase in FE intensity.

To rule out the role of curing agent residues we induced cross-linking in BR by exposure to γ and UV-radiation. Samples of Diene 35 NFA (Firestone Tire and Rubber Co.) were pressed at 100°C for 1 minute to create thin sheets of weakly cross linked BR. Some of these samples were then exposed to radiation. The γ-radiation was a calibrated 3000 Curie ^{60}Co source, and exposures were for 24 hours. The UV source was a laboratory Hg lamp rich in 2500 Å UV light. UV intensities were not measured but exposures were carried out at a constant distance (20 cm) for 24 hours. The cross-link densities of these materials were not measured but the exposed samples were considerably stronger, indicating an increased number of linkages. In Fig. 13 we see the resulting EE curves for the unexposed BR as well as the exposed samples showing the dramatic differences in intensity induced by radiation.

IV. DISCUSSION AND CONCLUSIONS

We have tried to show a variety of EE and PIE results on a number of systems involving fracture of filled and unfilled elastomers and consider some of the parameters that are influencing this emission. The need for careful studies of the physics and chemistry of these phenomena is obvious. The

usefulness of FE as a tool for investigation of failure mechanisms and fracture phenomena in elastomers requires a broad-based attack combining fracture mechanics, materials science, and fundamental fracto-emission studies on well-characterized elastomers. Since the field is relatively unexplored, we will conclude by speculating on some potential areas of usefulness of FE, many of which depend critically on further understanding of FE itself.

POTENTIAL APPLICATIONS OF FE

1. A probe of crack growth on an extremely wide range of time scales. This crack growth need not be catastrophic fracture and might involve crazing, micro-cracking, linking of microcracks, and other pre-failure events.

2. A probe of the departure of the fracture surface from equilibrium. As the surface charge and defects/free radicals decay away, FE may well be a measure of the initial concentrations and the rate of surface reactions such as free radical recombination.

3. The energies of the FE components may serve as a measure of the density of the charge distributions created on the fracture surface.

4. FE may serve as a way to measure the surface temperature at the crack tip by careful modeling of the emission curves at short times after fracture. Our modeling to date has required an elevated temperature of fracture that decays quickly away.

5. FE may serve as a means of measuring instantaneous crack velocity.

6. FE may serve as a probe of the locus of fracture in composite materials e.g. filled elastomers, and help in illuminating failure mechanisms. The roles of contact charging and chemical bonding in [illegible] may be determined by FE studies.

7. FE may serve as an NDT tool, perhaps in conjuction with acoustic emission. FE would be particularly useful when sensitivity to events near the surface is desired.

8. FE may be related in important ways to fracture mechanics parameters such as surface energy, fracture strength, or fracture toughness. If reliable connections could be made to such parameters, FE might be used to measure them.

VII. ACKNOWLEDGEMENTS

We wish to thank E. E. Donaldson and B. H. Carroll for their contributions to this work. We also wish to thank A.N. Gent, University of Akron Institute of Polymer Science, for contributing the polybutadiene samples, and H. M. Leeper, Alza corporation, for the isoprene samples.

This work was supported by the Office of Naval Research contract N0014-80-C-0213 and a grant from the M. J.Murdock Charitable Trust.

REFERENCES

1. J. T. Dickinson, P. F. Braunlich, L. Larson, and A. Marceau, Appl. Surf. Sci. 1, 515 (1978).

2. D. L. Doering, T. Oda, J. T. Dickinson, and P. F. Braunlich, Appl. Surf. Sci. 3, 196 (1979).

3. L. A. Larson, J. T. Dickinson, P. F. Braunlich, and D. B. Snyder, J. Vac. Sci. Technol. 16, 590 (1979).

4. J. T. Dickinson, D. B. Snyder, and E. E. Donaldson, J. Vac. Sci. Technol. 17, 429 (1980).

5. J. T. Dickinson, D. B. Snyder, and E. E. Donaldson, Thin Solid Films 72, 225 (1980).

6. J. T. Dickinson, E. E. Donaldson, and D. B. Snyder, J. Vac. Sci. Technol. 18, 238 (1981).

7. J. T. Dickinson, E. E. Donaldson, and M. K. Park, J. Mat. Sci. 16, 2897 (1981).

8. J. T. Dickinson and L. C. Jensen, J. Polymer Sci. Polymer Physics Ed., in press.

9. J. T. Dickinson, M. K. Park, E. E. Donaldson, and L. C. Jensen, J. Vac. Sci. Technol. 20, 436 (1982).

10. J. T. Dickinson, L. C. Jensen, and M. K. Park, J. Mat. Sci., in press.

11. J. T. Dickinson, L. C. Jensen, and M. K. Park, Appl. Phys. Letters 41, 443 (1982).

12. J. T. Dickinson, L. C. Jensen, and M. K. Park, Appl. Phys. Letters 41, (1982) in press.

13. H. Miles and J. T. Dickinson, Appl. Phys. Letters 41, (1982) in press.

14. J. T. Dickinson, to appear in Proceedings of the Symposium on Recent Developments in Adhesive Chemistry, ACS Seattle, 1983.

15. J. T. Dickinson, A. Jahan-Latibari, and L. C. Jensen, to appear in the Proceedings of the Symposium on Polymer Composites, Interfaces, ACS Seattle, 1983.

LIST OF TABLES

TABLE I .--Survey of Materials Investigated for EE and PIE

ELECTRONS

Materials	Approx. Decay Times of Fracto-Emission	Electrons Detected/ cm^2
INORGANIC		
Sapphire	<1 s, minutes	10^3
Alumina	<1 s, minutes	10^4
Al_2O_3 Anodized Layer	.1 - 20 μsec	10^5
BN	<1 s, minutes	10^6
Quartz	<1 s, minutes	10^6
LiF	<1 s	10^4
Mica (Muscovite)	<1 s, minutes	10^6
NaCl	<1 s	10^5
MgO	<1 s	10^5
Fused Silica	Several ms	10^3
Soda Lime Glass	Several ms	10^3
PZT	<1 s	10^6
Graphite	<1 s	10^2
ORGANIC CRYSTALS		
HMX	<1 s	10^4
PETN	<10 ms	10^4
Sucrose	Minutes	10^6
FIBERS		
Kevlar	45 μs	10^8
Graphite	10 μs	10^8
E-Glass	10 μs	10^8
S-Glass	10 μs	10^8
SiC	<10 μs	10^8
Al_2O_3	<1 ms	10^8
PLASTICS		
Epoxy (DER 332)	25 μs	10^3
Polymide	<1 s	10^5
PMMA	<50 μs	10^2
Lucite	<2 ms	10^2
PET Fibers	<1 s	10^5
Polystyrene	500 μs, 12.3 μs	10^3
Polyethylene	<1 s	10^4
PVF_2	<1 ms	10^3

TABLE I (continued)

POSITIVE IONS

Material	Approx. Decay Times of Fracto-Emission	Ions Detected/ cm^2
INORGANIC		
Mica (Muscovite)	1 s, minutes	10^6
FIBERS		
Kevlar 49	45 μs	10^8
Carbon	10 μs	10^8
E-Glass	10 μs	10^7
S-Glass	11 μs	10^8
PLASTICS		
Epoxy (DER 332)	25 μs	10^3
Polyurethane		10^6
Lucite	<2 msec	10^2
Polystyrene	35 μs	10^4
Nylon 66	<1 s	10^4
ELASTOMERS		
Buna N	<1 s, minutes	10^3
Natural Rubber	<1 s	10^4
Natural Rubber (abraded)	Minutes	10^7
Silicone Rubber	<1 s, minutes	10^3
Solithane	<.1 s	10^6
Vinyl Rubber-filled	<1 s, minutes	10^5
Polybutadiene	<.04 s, minutes	10^5
Polybutadiene-filled	<.2 s, minutes	10^6
SBR-filled	<1 s	10^6

TABLE I (continued)

Materials	Approx. Decay Times of Fracto-Emission	Electrons Detected/cm^2
ELASTOMERS		
Neoprene	<1 s	10^2
Viton	<1 s	10^3
Buna N	<1 s	10^2
Natural Rubber	<1 s	10^3
Natural Rubber (abraded)	Minutes	10^7
Silicone Rubber	<1 s, minutes	10^5
Solithane	<.2 s	10^4
Vinyl Rubber-filled	<1 s, minutes	10^4
Polybutadiene	0.04 s, minutes	10^3
Polybutadiene-filled	<1 s, minutes	10^7
Nylon-66	<1 s	10^4
Isoprene	<1 s	10^6
Amber Rubber	<1 s	10^5
BAMO	<1 s	10^4
FIBER-EPOXY COMPOSITE		
Graphite	<1 ms	10^5
Al_2O_3	<1 s	10^7
Kevlar	<1 s	10^6
E-Glass	<1 s	10^6

TABLE II .--Ions from Polybutadiene

Peak	$\frac{M}{q}$ $\frac{amu}{e}$		Possible Fragments
A	85 ± 6	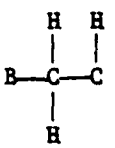	(81)
B	123 ± 6	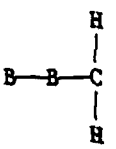	(122)
C	170 ± 6	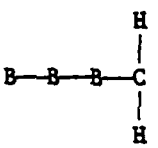	(176)
D	230 ± 6	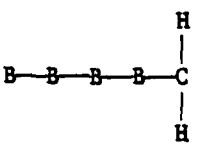	(230)

Figure Captions

1. Schematic diagram of experimental arrangement for fracto-emission investigations.

2. EE from the fracture of isoprene(IR).

3. EE and PIE from the fracture of polybutadiene with and without glass beads.

4. Total emission (counts accumulated over 200 s) as a function of the percent of glass beads (30-95 μm in diameter) in polybutadiene.

5. Total emission (counts accumulated over 200 s) as a function of the percent of glass beads (250-500 μm in diameter) in polybutadiene.

6. EE vs crack velocity on a linear scale for the first part of the velocity scale. The data shown for SI are from two samples.

7. EE vs crack velocity on a linear scale for the complete range of low and high velocities.

8. PIE from the peeling of polybutadiene from a soda-lime plate glass surface.

9. Schematic illustration of the experimental apparatus for a) time correlations and b) time-of-flight (TOF) measurements. The distances are d_1=1 cm, d_2=25 cm.

10. Time-delay spectrum of the particles detected at the CEM-PIE relative to the electrons detected at the CEM-EE. The two curves are for two different voltages applied to the front cone of the CEM-PIE. The peak at 1.5 μs did not shift with this voltage, implying an exited neutral molecule.

11. A typical TOF distribution for PIE from polybutadiene filled with glass beads. The drift tube was at -2 kV. Four major peaks labeled A, B, C, and D are observed.

12. The peak and total EE and PIE from polybutadiene for three different cross-link densities. The letters A, B, and C represent samples cross-linked with 0.025, 0.05, and 0.075% by weight dicumyl peroxide.

13. The effect of cross-linking with radiation on EE from polybutadiene. The very small emission was from a weakly cross-linked sample of Diene 35 NFA; the high emission is from the same material exposed to γ and UV radiation.

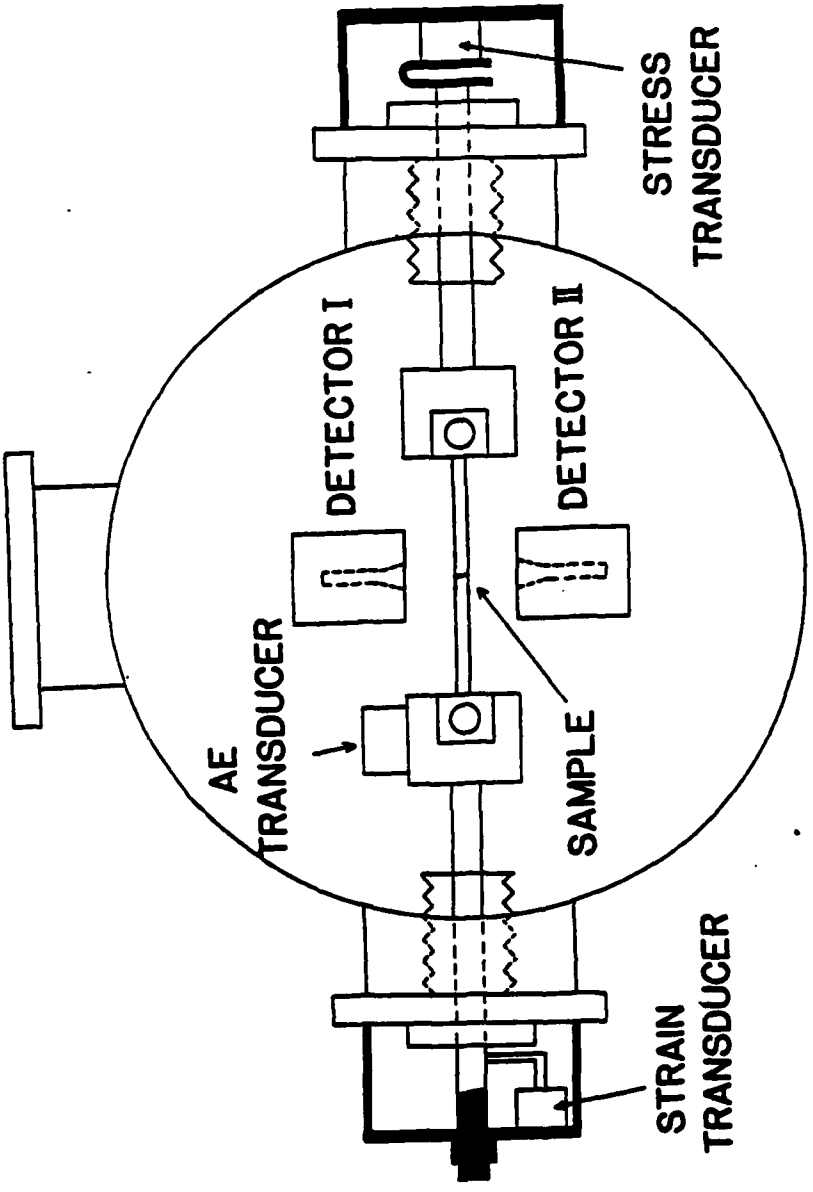

EXPERIMENTAL CONFIGURATION

Fig 1

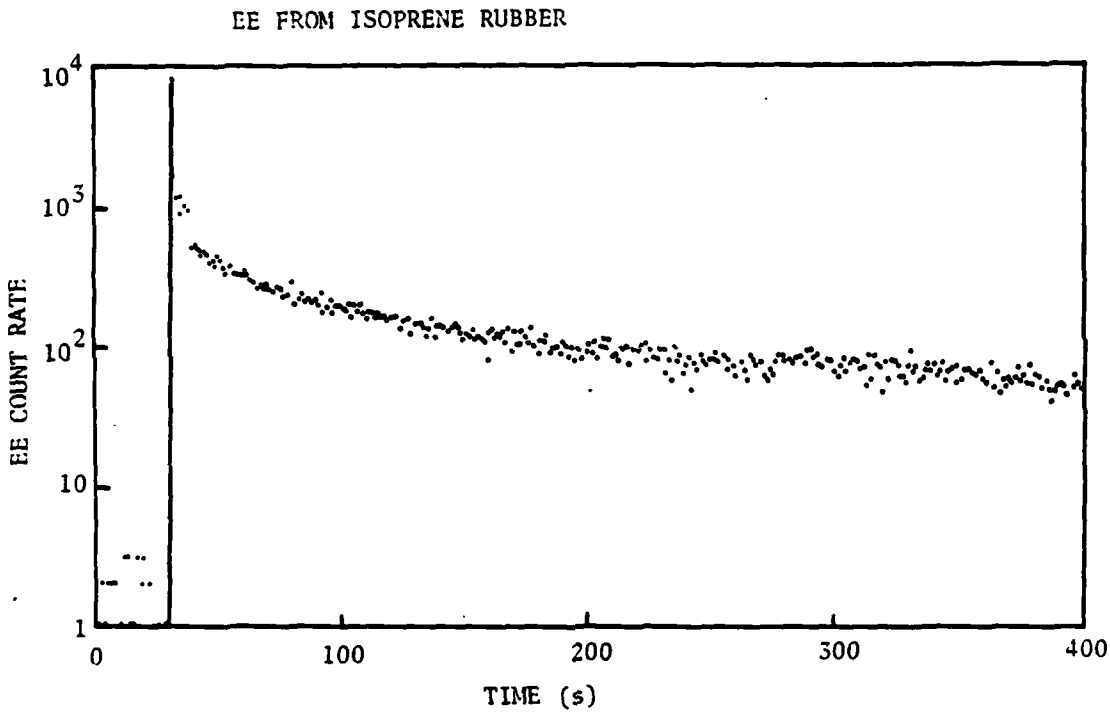
EE FROM ISOPRENE RUBBER
EE COUNT RATE
10^4
10^3
10^2
10
1
0
100
200
300
400
TIME (s)

Fig. 2

Fig. 9, and associated pulse circuitry (e.g. [illegible]

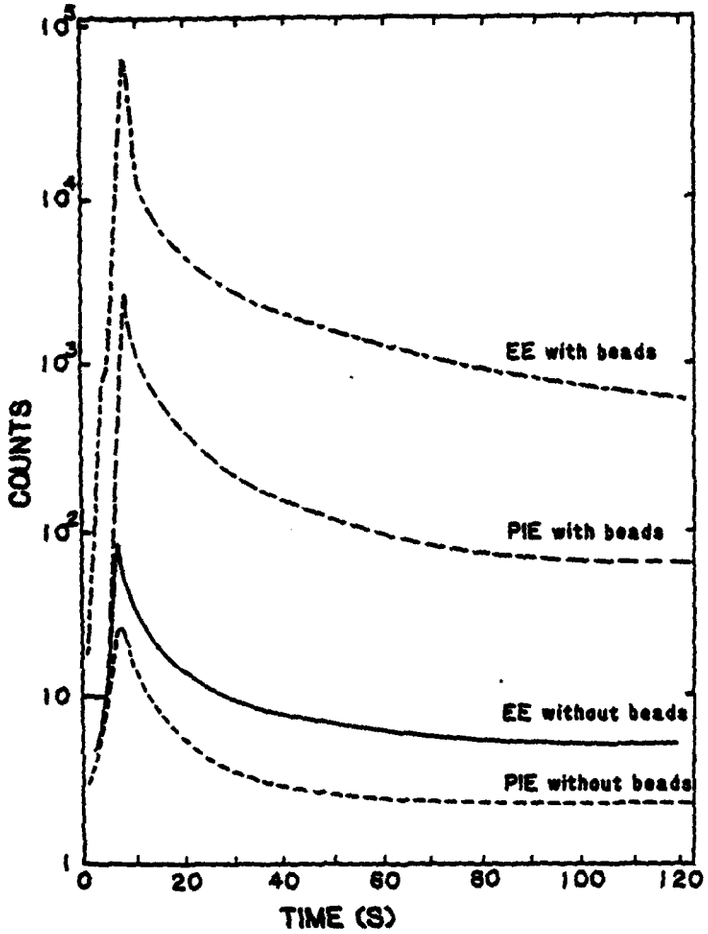

Fig 3

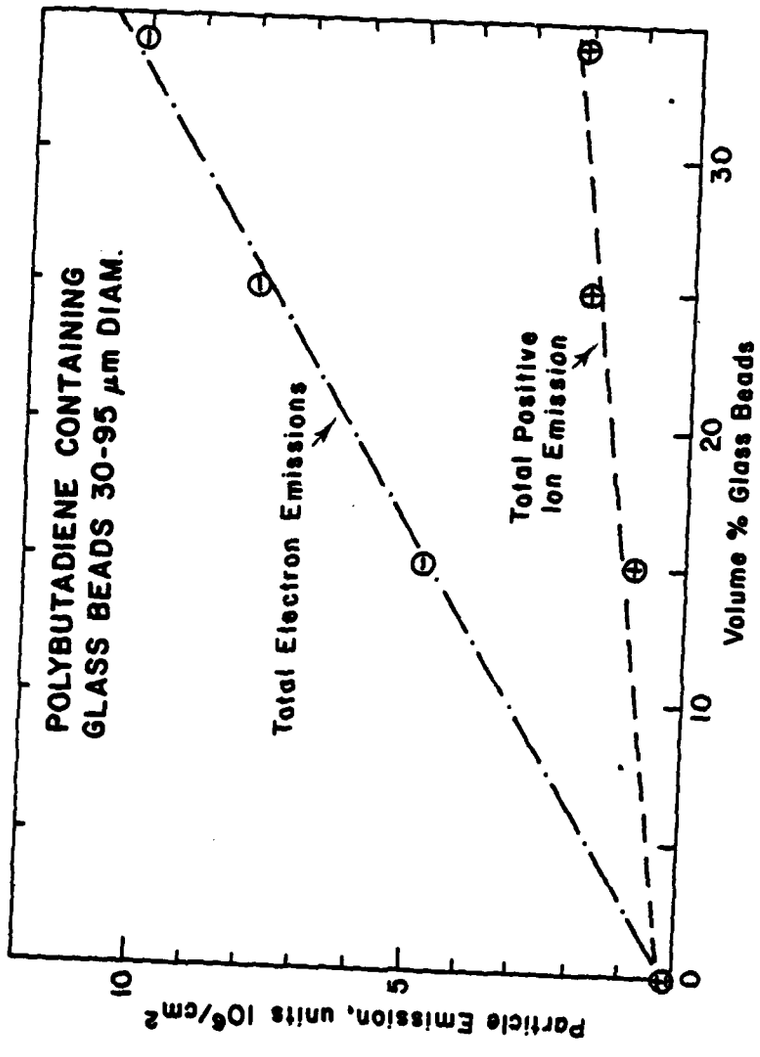
POLYBUTADIENE CONTAINING
GLASS BEADS 30-95 μm DIAM.
Total Electron Emissions
Total Positive
Ion Emission
Particle Emission, units 10⁶/cm²
Volume % Glass Beads
0
10
5
10
20
30

Fig. 4

Fig. 4

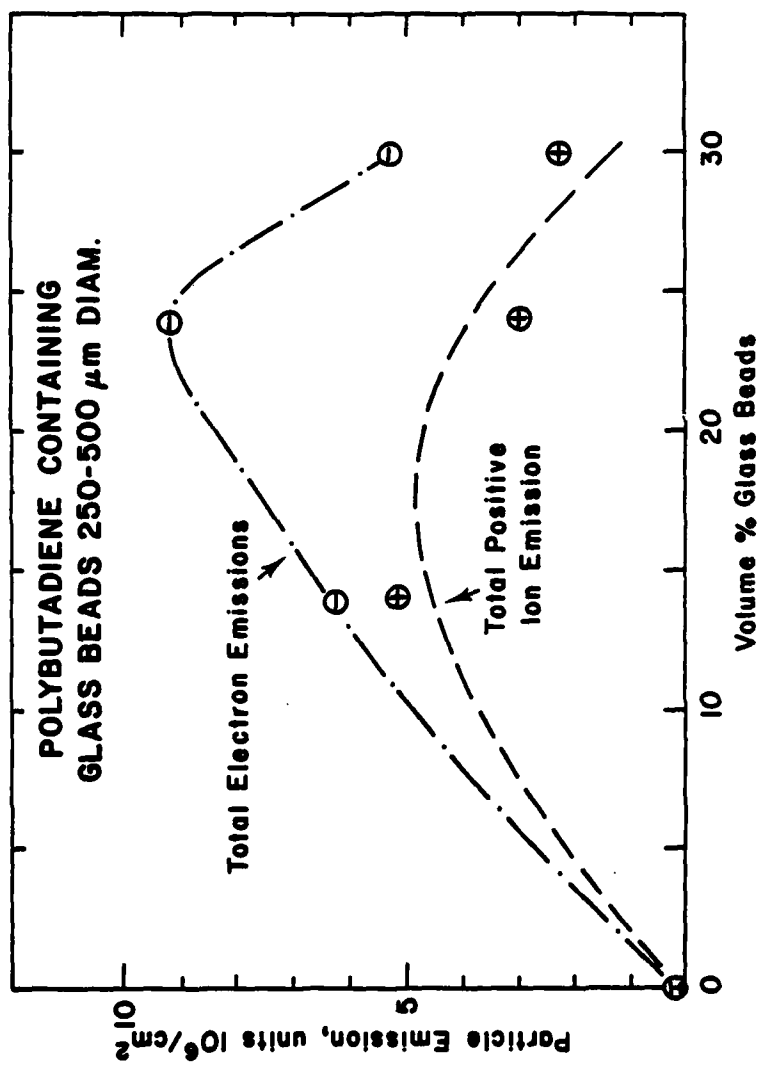
POLYBUTADIENE CONTAINING
GLASS BEADS 250-500 μm DIAM.
Total Electron Emissions
Total Positive
Ion Emission
Particle Emission, units $10^6/cm^2$
0
5
10
0
10
20
30
Volume % Glass Beads

Fig. 5

Figs

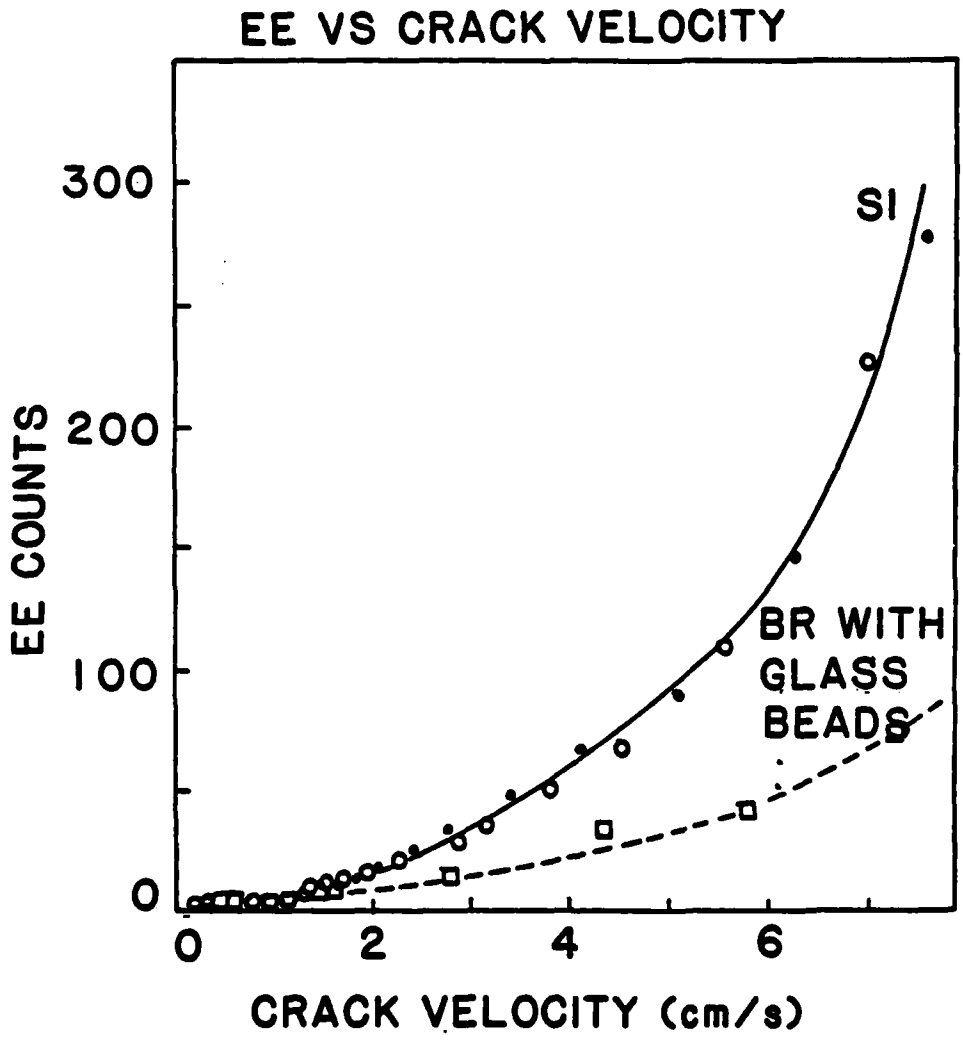
EE VS CRACK VELOCITY
EE COUNTS
300
200
100
0
0
2
4
6
CRACK VELOCITY (cm/s)
SI
BR WITH
GLASS
BEADS

Fig 6

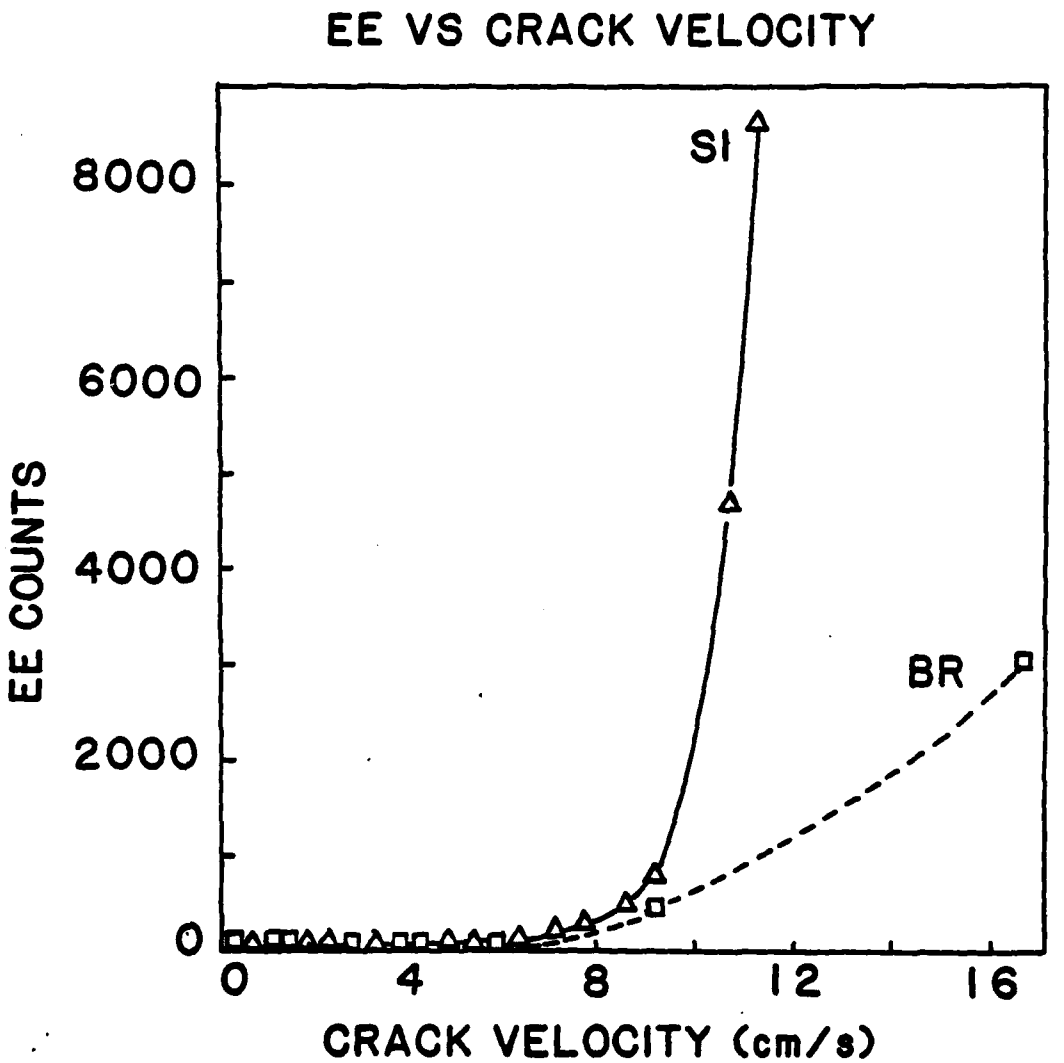
EE VS CRACK VELOCITY
SI
BR
8000
6000
4000
2000
0
EE COUNTS
0
4
8
12
16
CRACK VELOCITY (cm/s)

Fig 7

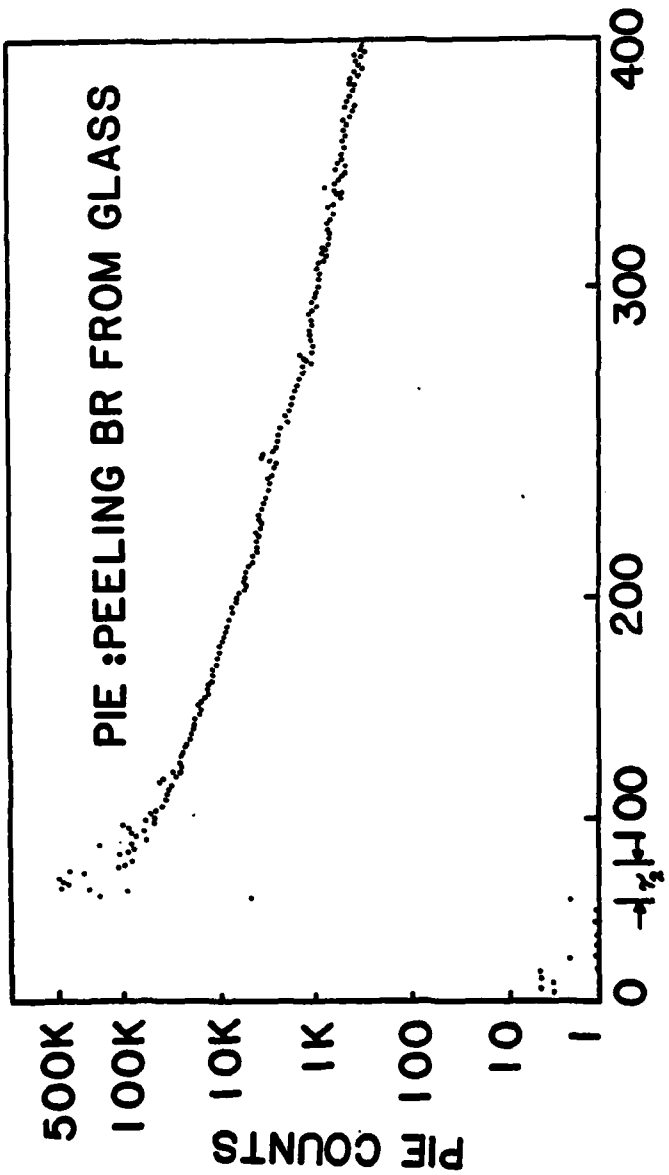
PIE :PEELING BR FROM GLASS
PIE COUNTS
500K
100K
10K
1K
100
10
1
0
100
200
300
400
TIME(s)

(a)

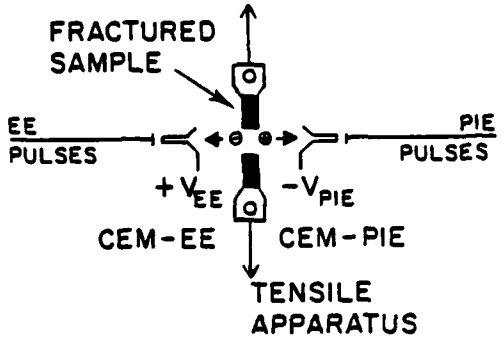
FRACTURED
SAMPLE
EE
PULSES
PIE
PULSES
+V_EE
-V_PIE
CEM-EE
CEM-PIE
TENSILE
APPARATUS

(b)

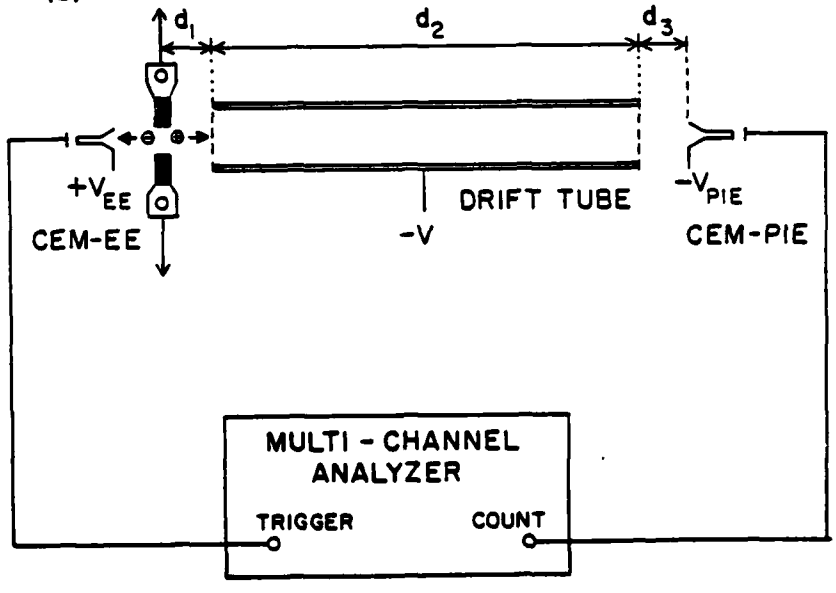
d1
d2
d3
+V_EE
CEM-EE
DRIFT TUBE
-V
-V_PIE
CEM-PIE
MULTI - CHANNEL
ANALYZER
TRIGGER
COUNT

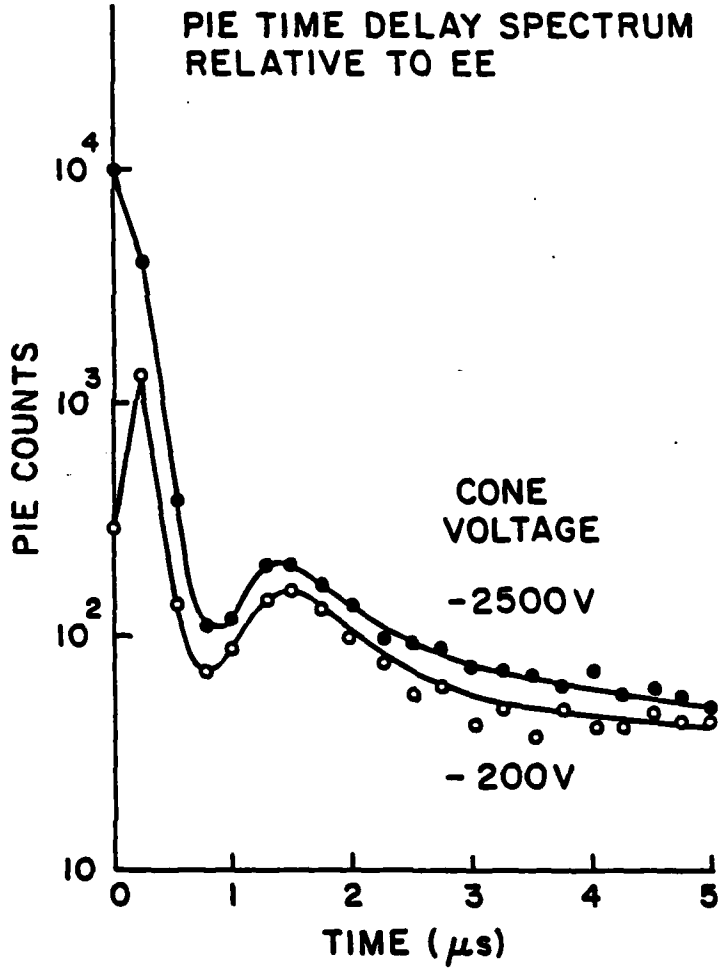
PIE TIME DELAY SPECTRUM
RELATIVE TO EE
PIE COUNTS
10^4
10^3
10^2
10
CONE
VOLTAGE
-2500V
-200V
0
1
2
3
4
5
TIME (μs)

Fig. 20

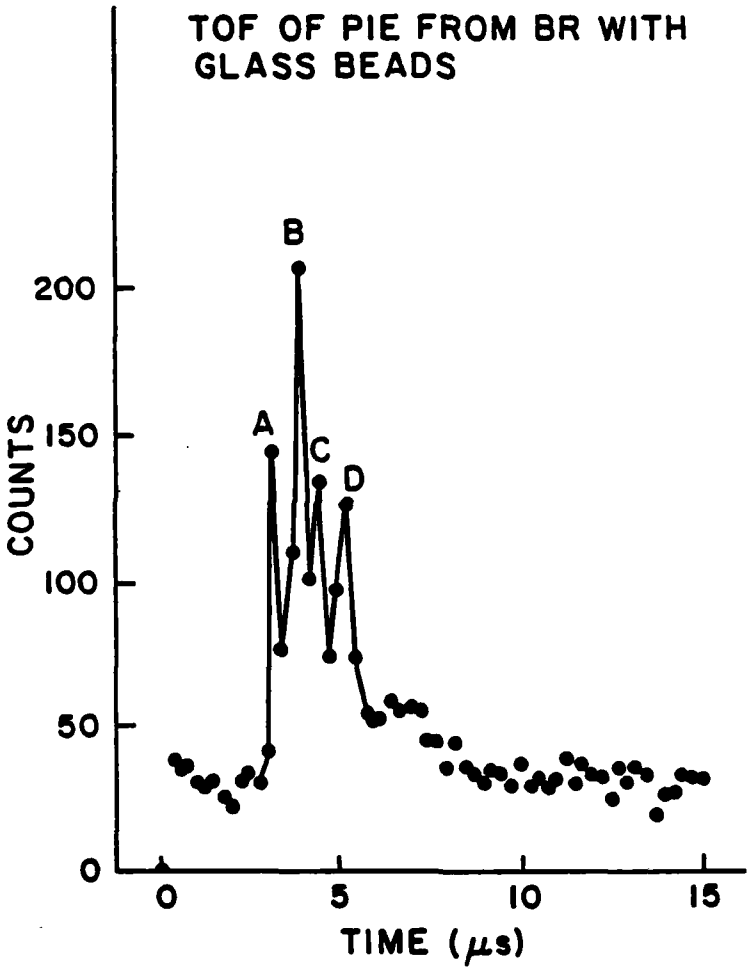
TOF OF PIE FROM BR WITH
GLASS BEADS
COUNTS
200
150
100
50
0
A
B
C
D
0
5
10
15
TIME (μs)

Fig 11

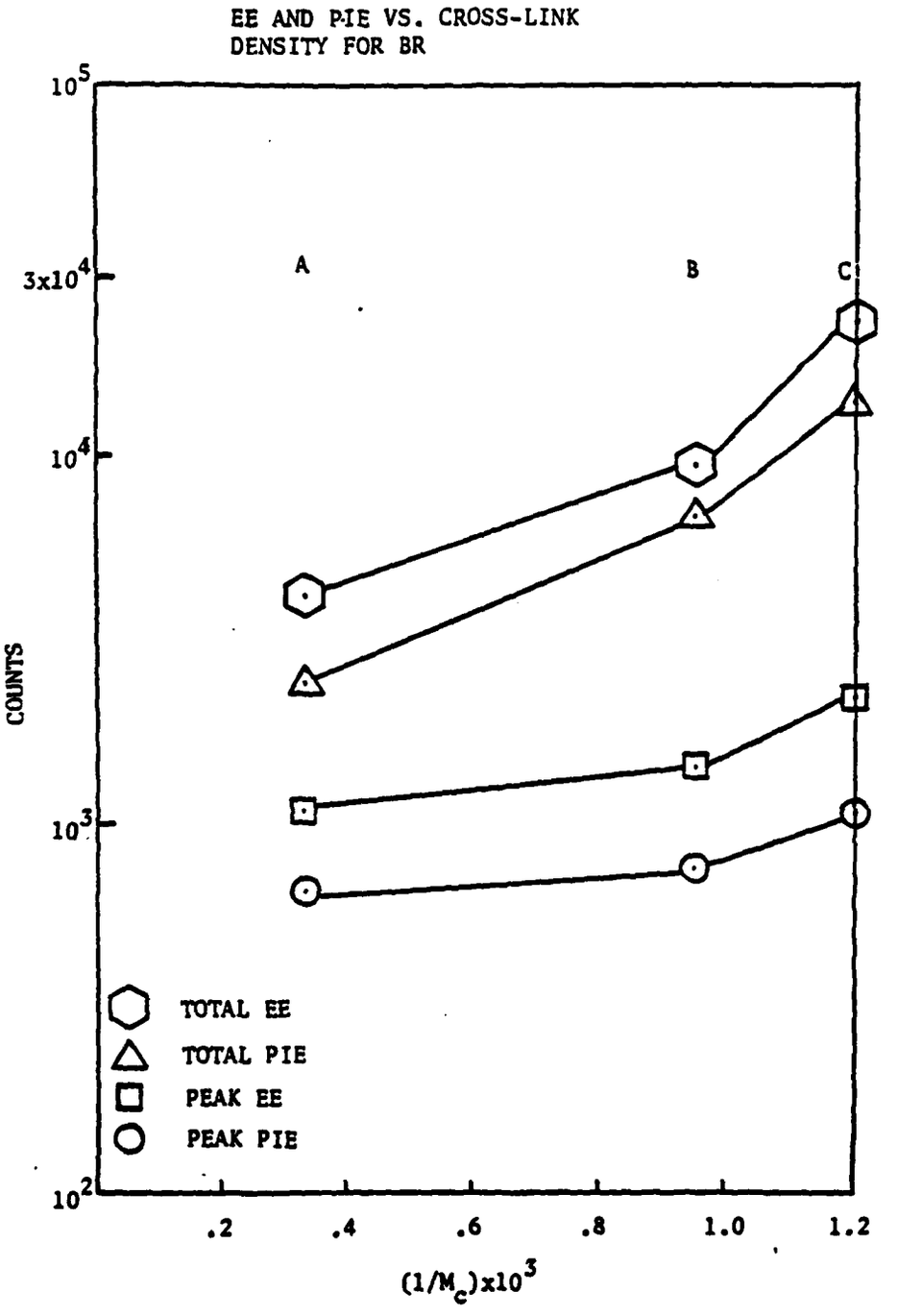
EE AND PIE VS. CROSS-LINK DENSITY FOR BR
10^5
$3x10^4$
10^4
10^3
10^2
A
B
C
COUNTS
TOTAL EE
TOTAL PIE
PEAK EE
PEAK PIE
.2
.4
.6
.8
1.0
1.2
$(1/M_c)x10^3$

Fig. 12

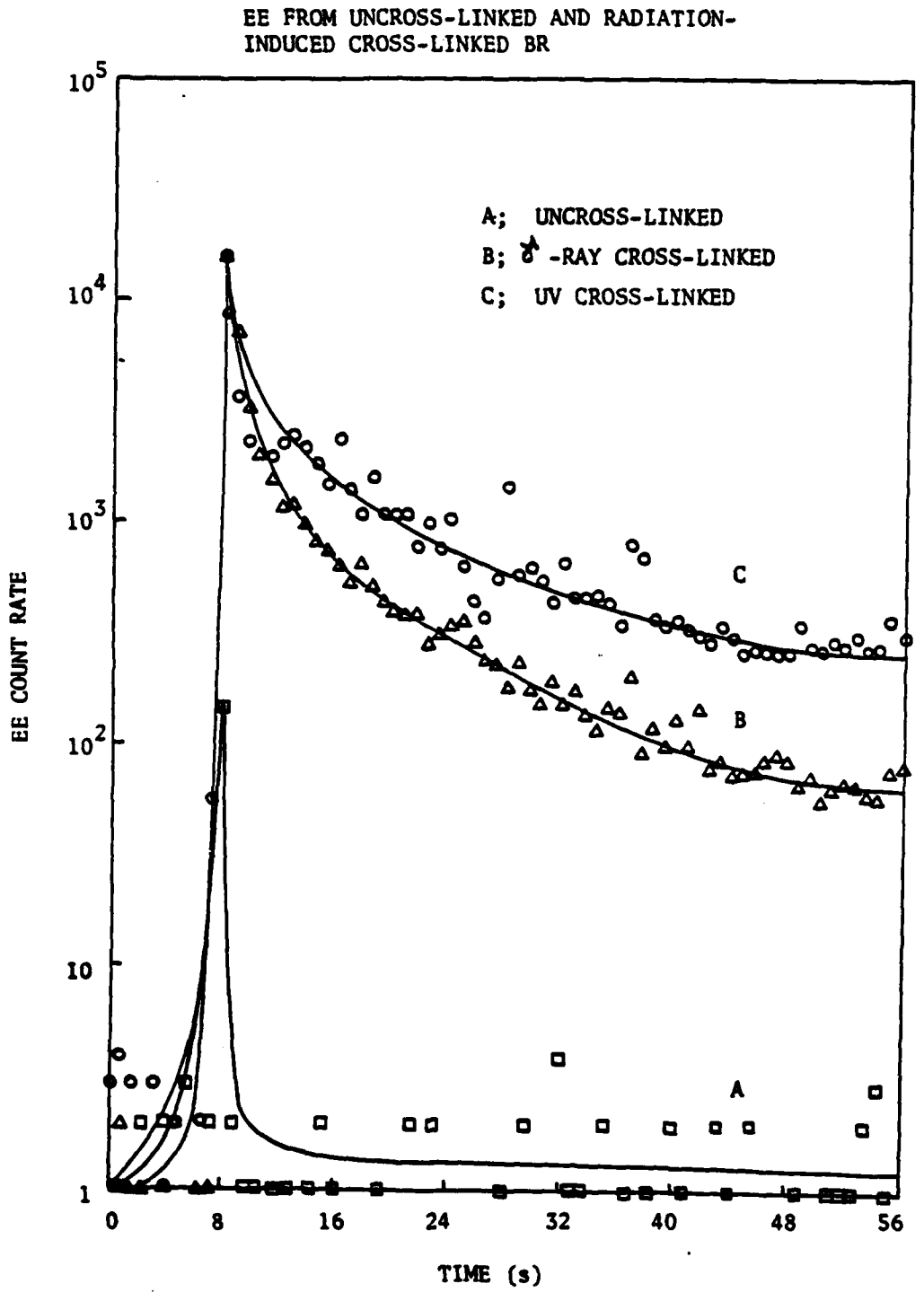
EE FROM UNCROSS-LINKED AND RADIATION-INDUCED CROSS-LINKED BR
A; UNCROSS-LINKED
B; γ-RAY CROSS-LINKED
C; UV CROSS-LINKED
EE COUNT RATE
TIME (s)
10^5
10^4
10^3
10^2
10
1
0
8
16
24
32
40
48
56
A
B
C

Fig. 13

VIII. WORK IN PROGRESS

The following is a summary of some of our work in progress and our intentions for future research:

1. BAMO/THF: We have measured the EE and NE from a copolymer of 3,3-bis (azidomethyl) oxetane (BAMO) and tetrahydrofuran (THF). This material was provided by Y. Gupta, Washington State University. Both components of FE had a strong strain-rate dependence, showing increasing emission with increasing strain rates over a range of elongation rates extending from 0.05 cm/s to 200 cm/s. The EE from a piece of BAMO/THF with a cross-section of 2 mm x 5 mm, elongated at approximately 100 cm/s, is shown in Fig. 1. The after-emission (following separation) observed here is entirely missing from samples which are fractured slowly; at this point we do not know why.

The fracture-induced NE mass peaks from BAMO/THF that we have examined so far with a quadrupole mass spectrometer are: 28 (N_2), 15 (CH_3), 18 (H_2O), and 19 (F?). Other than mass 19, the peak assignments are those of Farber. In Fig. 2 we show the changes in total pressure and mass 28 peaks accompanying fracture of BAMO/THF for two different elongation rates. The mass spectrometer and recorder sensitivities are identical for the two rates. As can be seen, there is a substantial increase in both total pressure and N_2 released during fracture.

Prior to fracture we have heated the BAMO/THF to 100°C for two hours to outgas the material (considerable gas including N_2 was released). Subsequent fracture still yielded the same bursts.

Although not conclusive, these results do support the hypothesis that the N_2 observed is due at least in part to fracture-induced decomposition. Further studies to prove or disprove this idea are in progress.

2. Inorganic Crystals: Our initial work on fracture of inorganic crystals has been done on LiF, MgO, and MgF_2. The purpose of these studies is to probe possible mechanisms of hot spot production in explosive crystals, using model inert materials. K. C. Yoo, University of Maryland, has provided crystals of these materials with known crystallographic orientations. We have fractured the materials in a three-point flexure mode. The emission curves shown in Figs. 3a and b are the EE count rates vs. time, taken simultaneously on two different time scales, from the fracture of MgO. The crystal was strained in such a manner that the fracture surface would tend to be a (100) surface.

The emission appears to be of average intensity for pure, crystalline, inorganic materials, e.g. alkali halides. The observed rapid decay suggests a relatively low activation energy for the emission rate-limiting step

In MgF_2 we have observed a striking difference in the emission intensities for two different crystal orientations. In light of the model presented in section III, this difference may be related to differences in charge separation and/or gases desorbed into the crack tip changing the intensity of the gas discharge occurring during fracture. Incidentally, we have observed evidence of this discharge occurring during the fracture of MgO (e.g. RE and phE during fracture).

A number of experiments on these crystalline materials are planned in

order to gain further understanding of the role of defects, dislocation motion, and crack velocity in the energetics of creating fracture surfaces in crystalline materials.

3. Filled and Unfilled Polyurethane: Gene Martin from NWC, China Lake, has sent us small pieces of polyurethane made from R45M (ARCO-produced hydroxyl-terminated polybutadiene) containing 1% antioxidant, and cured with IPDI (3-isocyanate-methyl-3,5,5-trimethylcyclohexyl-isocyanate).

We have also received polyurethane filled with glass beads, both treated and untreated, and will begin to study these samples soon. The unfilled material is quite soft and sticky at room temperature; if pressed against a solid surface, such as a metal, it adheres quite strongly.

When the unfilled polyurethane (2 mm x 5mm notched samples) is fractured in tension in a vacuum, only a small amount of electron emission is observed (see Fig. 4). However, the polyurethane would occasionally slip during elongation in the metal clamps, and this resulted in much more intense emission. Suspecting that the increased emission might be due to contact charging at the polymer/metal interface, we investigated the emission which occurs when a sample of polyurethane was pressed against metal or glass and then peeled from the surface. The resulting electron and photon emission curves are shown in Figs. 5a and 5b (metal), and Figs. 6a and 6b (glass). The amount of electron emission is considerably higher than in the case of cohesive failure and has a long decay time (typically hundreds of seconds). The intensity is also dependent on the time of contact prior to separating the surfaces, increasing with longer contact times.

Accompanying the peak electron emission, just as the sample is being pulled off the surface, we see a burst of photons whose characteristics are consistent with an electrical breakdown at the interface. We are continuing these polymer-surface interface studies, and will next look at filled polyurethane to see whether the emission produced by this material during fracture is consistent with our observations on interfacial failure.

4. Interfacial Failure Between Polybutadiene and Glass: In the case of polybutadiene (BR) filled with small glass beads, we saw a strong dependence of emission intensity (both during and after fracture) on the presence and concentration of the filler particles. The EE and PIE curves for filled and unfilled BR are shown in Fig. 7, where the concentration of glass beads for the filled material is 34% by volume. A number of supporting experiments have shown that the likely cause of the observed increase in both peak and after-emission is the interfacial failure between the polymer and glass surfaces. This leads to intense charge separation, with subsequent particle bombardment of the fracture surfaces as discussed in Section III.

We have recently performed peel tests between macroscopic surfaces of BR (samples provided by Alan Gent, University of Akron) and soda-lime plate glass. The EE and PIE observed (taken separately) during and after peeling of 1 cm^2 of BR from the glass are shown in Fig. 8. The total EE and PIE for a 400 second time interval are 12.4×10^6 and 8.5×10^6, respectively. The strong, long-lasting emission observed from this interfacial (or adhesive) failure supports the hypothesis that this type of failure is responsible for the intense emission from filled

materials.

Figure Captions

Fig. 1. Electron emission accompanying fracture of BAMO/THF at a high strain rate.

Fig. 2. Neutral emission (mass 28 and total pressure) accompanying fracture of BAMO/THF.

Fig. 3. Electron emission on two different time scales from the fracture of single-crystal MgO.

Fig. 4. EE from the fracture of unfilled polyurethane.

Fig. 5. (a) Electron and (b) photon emission during and following the separation of polyurethane from a stainless steel substrate.

Fig. 6. (a) Electron and (b) photon emission during and following the separation of polyurethane from a glass substrate.

Fig. 7. EE and PIE from the fracture of filled and unfilled polybutadiene.

Fig. 8. Electron and positive ion emission during and following the separation of BR from a glass substrate.

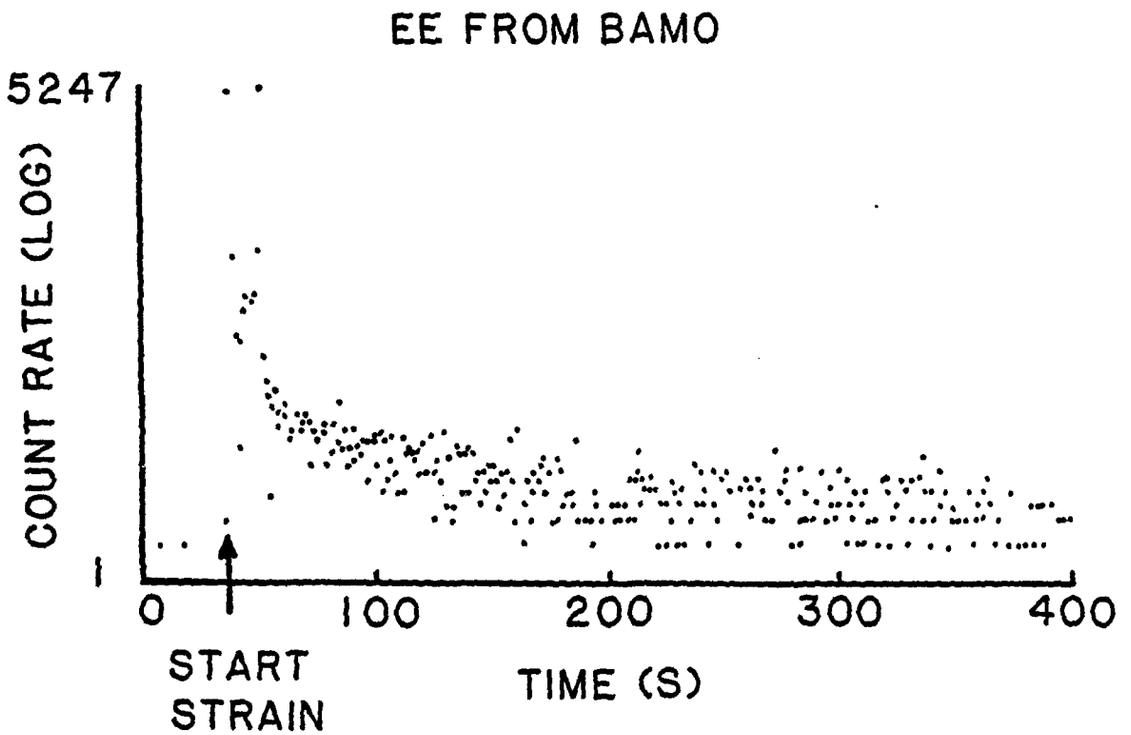
EE FROM BAMO
5247
1
COUNT RATE (LOG)
0
100
200
300
400
START
STRAIN
TIME (S)

Fig 1

NEUTRAL EMISSION FROM BAMO

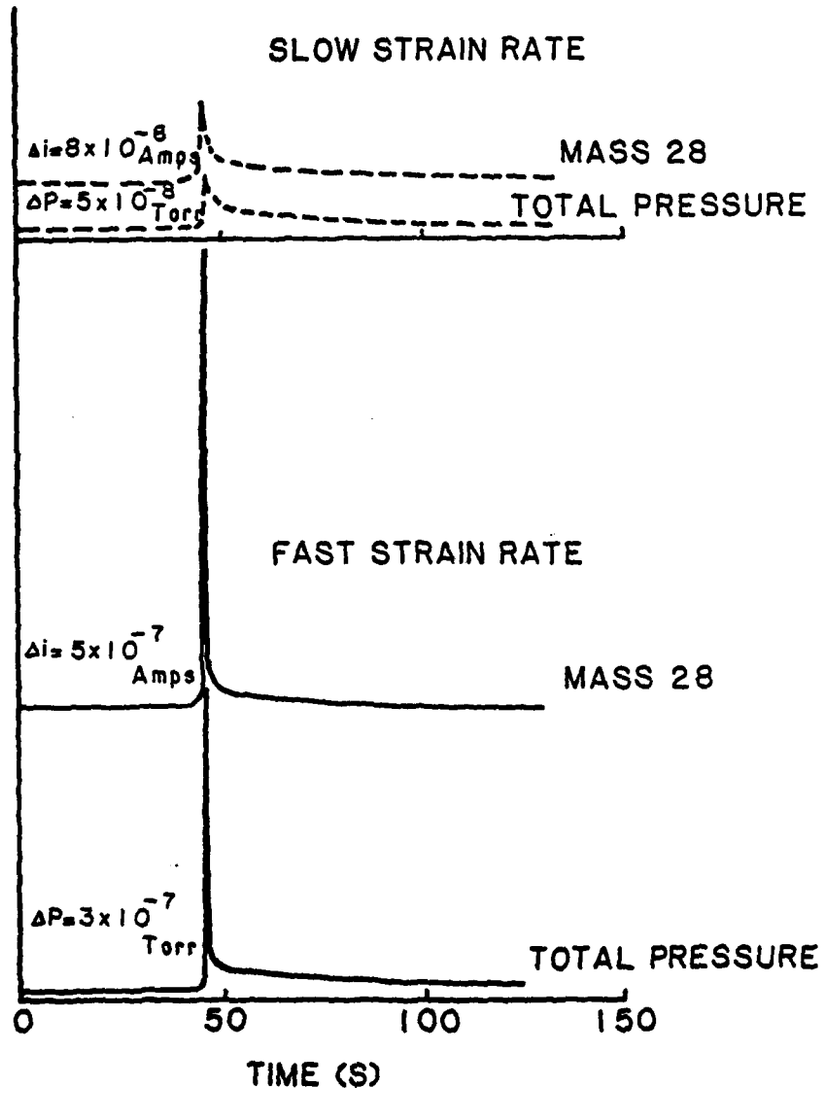

Fig 25

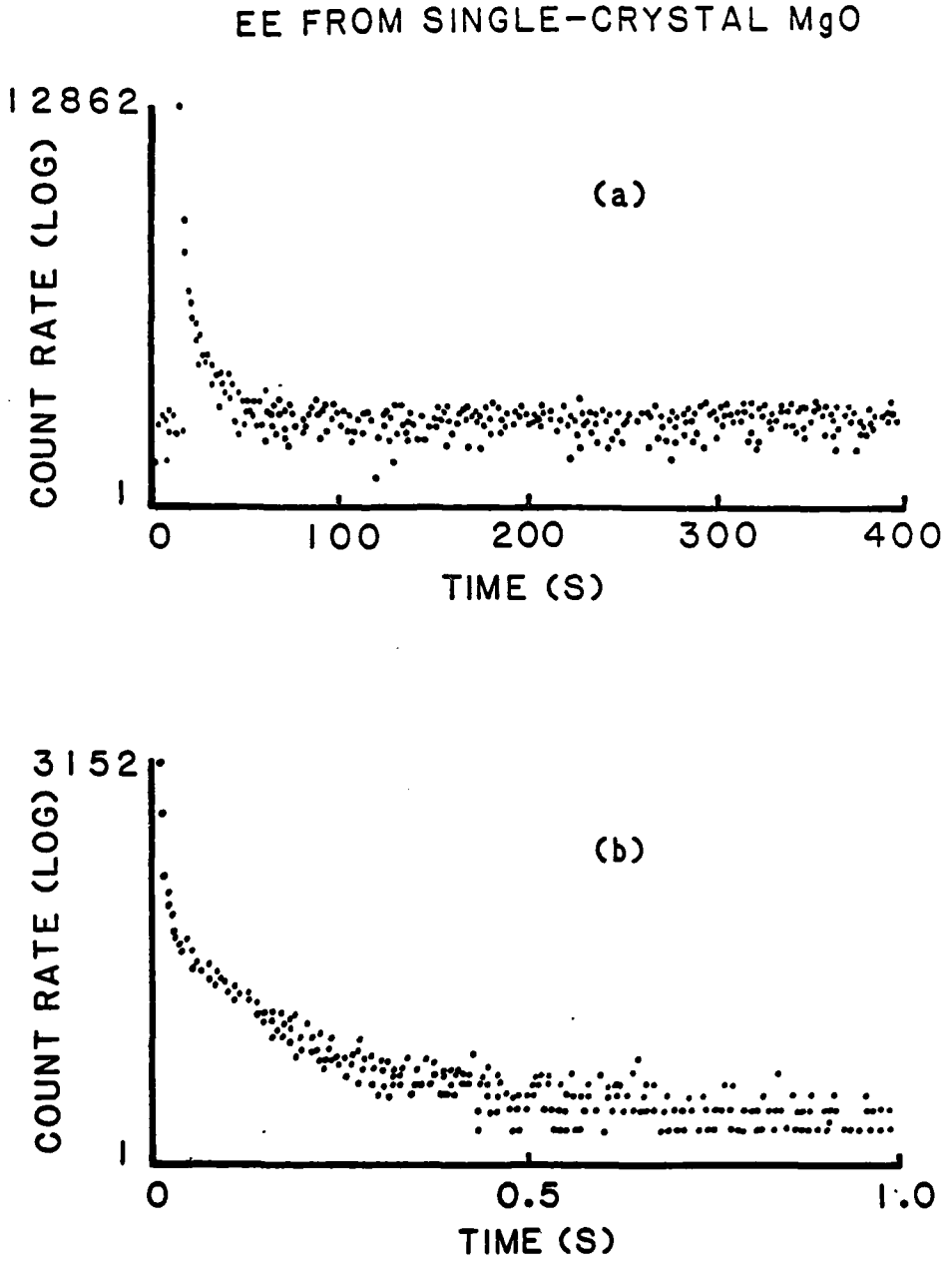
EE FROM SINGLE-CRYSTAL MgO
12862
COUNT RATE (LOG)
1
(a)
0
100
200
300
400
TIME (S)
3152
COUNT RATE (LOG)
1
(b)
0
0.5
1.0
TIME (S)

Fig 3c

Electron Emission From the Fracture
of Unfilled Polyurethane

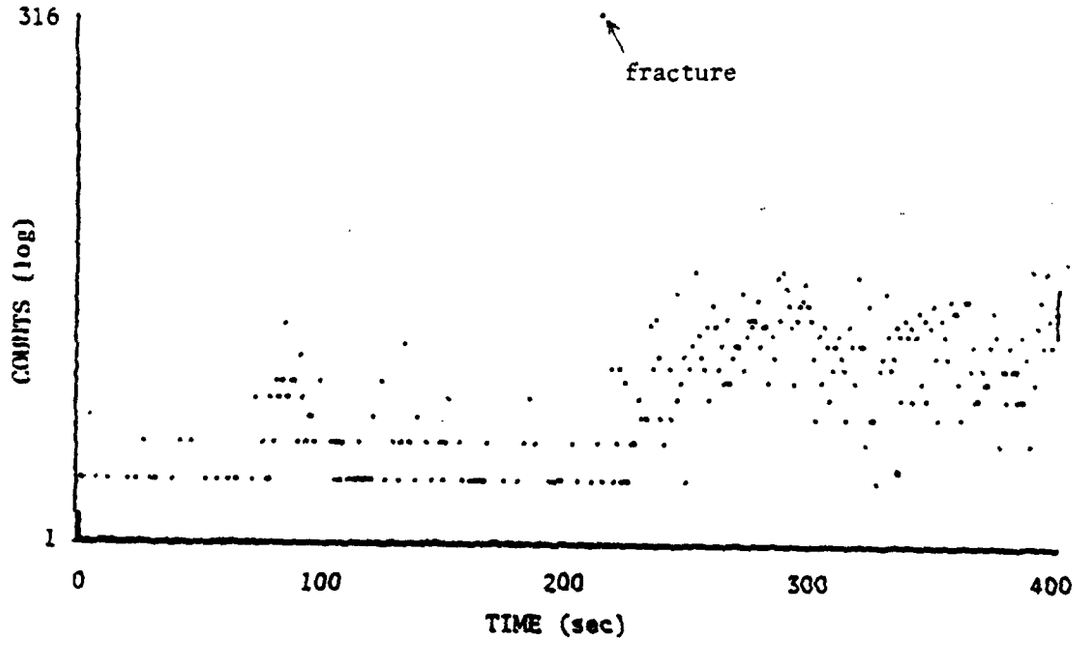

4

Fracto-Emission From the Separation of Polyurethane From a Stainless Steel Surface

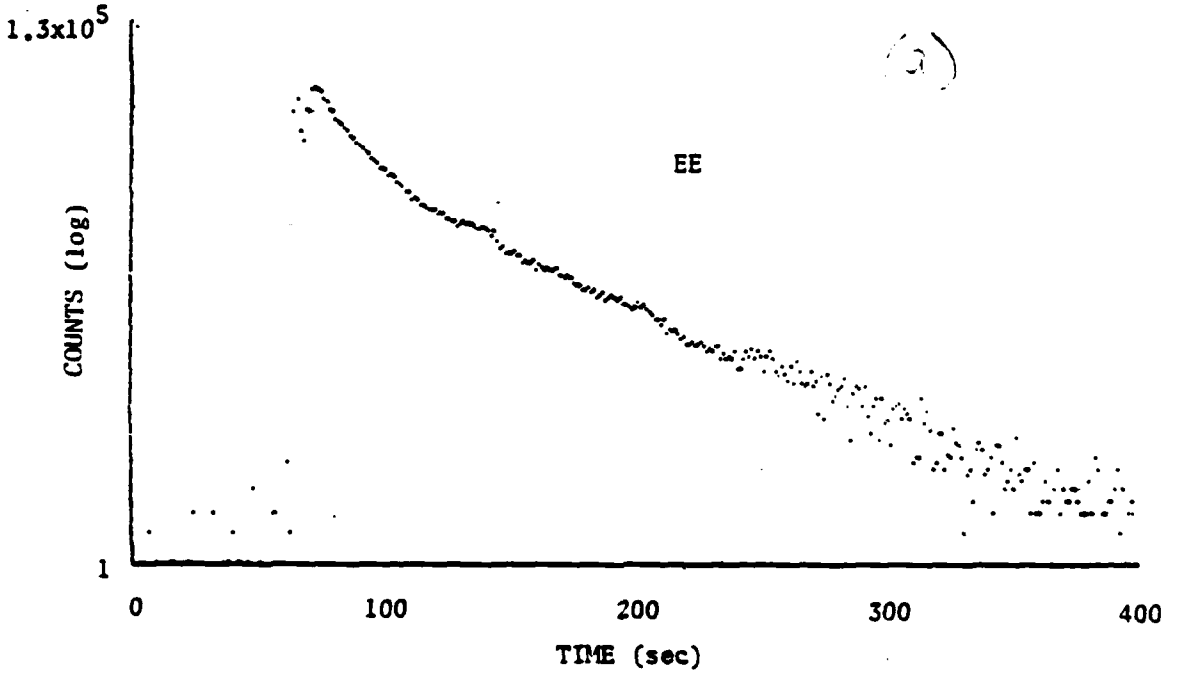

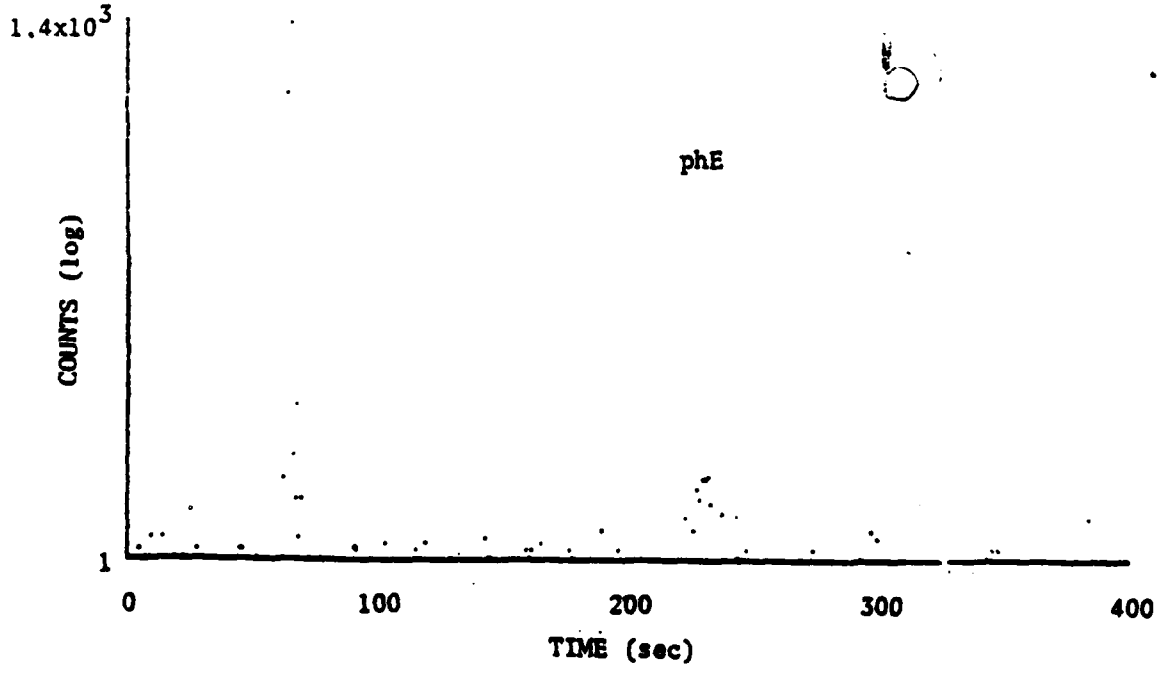

Fig. 5

Fracto-Emission From the Separation of Polyurethane From a Glass Surface

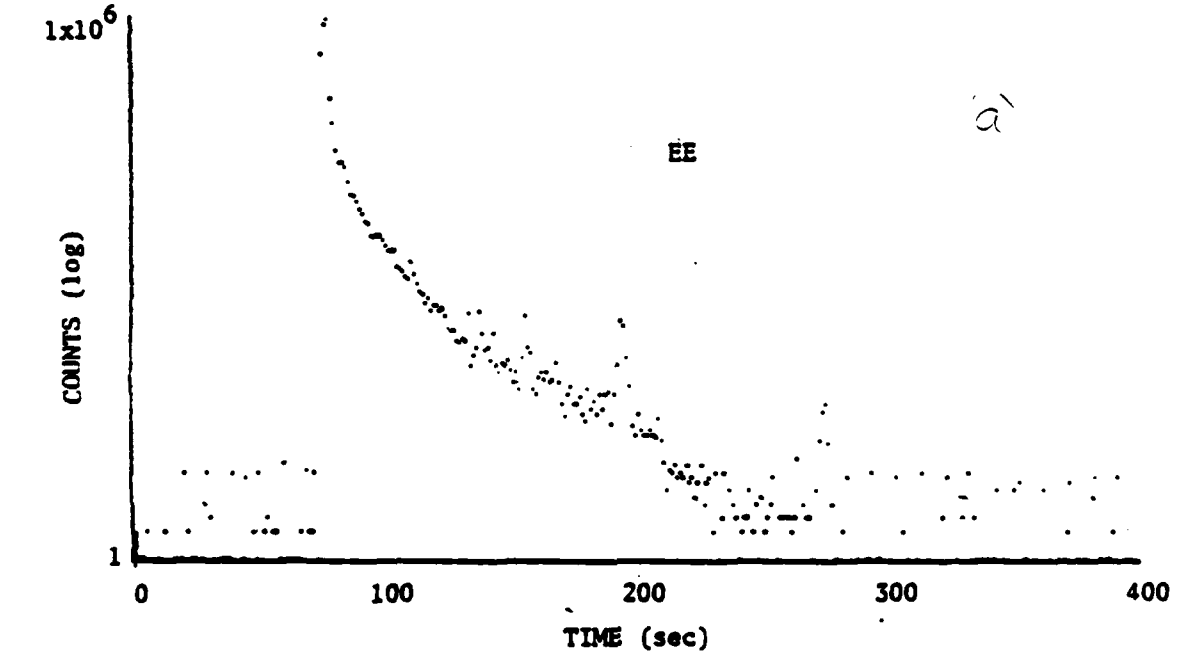

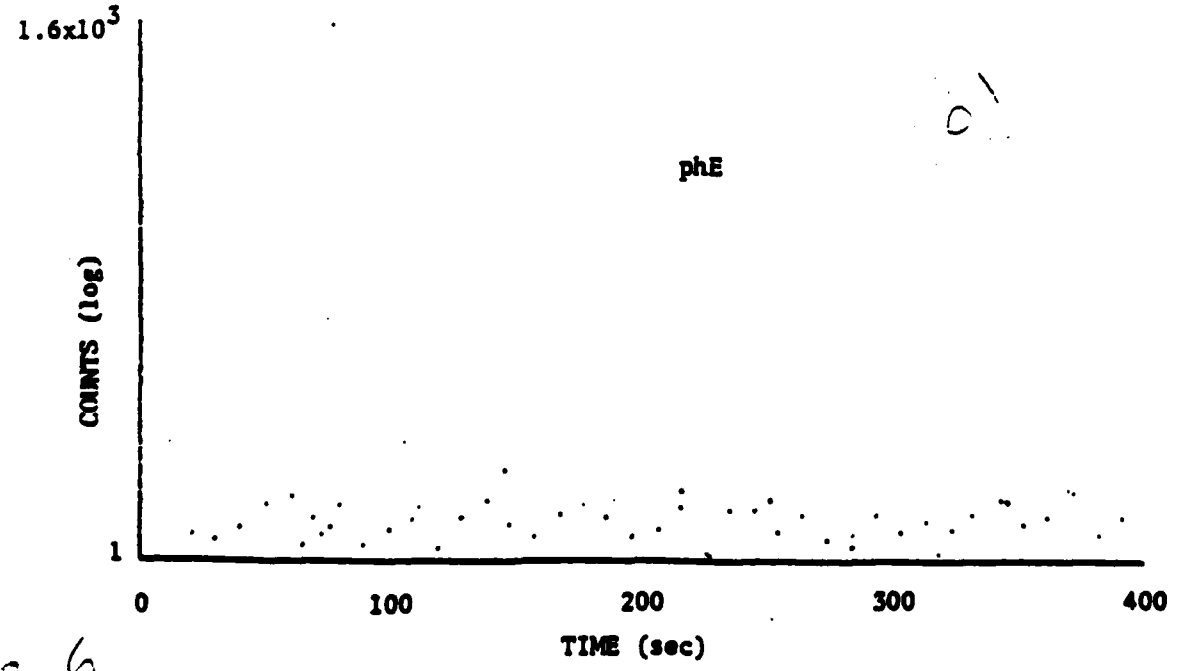

Fig 6

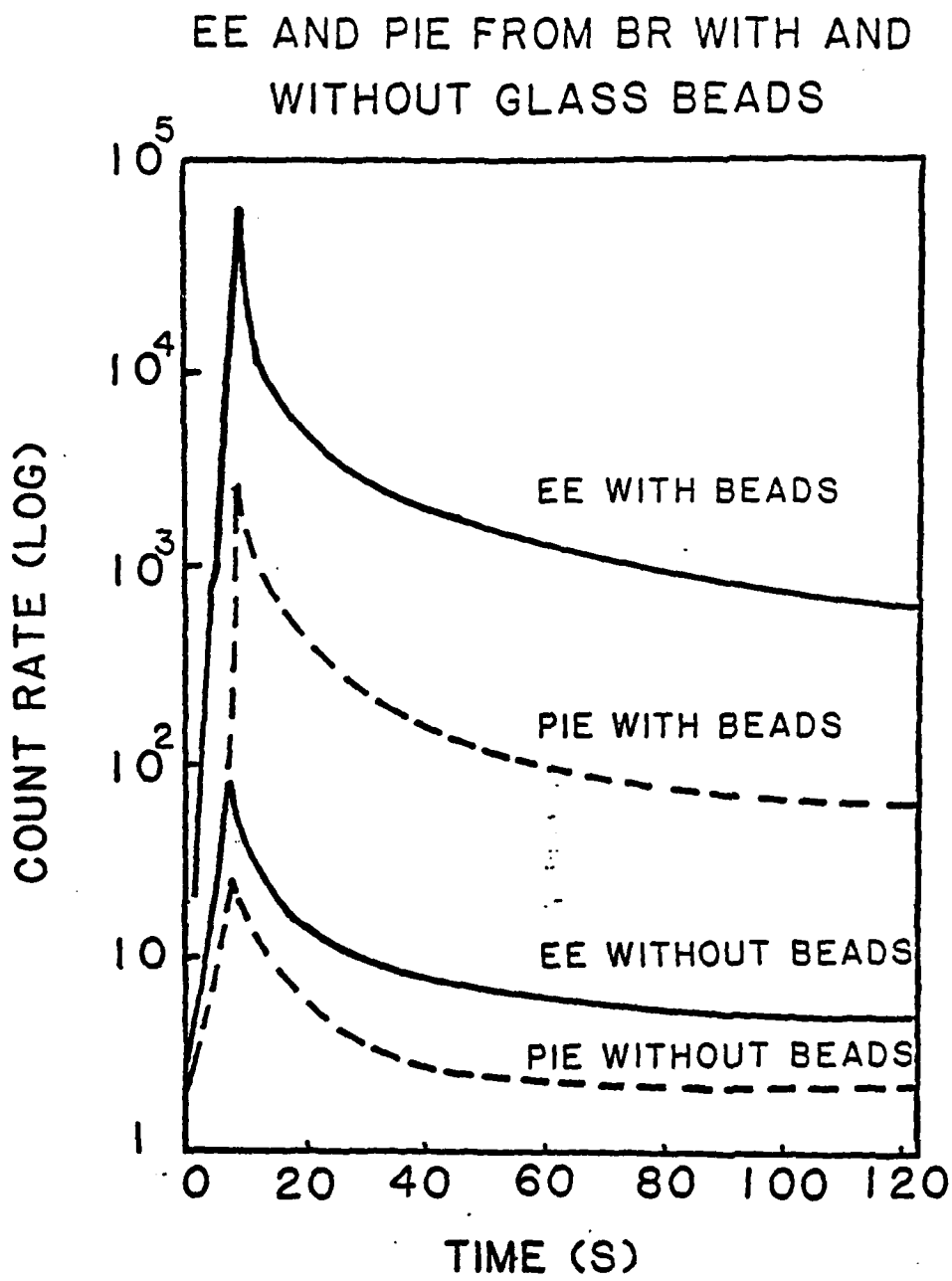
EE AND PIE FROM BR WITH AND WITHOUT GLASS BEADS
COUNT RATE (LOG)
10^5
10^4
10^3
10^2
10
1
EE WITH BEADS
PIE WITH BEADS
EE WITHOUT BEADS
PIE WITHOUT BEADS
0 20 40 60 80 100 120
TIME (S)

Fig 7

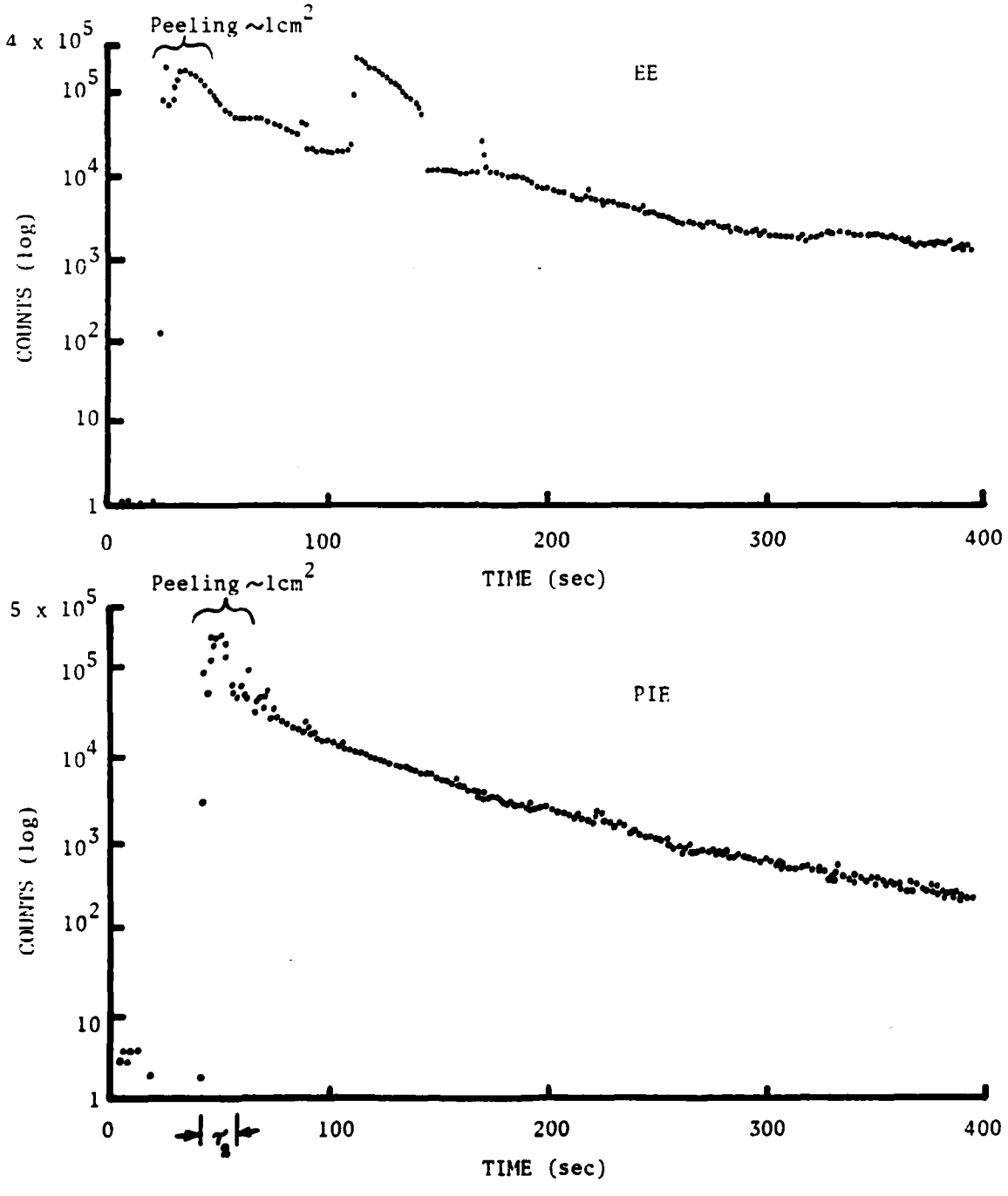
Peeling ~1cm²
4 x 10⁵
10⁵
10⁴
10³
10²
10
1
COUNTS (log)
EE
0
100
200
300
400
TIME (sec)
Peeling ~1cm²
5 x 10⁵
10⁵
10⁴
10³
10²
10
1
COUNTS (log)
PIE
0
100
200
300
400
TIME (sec)

Fig. 8

IX. CONCLUSIONS

In this year we have made considerable progress in our understanding of the emission of electrons positive ions, and photons during and following fracture polymers, inorganic crystals, and organic crystals. The concepts of charge separation, gas desorption, a gaseous discharge, and particle bombardment of the fracture surfaces followed by subsequent relaxation processes provide the foundation for making predictions and suggest routes to quantitative models and numerous additional experiments. In addition we have shown that material properties, e.g. cross-link density in an elastomer, can influence FE greatly. Also, we have shown that an energetic binder, BAMO/THF, emits copious amounts of N_2 during fracture and may be undergoing decomposition along the fracture path. Finally, the FE from the molecular crystals sucrose and RDX suggests that the charged particle emission may involve a gaseous discharge during fracture, which means that the surfaces are charging and are being bombarded with discharge products, i.e. electrons, ions, and reactive neutrals.

X. FRACTO-EMISSION TALKS AND PAPERS PRESENTED

1. "Fracto-Emission from Elastomers," Gordon Conference on Elastomers, New Hampshire, July 1982.

2. "Correlations in Time of Electron and Positive Ion Emission Accompanying Fracture," American Vacuum Society, Baltimore, November 1982.

3. "Fracto-Emission from Composites," Gordon Conference on Composites, Santa Barbara, January 1983.

4. "Fracto-Emission Accompanying Adhesive Failure," ACS Symposium on Adhesion, Seattle, March 1983.

5. "Fracto-Emission from Fiber-Reinforced Composites and Adhesive Failure," ACS Symposium on Composites, Seattle, March 1983.

6. "Fracto-Emission from Filled and Unfilled Elastomers," ACS Symposium on Frontiers of Rubber Science, Toronto, May 1983.

7. "Fracto-Emission," DOW Chemical Company, Midland, MI, May 1983.

DISTRIBUTION LIST

	No. Copies
Dr. L.V. Schmidt Assistant Secretary of the Navy (R,E, and S) Room 5E 731 Pentagon Washington, D.C. 20350	1
Dr. A.L. Slafkosky Scientific Advisor Commandant of the Marine Corps Code RD-1 Washington, D.C. 20380	1
Dr. Richard S. Miller Office of Naval Research Code 413 Arlington, VA 22217	10
Mr. David Siegel Office of Naval Research Code 260 Arlington, VA 22217	1
Dr. R.J. Marcus Office of Naval Research Western Office 1030 East Green Street Pasadena, CA 91106	1
Dr. Larry Peebles Office of Naval Research East Central Regional Office 666 Summer Street, Bldg. 114-D Boston, MA 02210	1
Dr. Phillip A. Miller Office of Naval Research San Francisco Area Office One Hallidie Plaza, Suite 601 San Francisco, CA 94102	1
Mr. Otto K. Heiney AFATL - DLDL Elgin AFB, FL 32542	1
Mr. R. Geisler ATTN: MKP/MS24 AFRPL Edwards AFB, CA 93523	1
Dr. F. Roberto Code AFRPL MKPA Edwards AFB, CA 93523	1
Dr. L.H. Caveny Air Force Office of Scientific Research Directorate of Aerospace Sciences Bolling Air Force Base Washington, D.C. 20332	1
Mr. Donald L. Ball Air Force Office of Scientific Research Directorate of Chemical Sciences Bolling Air Force Base Washington, D.C. 20332	1
Dr. John S. Wilkes, Jr. FJSRL/NC USAF Academy, CO 80840	1
Dr. R.L. Lou Aerojet Strategic Propulsion Co. P.O. Box 15699C Sacramento, CA 95813	1
Dr. V.J. Keenan Anal-Syn Lab Inc. P.O. Box 547 Paoli, PA 19301	1
Dr. Philip Howe Army Ballistic Research Labs ARRADCOM Code DRDAR-BLT Aberdeen Proving Ground, MD 21005	1
Mr. L.A. Watermeier Army Ballistic Research Labs ARRADCOM Code DRDAR-BLI Aberdeen Proving Ground, MD 21005	1
Dr. W.W. Wharton Attn: DRSMI-RKL Commander U.S. Army Missile Command Redstone Arsenal, AL 35898	1

DISTRIBUTION LIST

	No. Copies
Mr. J. Murrin Naval Sea Systems Command Code 62R2 Washington, D.C. 20362	1
Dr. D.J. Pastine Naval Surface Weapons Cneter Code R04 White Oak Silver Spring, MD 20910	1
Mr. L. Roslund Naval Surface Weapons Center Code R122 White Oak, Silver Spring MD 20910	1
Mr. M. Stosz Naval Surface Weapons Center Code R121 White Oak Silver Spring, MD 20910	1
Dr. E. Zimmet Naval Surface Weapons Center Code R13 White Oak Silver Spring, MD 20910	1
Dr. D. R. Derr Naval Weapons Center Code 388 China Lake, CA 93555	1
Mr. Lee N. Gilbert Naval Weapons Center Code 3205 China Lake, CA 93555	1
Dr. E. Martin Naval Weapons Center Code 3858 China Lake, CA 93555	1
Mr. R. McCarten Naval Weapons Center Code 3272 China Lake, CA 93555	1
Dr. A. Nielsen Naval Weapons Center Code 385 China Lake, CA 93555	1
Dr. R. Reed, Jr. Naval Weapons Center Code 388 China Lake, CA 93555	1
Dr. L. Smith Naval Weapons Center Code 3205 China Lake, CA 93555	1
Dr. B. Douda Naval Weapons Support Center Code 5042 Crane, Indiana 47522	1
Dr. A. Faulstich Chief of Naval Technology MAT Code 0716 Washington, D.C. 20360	1
LCDR J. Walker Chief of Naval Material Office of Naval Technology MAT, Code 0712 Washington, D.C. 20360	1
Mr. Joe McCartney Naval Ocean Systems Center San Diego, CA 92152	1
Dr. S. Yamamoto Marine Sciences Division Naval Ocean Systems Center San Diego, CA 91232	1
Dr. G. Bosmajian Applied Chemistry Division Naval Ship Research & Development Center Annapolis, MD 21401	1
Dr. H. Shuey Rohn and Haas Company Huntsville, Alabama 35801	1

DYN

6/81

DISTRIBUTION LIST

	No. Copies
Mr. R. Brown Naval Air Systems Command Code 330 Washington, D.C. 20361	1
Dr. H. Rosenwasser Naval Air Systems Command AIR-310C Washington, D.C. 20360	1
Mr. B. Sobers Naval Air Systems Command Code 03P25 Washington, D.C. 20360	1
Dr. L.R. Rothstein Assistant Director Naval Explosives Dev. Engineering Dept. Naval Weapons Station Yorktown, VA 23691	1
Dr. Lionel Dickinson Naval Explosive Ordnance Disposal Tech. Center Code D Indian Head, MD 20640	1
Mr. C.L. Adams Naval Ordnance Station Code PM4 Indian Head, MD 20640	1
Mr. S. Mitchell Naval Ordnance Station Code 5253 Indian Head, MD 20640	1
Dr. William Tolles Dean of Research Naval Postgraduate School Monterey, CA 93940	1
Naval Research Lab. Code 6100 Washington, D.C. 20375	1
Dr. J. Schnur Naval Research Lab. Code 6510 Washington, D.C. 20375	1
Mr. R. Beauregard Naval Sea Systems Command SEA 64E Washington, D.C. 20362	1
Mr. G. Edwards Naval Sea Systems Command Code 62R3 Washington, D.C. 20362	1
Mr. John Boyle Materials Branch Naval Ship Engineering Center Philadelphia, PA 19112	1
Dr. H.G. Adolph Naval Surface Weapons Center Code R11 White Oak Silver Spring, MD 20910	1
Dr. T.D. Austin Naval Surface Weapons Center Code R16 Indian Head, MD 20640	1
Dr. T. Hall Code R-11 Naval Surface Weapons Center White Oak Laboratory Silver Spring, MD 20910	1
Mr. G.L. Mackenzie Naval Surface Weapons Center Code R101 Indian Head, MD 20640	1
Dr. K.F. Mueller Naval Surface Weapons Center Code R11 White Oak Silver Spring, MD 20910	1

DISTRIBUTION LIST

	No. Copies
Dr. R.G. Rhoades Commander Army Missile Command DRSMI-R Redstone Arsenal, AL 35898	1
Dr. W.D. Stephens Atlantic Research Corp. Pine Ridge Plant 7511 Wellington Rd. Gainesville, VA 22065	1
Dr. A.W. Barrows Ballistic Research Laboratory USA ARRADCOM DRDAR-BLP Aberdeen Proving Ground, MD 21005	1
Dr. C.M. Frey Chemical Systems Division P.O. Box 358 Sunnyvale, CA 94086	1
Professor F. Rodriguez Cornell University School of Chemical Engineering Olin Hall, Ithaca, N.Y. 14853	1
Defense Technical Information Center DTIC-DDA-2 Cameron Station Alexandria, VA 22314	12
Dr. Rocco C. Musso Hercules Aerospace Division Hercules Incorporated Alleghany Ballistic Lab P.O. Box 210 Washington, D.C. 21502	1
Dr. Ronald L. Simmons Hercules Inc. Eglin AFATL/DLDL Eglin AFB, FL 32542	1
Dr. E.H. Debutts Hercules Inc. Baccus Works P.O. Box 98 Magna, UT 84044	1
Dr. James H. Thacher Hercules Inc. Magna Baccus Works P.O. Box 98 Magna, UT 84044	1
Mr. Theordore M. Gilliland Johns Hopkins University APL Chemical Propulsion Info. Agency Johns Hopkins Road Laurel, MD 20810	1
Dr. R. McGuire Lawrence Livermore Laboratory University of California Code L-324 Livermore, CA 94550	1
Dr. Jack Linsk Lockheed Missiles & Space Co. P.O. Box 504 Code Org. 83-10, Bldg. 154 Sunnyvale, CA 94088	1
Dr. B.G. Craig Los Alamos National Lab P.O. Box 1663 NSP/DOD, MS-245 Los Alamos, NM 87545	1
Dr. R.L. Rabie WX-2, MS-952 Los Alamos National Lab. P.O. Box 1663 Los Alamos NM 37545	1
Dr. R. Rogers, WX-2 Los Alamos Scientific Lab. P.O. Box 1663 Los Alamos, NM 87545	1

DISTRIBUTION LIST

	No. Copies
Dr. J.F. Kincaid Strategic Systems Project Office Department of the Navy Room 901 Washington, D.C. 20376	1
Strategic Systems Project Office Propulsion Unit Code SP2731 Department of the Navy Washington, D.C. 20376	1
Mr. E.L. Throckmorton Strategic Systems Project Office Department of the Navy Room 1048 Washington, D.C. 20376	1
Dr. D.A. Flanigan Thiokol Huntsville Division Huntsville, Alabama 35807	1
Mr. G.F. Mangum Thiokol Corporation Huntsville Division Huntsville, Alabama 35807	1
Mr. E.S. Sutton Thiokol Corporation Elkton Division P.O. Box 241 Elkton, MD 21921	1
Dr. G. Thompson Thiokol Wasatch Division MS 240 P.O. Box 524 Brigham City, UT 84302	1
Dr. T.E. Davidson Technical Director Thiokol Corporation Government Systems Group P.O. Box 9258 Ogden, Utah 84409	1
Dr. C.W. Vriesen Thiokol Elkton Division P.O. Box 241 Elkton, MD 21921	1
Dr. J.C. Hinshaw Thiokol Wasatch Division P.O. Box 524 Brigham City, Utah 83402	1
U.S. Army Research Office Chemical & Biological Sciences Division P.O. Box 12211 Research Triangle Park NC 27709	1
Dr. R.F. Walker USA ARRADCOM DRDAR-LCE Dover, NJ 07801	1
Dr. T. Sinden Munitions Directorate Propellants and Explsoives Defence Equipment Staff British Embassy 3100 Massachusetts Ave. Washington, D.C. 20008	1
LTC B. Loving AFROL/LK Edwards AFB, CA 93523	1
Professor Alan N. Gent Institute of Polymer Science University of Akron Akron, OH 44325	1
Mr. J. M. Frankle Army Ballistic Research Labs ARRADCOM Code DRDAR-BLI Aberdeen Proving Ground, MD 21005	1

DISTRIBUTION LIST

	No. Copies
Dr. Ingo W. May Army Ballistic Research Labs ARRADCOM Code DRDAR-BLI Aberdeen Proving Ground, MD 21005	1
Professor N.W. Tschoegl California Institute of Tech Dept. of Chemical Engineering Pasadena, CA 91125	1
Professor M.D. Nicol University of California Dept. of Chemistry 405 Hilgard Avenue Los Angeles, CA 90024	1
Professor A. G. Evans University of California Berkeley, CA 94720	1
Professor T. Litovitz Catholic Univ. of America Physics Department 520 Michigan Ave., N.E. Washington, D.C. 20017	1
Professor W. G. Knauss Graduate Aeronautical Lab California Institute of Tech. Pasadena, CA 91125	1
Professor Edward Price Georgia Institute of Tech. School of Aerospace Engin. Atlanta, Georgia 30332	1
Dr. Kenneth O. Hartman Hercules Aerospace Division Hercules Incorporated P.O. Box 210 Cumberland, MD 21502	1
Dr. Thor L. Smith IBM Research Lab D42.282 San Jose, CA 95193	1
Dr. J. P. Marshall Dept. 52-35, Bldg. 204/2 Lockheed Missile & Space Co. 3251 Hanover Street Palo Alto, CA 94304	1
Ms. Joan L. Janney Los Alamos National Lab Mail Stop 920 Los Alamos, NM 87545	1
Dr. J. M. Walsh Los Alamos Scientific Lab Los Alamos, NM 87545	1
Professor R. W. Armstrong Univ. of Maryland Department of Mechanical Eng. College Park, MD 20742	1
Prof. Richard A. Reinhardt Naval Postgraduate School Physics & Chemistry Dept. Monterey, CA 93940	1
Dr. R. Bernecker Naval Surface Weapons Center Code R13 White Oak, Silver Spring, MD 20910	1
Dr. M. J. Kamlet Naval Surface Weapons Center Code R11 White Oak, Silver Spring, MD 20910	1
Professor J. D. Achenbach Northwestern University Dept. of Civil Engineering Evanston, IL 60201	1
Dr. N. L. Basdekas Office of Naval Research Mechanics Program, Code 432 Arlington, VA 22217	1
Professor Kenneth Kuo Pennsylvania State Univ. Dept. of Mechanical Engineering University Park, PA 16802	1

DISTRIBUTION LIST

	No. Copies	No. Copies
Dr. S. Sheffield Sandia Laboratories Division 2513 P.O. Box 5800 Albuquerque, NM 87185	1	
Dr. M. Farber Space Sciences, Inc. 135 Maple Avenue Monrovia, CA 91016	1	
Dr. Y. M. Gupta SRI International 333 Ravenswood AVenue Menlo Park, CA 94025	1	
Mr. M. Hill SRI International 333 Ravenswood Avenue Menlo Park, CA 94025	1	
Professor Richard A. Schapery Texas A&M Univ. Dept of Civil Engineering College Station, TX 77843	1	
Dr. Stephen Swanson Univ. of Utah Dept. of Mech. & Industrial Engineering MEB 3008 Salt Lake City, UT 84112	1	
Mr. J. D. Byrd Thiokol Corp. Huntsville Huntsville Div. Huntsville, AL 35807	1	
Professor G. D. Duvall Washington State University Dept. of Physics Pullman, WA 99163	1	
Prof. T. Dickinson Washington State University Dept. of Physics Pullman, WA 99163	1	

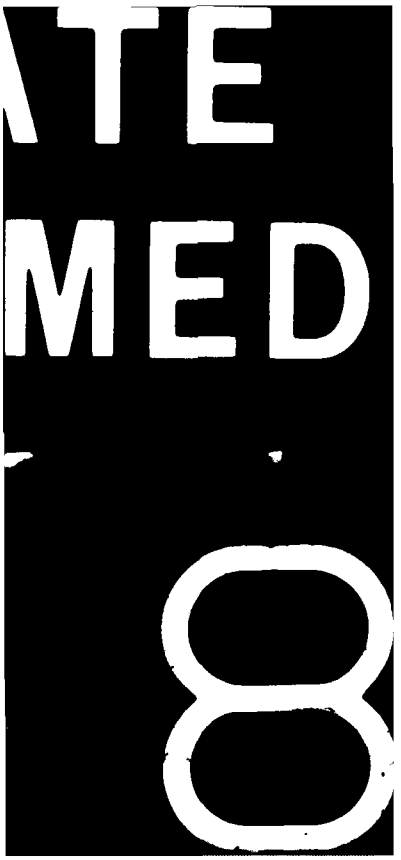
TE
MED
8